BEZMIALEM VAKIF UNIVERSITY
INSTITUTE OF HEALTH SCIENCES

GENERATION OF PLASMID-BASED EUKARYOTIC MODEL TO INVESTIGATE BIOLOGY OF CRIMEAN-CONGO HEMORRHAGIC FEVER VIRUS NUCLEOPROTEIN AND GLYCOPROTEINS

PhD THESIS

Nesibe Selma ÇETİN

Department of Biotechnology

PhD Programme

Thesis Advisor: Prof. Dr. Mehmet Ziya Doymaz

JANUARY 2023

BEZMIALEM VAKIF UNIVERSITY
INSTITUTE OF HEALTH SCIENCES

GENERATION OF PLASMID-BASED EUKARYOTIC MODEL TO INVESTIGATE BIOLOGY OF CRIMEAN-CONGO HEMORRHAGIC FEVER VIRUS NUCLEOPROTEIN AND GLYCOPROTEINS

PhD THESIS

Nesibe Selma ÇETİN
(160506002)

Biotechnology Department

Biotechnology PhD Programme

Thesis Advisor: Prof. Dr. Mehmet Ziya DOYMAZ

JANUARY 2023

After fulfilling all the necessary conditions determined by the related regulations, PhD student Nesibe Selma ÇETİN (student ID number: 160506002) successfully presented her thesis titled as " GENERATION OF PLASMID-BASED EUKARYOTIC MODEL TO INVESTIGATE BIOLOGY OF CRIMEAN-CONGO HEMORRHAGIC FEVER VIRUS NUCLEOPROTEIN AND GLYCOPROTEINS" in front of the jury members.

Thesis Advisor : **Prof. Dr. Mehmet Ziya DOYMAZ** .....
Bezmialem Vakif University

Jury Members : **Asst. Prof. A. Matteen RAFIQI** .....
Bezmialem Vakif University

Assoc. Prof. Bilge SÜMBÜL .....
Bezmialem Vakif University

Prof. Dr. Ali Osman KILIÇ .....
Karadeniz Technical University

Assoc. Dr. Orkide COŞKUNER WEBER .....
Turkish-German University

Date of Submission : 3 January 2023
Date of defense Exam : 23 January 2023

To my family,

FOREWORD

I would like to express my great gratitude to my advisor, Prof Dr Mehmet Ziya Doymaz, for his expertise, generous guidance, understanding and support in this study. I would like to thank my colleagues Dr. Elif Karaaslan, Dr. Merve Yazıcı, Dr. Ayşegül Pirinçal, MSc. Sevde Sayın, MSc. Filiz Kaptan, MSc. Sercan Keskin, MSc. Burcu Nur Aydın, Özlem Bakangil and Esmahan Avcı for their contributions to the realization of this thesis. I would like to thank also my parents for their unwavering support in every difficulty I encountered in my life, and especially for their sacrifices and efforts so that I could enjoy the unrestricted universal right of education.

I would like to dedicate this thesis to my dear parents, my dear wife Yasin, who helped me complete this work with her patience and devotion, and Yunus, who has just started his educational journey in the hope that this thesis will be an inspiration.

January 2023 Nesibe Selma Çetin

DECLARATION

I declare that; this thesis study is mine, I do not have any unethical behavior at all stages of the thesis, I have obtained all the information within academic and ethical rules, I have referred to all information and comments that have not been obtained through this thesis study and I have included them in the list of references, I have not violated any patent and copyright during the study and writing of this thesis.

Nesibe Selma Çetin

Signature

TABLE OF CONTENTS

Page

ABBREVIATIONS

CCHF : Crimean Congo Hemorrhagic Fever
CCHFV : Crimean Congo Hemorrhagic Fever Virus
SARS-CoV-2 : Severe Acute Respiratory Syndrome Coronavirus 2
COVID-19 : Coronavirus Disease 2019
VLP : Virus like particles
PEG : Poly(ethylene glycol)
PEI : Polyethylenimine
DNA : Deoxyribonucleic Acid
RNA : Ribonucleic Acid
WHO : World Health Organization
NIH/NIAID : National Institute of Allergy and Infectious Diseases
HFV : Hemorrhagic fever virus
VHF : Viral hemorrhagic fever
CHF : Crimean Hemorrhagic Fever
UTR : Untranslated region
HBV : Hepatitis B Virus
HPV : Human Papilloma Virus
HIV : Human Immunodeficiency Virus
cDNA : Complementary DNA
vRNA : Viral RNA
cRNA : Copy RNA
BSL-2 : Biosafety level 2
BSL-4 : Biosafety level 4
RNP : Ribonucleoprotein
Pol : Polymerase
ICTV : International Committee on Taxonomy of Viruses
OTU : Ovarian tumor
MHC : Major histocompatibility complex
TLR : Toll-like receptor
IL : Interleukin
Ub : Ubiquitin
ISG : Interferon stimulated gene
ER : Endoplasmic reticulum
SKI-1/S1P : Subtilisin-kexin isoenzyme-1/site-1-protease
MLD : Mucin-like domain
RdRp : RNA-dependent RNA polymerase
Np : Nucleoprotein of CCHFV
Gn : CCHFV Glycoprotein on N-terminal of M segment
Gc : CCHFV Glycoprotein on C-terminal of M segment
STAT-1 : Signal transducer and activator of transcription 1
KO : Knockout
IVIG : Intravenous immunoglobulin

SARS-CoV	**:** Severe acute respiratory syndrome coronavirus 2
S	**:** Spike protein of SARS-CoV-2
M	**:** Membrane protein of SARS-CoV-2
E	**:** Envelope protein of SARS-CoV-2
N	**:** Nucleoprotein of SARS-CoV-2
ACE-2	**:** Angiotensin convertase enzyme 2
TMPRSS2	**:** Transmembrane serine protease 2
CatL	**:** Cathepsin L
TNF	**:** Tumor necrosis factor
GM-CSF	**:** Granulocyte-macrophage colony-stimulating factor
GI	**:** Gastrointestinal tract
RAAS	**:** Renin-angiotensin-aldosterone system
BHK-21	**:** Baby hamster kidney-21 cells
HEK293T	**:** Human embryonic kidney cells
Vero E6	**:** African green monkey kidney epithelial cells
DMEM	**:** Dulbecco's modified Eagle's medium
FBS	**:** Fetal Bovine Serum
PenStrep	**:** Penicilline-Streptomycine
SDS	**:** Sodium dodecyl sulfate
TCA	**:** Trichloroacetic acid
ELISA	**:** Enzyme-Linked Immuno Sorbent Assay
CMV	**:** Cytomegalovirus
BUNV	**:** Bunyamwera
RVFV	**:** Rift Valley Fever Virus
tc-VLP	**:** Transcription and entry competent virus-like particle

SYMBOLS

ºC	**:** Degree Celcius
Δ	**:** Delta
h	**:** Hour
min	**:** Minute
bp	**:** Base pair
Ct	**:** Cycle threshold
g	**:** Gravity force

LIST OF TABLES

Page

LIST OF FIGURES

Page

GENERATION OF PLASMID-BASED EUKARYOTIC MODEL TO INVESTIGATE BIOLOGY OF CRIMEAN CONGO HEMORRHAGIC FEVER VIRUS NUCLEOPROTEIN AND GLYCOPROTEINS

SUMMARY

RNA viruses are the main cause of many pandemics that shape human history by causing the death of millions of people. The rapid adaptability of RNA viruses, which allows them to circulate for thousands of years, and the increased contact of humans with wild animals can trigger the emergence of virus variants that can cause new pandemics. Virus-like particle studies (VLPs) to elucidate unknown mechanisms in the virus life cycle and pathophysiology of disease are of vital importance in the development of effective antiviral strategies against these viruses that affect human life. The lack of genomic material that can cause virus infection paves the way for these viruses to be studied in BSL-2 laboratories, which are easily accessible to many researchers around the world. In recent years, the World Health Organization (WHO) has published a list of infectious agents that should be primarily investigated. Crimean-Congo Hemorrhagic Fever Virus (CCHFV) and Severe Acute Respiratory Syndrome Coronavirus 2 (SARS-CoV-2) viruses, which are also clinically important for our country, are included in this list. From this point of view, in this thesis, various viral protein expression studies have been carried out to develop different VLP systems that can both study the biology and immunology of CCHFV and form the basis of vaccine candidate development studies for SARS-CoV-2. For this purpose, firstly, CCHFV viral proteins were produced in Huh-7 cells via pcDNA 3.1 plasmid, and their expression was confirmed by both post-transcriptional and post-translational analyses. Furthermore, immunological analyzes by in-house ELISA revealed that various viral protein combinations may promote the production of different CCHFV proteins. In addition, a unique ambisense minigenome system has been developed. The inclusion of this system in future VLP studies might result in the generation of a transcription and entry competent VLPs for CCHFV Kelkit 06 strain. Second, four different plasmids carrying multiple expression cassettes in various combinations were constructed to produce four different VLP-based vaccine candidates against SARS-CoV-2 in *P. pastoris*.

In conclusion, the experiments conducted in this thesis have shown the expression and detection of immunologically significant viral antigenic proteins of CCHFV and SARS CoV-2, two of the most serious human viral pathogens of our time, in eukaryotic cells. These studies have established a critical infrastructure at our laboratory which will be imperative for future studies. It appears that for generation and demonstration at sufficient quantities and commercially meaningful VLPs from plasmid-based expression systems, further optimizations are needed. It should be underlined that to address the questions on the biology and immunology of these viruses through VLP and minigenome approaches, these optimizations such as exhaustive trials with

different expression models, optimization of sequences, alternative transfection systems and stable expressions should be undertaken.

Keywords: RNA viruses, RNA virus infections, Arboviruses, Corona virus infections, COVID-19 vaccines

KIRIM KONGO KANAMALI ATEŞİ VİRÜSÜ NÜKLEOPROTEİNİN VE GLİKOPROTEİNLERİNİN BİYOLOJİSİNİN ÇALIŞILMASINDA PLAZMİT TEMELLİ ÖKARYOTİK MODEL OLUŞTURULMASI

ÖZET

Milyonlarca insanın ölümüne sebep olarak insanlık tarihinine yön veren pek çok farklı pandemiye RNA virüsleri sebep olmuştur. İnfluenza A virüsü, çocuk felci virüsü, rotavirüsler, dang virüsü, hepatit C virüsü, Batı Nil humması virüsü, sarı humma virüsü ve kızamık virüsü gibi ciddi insan patojenlerinin çoğu RNA virüsleridir. Küreselleşmeyle birlikte insanların birbirleriyle ve doğadaki diğer canlılarla etkileşimi günden güne artmaktadır. Bu durum, RNA virüslerinin binlerce yıldır dolaşımda kalmalarını sağlayan hızlı uyum yetenekleri sebebiyle yeni konakçılar bulmasını kolaylaştırabilmekte ve yeni pandemilerin önünü açabilecek virüs varyantlarının ortaya çıkmasını tetikleyebilmektedir. Son COVID-19 salgınında da görüldüğü gibi, RNA virüsleri zamanla daha da endişe verici bir halk sağlığı sorunu haline gelmektedir. RNA virüslerinin bağışıklık sisteminden kaçma konusundaki mahir yetenekleri bazı durumlarda etkin antiviral ilaçların geliştirilmesini zorlaştırmaktadır. Aşı ve antivirallerin üretimi için de öncelikle virüs yaşam döngüsünün aydınlatılması gerekmektedir. Bu amaca hizmet eden sağlam yöntemlerin oluşturulması, hastalığın altında yatan moleküler mekanizmaların araştırılmasında kritik bir role sahiptir.

Genel terminolojide, ileri genetik, bir fenotipin genetik temelinin araştırılmasını ifade ederken, ters genetik, genetik değişikliklerin fenotip üzerindeki etkisinin incelenmesini ifade eder ki, viroloji bağlamında ters genetik, bir virüsün tamamen cDNA'dan üretilmesi anlamına gelir. Ters genetik sistemleri yüksek patojeniteye sahip virüslerin yaşam döngüleri, bağışıklık yanıtlarından kaçış yolları, virüs-konakçı etkileşimleri, aşı geliştirilme veya vektör olarak kullanılabilecek özelleştirilmiş virüslerin üretimi gibi çalışmaların BSL-2 koşullarında yapılabilmesine imkan tanıyan etkili ve kullanışlı araçlardır. Bu sistemler, virüslere ait yaşam döngüsünün moleküler temelinin tüm yönleriyle belirlenebileceği mutasyon analizlerine imkan tanımaktadır. Pek çok yüksek derecede patojenik RNA virüsünün biyolojisi hakkında muazzam miktarda bilgi, özellikle minigenomların da dahil olduğu VLP sistemlerini içeren araştırmalardan elde edilmiştir. Viral genomların replikasyonu ve transkripsiyonu minigenom sistemleri kullanılarak modellenirken, hedef hücrelerin morfogenezi, tomurcuklanması ve enfeksiyonu, transkripsiyon ve replikasyon açısından yetkin virüs benzeri partiküller kullanılarak simüle edilmektedir. Virüs yaşam döngüsü ve hastalığın patofizyolojisi konusundaki bilinmeyen mekanizmaları aydınlatmak üzere yapılan virüs benzeri parçacık çalışmaları (VLPs), insan hayatını etkileyen bu virüslere karşı etkili antiviral stratejilerin geliştirilmesinde hayati öneme sahiptir. Virüs benzeri parçacıkların, enfeksiyona sebep olabilecek genomik materyalden yoksun olması, dünyadaki birçok araştırmacının kolayca erişebildiği BSL-2 laboratuvarlarında bu tarz virüslerle yapılacak çalışmaları kolaylaştırmaktadır.

Geçtiğimiz yıllarda, Dünya Sağlık Örgütü (DSÖ), salgın potansiyelleri ve karşı önlemlerin olmaması veya yetersiz olması nedeniyle en fazla halk sağlığı riski taşıyan ve öncelikli olarak araştırılması gereken enfeksiyon ajanları hakkında bir liste yayınlamıştır. Ülkemiz için de klinik öneme sahip Kırım Kongo Kanamalı Ateşi (KKKA) ve COVID-19 hastalıkları bu listede ilk iki sırayı paylaşmaktedır. Buradan hareketle, bu tezde hem KKKA'nın etiyololojik ajanı olan Kırım Kongo Kanamalı Ateşi Virüsü (KKKAV)'nin biyolojisinin ve immunolojisinin çalışılabildiği, hem de COVID-19 pandemisinin müsebbibi Şiddetli Akut Solunum Sendromu Coronavirüs 2 (SARS-CoV-2)'ye yönelik aşı adayı geliştirme çalışmalarına temel oluşturacak farklı VLP sistemlerinin geliştirmesi adına çeşitli viral protein ekspresyon çalışmaları yapılmıştır.

Kırım- Kongo Kanamalı Ateşi, KKKAV'nin neden olduğu kene kaynaklı viral hemorajik bir hastalıktır. KKKA, insanlarda, sağlık sisteminin kalitesine göre %5 ila %80 arasında değişen ölüm oranlarına sahip sporadik salgınlara neden olmaktadır. Şimdiye kadar Afrika, Asya ve Avrasya'yı kapsayan geniş bir coğrafi alanda 30'dan fazla ülkede virüs izolasyonu ve/veya hastalık bildirilmiştir. Virüsün *Hyalomma* keneleri aracılığıyla artan bulaşı nedeniyle üç milyar insan hastalığa yakalanma riski altındadır. Bununla birlikte, dünyada en fazla vaka Türkiye'den bildirilmektedir. 2002 ile 2018 yılları arasında 11.041 vaka bildirildiğinden, KKKA Türkiye'de halk sağlığını tehdit eden ve büyüyen bir endişe haline geldi. Enzootik alanda bulunan enfekte keneler ile temas insanlarda KKKA'ya neden olmaktadır. İnsanlar dışındaki omurgalı konakçılar, enfeksiyondan sonra yalnızca asemptomatik geçici viremiden muzdariptir. Vücut sıvıları veya kontamine tıbbi ekipman ile doğrudan temas, nozokomiyal enfeksiyonların ana nedenleridir ve kesim sırasında viremik bir hayvanın dokuları veya sıvıları ile temas, insana bulaşmanın başka bir yoludur. İnsanlarda KKKA çok farklı klinik tablo ile seyredebilir.Hafif seyreden bir hastalıktan, şiddetli ve ölümcül seviyelere ulaşan bir hastalığa dönüşebilir. Şu anda KKKA için onaylanmış bir aşı veya ilaç bulunmadığından, tedavinin birincil odak noktası hastalara destekleyici bakım sağlamaktır.

Kırım Kongo Kanamalı Ateşi Virüsü negatif tek sarmallı zarflı bir RNA virüsüdür. Viral genom, sırasıyla RNA'ya bağımlı viral RNA polimeraz, glikoproteinler ve nükleoproteinler gibi yapısal proteinleri kodlayan L, M ve S segmentleri olarak adlandırılan üç tek sarmallı negatif RNA moleküllerinden oluşur. Her segmentte tek bir açık okuma çerçevesi (ORF) ve yüksek düzeyde korunmuş ve birbirine komplementer kodlayıcı olmayan terminal tamamlayıcı diziler bulunmaktadır. Her iki uç arasındaki kovalent olmayan etkileşim, viral polimerazın bağlanması için fonksiyonel bir promotör bölge olma görevini üstlenmektedir. CCHFV M segmentinden iki viral glikoprotein, Gn ve Gc üretilmektedir ve konak hücreye bağlanma ve internalizasyondan sorumludur. S segmentten üretilen nükleoproteinler (Np), viral genomun kapsüllenmesi ve RNA'ya bağımlı RNA polimeraz (RdRp) ile birlikte bir ribonükleoprotein kompleksinin oluşturulması, ardından konakçı hücrede viral replikasyonun ve transkripsiyonun başlatılması için çok önemlidir.

Bulaş riskinin yüksek olması ve BSL-4 tesislerinin gerekliliği canlı virüs ile yapılan çalışmaları kısıtlamaktadır. Bu nedenle, virüs biyolojisi hakkında, özellikle tekil proteinler tarafından sağlanan her bilgi, literatüre değerli katkılar sağlayacaktır. Bu amaçla ilk olarak, KKKAV viral proteinleri Huh-7 hücrelerinde pcDNA 3.1 plazmidi aracılığıyla üretilmiş ve hem post-transkripsiyonel hem de post-translasyonel analizlerle viral proteinlerin ekspresyonları gösterilmiştir. ELISA ile yapılan immünolojik analizlerde, çeşitli viral protein kombinasyonlarının, farklı KKKAV

VLP'lerin üretimini destekleyebileceğine dair bazı veriler elde edilmiştir. Ayrıca, benzersiz bir ambisense minigenom sistemi geliştirilmiştir. Bu sistemin ileride yapılacak VLP çalışmalarına dahil edilmesi, KKKAV Kelkit 06 suşu için transkripsiyonel ve giriş yetkin bir VLP üretilmesinin yolunu açabileceği düşünülmektedir.

İkinci olarak, bu tezde, insanlık tarihinde dönüm noktası sayılabilecek ölçüde yıkıcı sonuçlarına mağruz kaldığımız COVID-19 pandemisinin müsebbibi SARS-CoV-2'ye yönelik çalışmalar yapılmıştır. 2019' un sonunda, Çin'in Wuhan şehrinde, kaynağı bilinmeyen bir dizi oldukça bulaşıcı şiddetli pnömoni vakası ortaya çıkmıştır. Moleküler biyolojideki modern gelişmeler sayesinde, bu durumun altında yatan viral ajan, ilk vakadan sonraki bir ay içinde tanımlandı ve SARS-CoV ile %79,6 sekans benzerliği nedeniyle SARS-CoV-2 olarak adlandırıldı. Yüksek bulaşma hızı nedeniyle birkaç ay içinde "koronavirüs hastalığı 2019" (COVID-19) olarak bilinen ve insan sağlığı ve kamu güvenliği için ciddi bir küresel tehdit oluşturan bir pandemiye dönüşmüştür. Ocak 2023 itibariyle 215 ülke ve bölgede 661 milyonu aşan vaka ve 6,69 milyondan fazla ölüm belgelenmiştir. İnsanlar arasında viral bulaşmanın, enfekte hastaların öksürmelerinden, hapşırmalarından veya konuşmalarından salınan solunum partikülleri yoluyla doğrudan meydana geldiği bilinmektedir. Bu yüzden, dünyanın birçok ülkesinde, çeşitli aralıklarla evde kalma emirleri, sokağa çıkma yasakları, karantinalar, güvenlik kordonları ve benzeri toplumsal kısıtlamalar gibi ilaç dışı müdahaleler uygulanmak zorunda kalınmıştır. Bu süreçte ek olarak, sporadik mutasyonlar ve rekombinasyonlar sebeiyle, virüsün daha geniş bir alana yayılmasına veya nötralize edici antikorlardan kaçabilmesine imkan tanıyan yeni varyantlar da ortaya çıkmıştır.

COVID-19'un etiyolojik ajanı SARS-CoV-2, zarflı, pozitif tek sarmallı bir RNA virüsüdür. Virionda S, M, N ve E olarak adlandırılan yapısal proteinleri bulunmaktadır. E proteini iyon kanalı aktivitesine sahiptir ve olgun virüs partikülünün oluşumunda önemli olduğu düşünülmektedir. Nükleoprotein (N), pozitif anlamda viral RNA'ya yüksek afinite ile bağlanır ve onu konakçı nükleazlardan korur. M proteini virionda bol miktarda bulunur ve nükleokapside bağlanarak viral genomun paketlenmesine yardımcı olur. S proteini, virüsün hücre yüzeyindeki anjiyotensin dönüştürücü enzim 2 (ACE2) reseptörlerine bağlanmasına ve ardından endozomlara alınmasına aracılık eder.

SARS-CoV-2 ile enfekte olan çoğu insan, virüs replikasyonunun esas olarak üst solunum yollarıyla sınırlı olduğu hafif ila orta şiddette bir hastalık geliştirse de, bazılarında hayatı tehdit eden bir pnömoniye dönüşmektedir ve yüzde %1 oranında fatalite görülmektedir. COVID-19' a yakalan kişilerin yaklaşık %3-20'sinde hastalık ağır seyretmektedir ve bunların yaklaşık %10-30'u için yoğun bakıma ihtiyaç duyulmaktadır. Bu durum sağlık sistemleri üzerinde büyük bir baskı oluşturmuştur. Şu anda, COVID-19' a karşı spesifik bir tedavinin henüz geliştirilmemesi COVID-19'un patogenezine ilişkin sınırlı anlayışımızı vurgulamaktadır.

COVID-19'a karşı aşı geliştirme çalışmaları, viral genom dizilimi yapılır yapılmaz eşi görülmemiş bir hızla başlatıldı. Spike proteinin virüs giriş mekanizmasındaki önemli rolü nedeniyle, tüm protein veya reseptör bağlanma alanı (RBD) gibi kritik parçalar aşı tasarımında ana hedef antijen olarak kullanılmıştır. Bu kapsamda, yalnızca Spike veya tüm yapısal proteinleri içeren VLP'lerle yapılan mevcut klinik çalışmaların aksine, bu çalışmada, viral proteinlerin değişik kombinasyonları ile farklı VLP'lerin üretimine odaklanılmıştır. SARS-CoV-2 proteinleriyle bir VLP yapısı oluşturmak için minimum protein içeriğinin M ve E proteinleri olduğu öngörüsü ve S ve N

proteinlerinin antijenik özellikleri nedeniyle SEM, SEN, SENM ve ENM olarak adlandırılan dört farklı SARS-CoV-2 VLP plazmidi tasarlanmıştır. amacıyla çeşitli kombinasyonlarda çoklu ekspresyon kasetleri taşıyan dört farklı plazmit oluşturulmuştur. Bu plazmitler, farklı viral ifade kasetleri kombinasyonlarının sıralı olarak klonlanmasıyla inşa edilmiştir. Viral genlerin maya genomuna entegrasyonu sonrası *P. pastoris* GS115 suşu ile yapılan expresyon çalışmalarında, viral proteinler çeşitli antikorlar kullanılarak tespit edilmiştir. Bu çalışmalar VLP sistemlerinin translasyonel biyoteknolojide kullanımına dair örnek bir çalışmayı temsil etmektedir ve aşı adaylarının immünojenisitesini ve güvenliğini inceleyen ileri klinik çalışmalara veri sağlayabileceği düşünülmektedir.

Sonuç olarak, bu tezde yapılan deneyler, zamanımızın en ciddi insan viral patojenlerinden ikisi olan CCHFV ve SARS CoV-2'nin immünolojik açıdan önemli viral antijenik proteinlerinin ökaryotik hücrelerde ekspresyonunu ve saptanmasını göstermiştir. Bu çalışmalar laboratuvarımızda ilerideki çalışmalar için gerekli olacak kritik bir altyapı oluşturmuştur. Plazmid bazlı ekspresyon sistemlerinden yeterli miktarlarda ve ticari olarak anlamlı VLP'lerin üretilmesi ve gösterilmesi için daha fazla optimizasyona ihtiyaç duyulmaktadır. Bu virüslerin biyolojisi ve immünolojisi ile ilgili soruları VLP ve minigenom yaklaşımları ile ele almak için, farklı ifade modelleri ile ayrıntılı denemeler, dizilerin optimizasyonu, alternatif transfeksiyon sistemleri ve kararlı ifadeler gibi bu optimizasyonların yapılması gerektiğinin altı çizilmelidir.

Anahtar Kelimeler: RNA virüsleri, RNA virüsü enfeksiyonları, Arbovirüsler, Corona virüsü enfeksiyonları, COVID-19 aşıları

1. INTRODUCTION

1.1 Purpose of Thesis

The majority of human infections that result in millions of mortalities each year are introduced by RNA viruses [1-5]. Because of globalization, people are now more mobile than ever before, leading to increased interaction with wildlife. This has made it easier for RNA viruses, which innately tend to evolve rapidly, to find new hosts. As evidenced by the recent COVID-19 pandemic, RNA viruses are becoming a growing public health concern. Working with live viruses is challenging because of the fascinating ability of RNA viruses to evade the immune system [6]. On the other hand, the reverse genetic systems used in virology allow studies that enable to understand of such viruses in all their aspects and to develop appropriate treatment strategies accordingly, without the need for high levels of biosecurity [7]. In this thesis, various studies have been carried out to develop virus-like particle (VLP) systems that serve different purposes for two viruses, Crimean Congo Hemorrhagic Fever Virus (CCHFV) and SARS-CoV-2, which are reported to be primarily studied by the World Health Organization (WHO). The CCHFV is a negative-stranded enveloped RNA virus and is one of the public health problems of our country, as it threatens the health of billions of people, as well as the fact that the highest number of cases in the world are reported in Türkiye [8, 9]. Also, the high risk of transmission and the necessity for BSL-4 facilities hampers the studies with live virus. So, any information on virus biology, especially that provided by individual proteins, will be a valuable contribution to the knowledge of CCHFV. Therefore, it is aimed to produce viral proteins in mammalian expression systems to establish a plasmid-based VLP system which can contribute to existing knowledge about CCHFV biology and immunology. It was also aimed to develop a minigenome system that can be utilized in other studies aiming to generate VLP models which can simulate one cycle of virus replication. Unlike studies in the literature, it is aimed to develop a unique minigenome system that eliminates the need for both T7-expressing cell lines and a viral ribonuclear protein complex (RNP) generally aided by either a helper virus or by plasmid transfections *in trans*. This, the

expression studies may further facilitate studies of the virus life cycle, the discovery of new therapeutics, and the development of diagnostic tools

Molecular virology studies with the reverse genetic approach led to many different biotechnological studies. Information from these studies has been used to develop VLP-based vaccines against many different viruses that cause infectious diseases [10]. For example, VLP vaccines developed against Hepatitis B Virus (HBV) and Human Papilloma Virus (HPV) are widely used due to their safety and effectiveness [11]. Because of this, the other objective of this thesis is to develop VLP-based vaccine candidates against the SARS-CoV-2 virus that emerged at the end of 2019 and caused a pandemic that resulted in millions of deaths worldwide [12]. Unlike existing clinical studies with VLPs containing only spikes or all structural proteins, this study focused on the production of different VLPs by combinations of viral proteins[13]. Due to the prediction that the minimum protein content to form a VLP structure is M and E proteins, and the antigenic properties of S and N proteins, four different SARS-CoV-2 VLPs plasmids, called SEM, SEN, SENM, and ENM according to encoded genes, were designed. Considering that cost-effective manufacturing is critical in the development of vaccines for mass production, the *P. pastoris* expression system was chosen to produce easily target antigens at lower production costs than other eukaryotic systems (such as mammalian, insect, and plant) while maintaining its immunogenicity [14]. To generate these VLPs by transforming a single plasmid, multiple expression cassettes encoding viral genes will be cloned sequentially into the same vector. As an exemplary usage of VLP systems in translational biotechnology, this study may provide data to the clinical studies examining the immunogenicity and safety of vaccine candidates in the future.

Virus-like particle systems have shed light on the biology, immunology, and pathogenesis of numerous RNA viruses. It is essential to conduct virus characterization studies safely in order to develop effective treatment methods for combating RNA viruses that threaten human health. The knowledge and experience brought on by this thesis will pave the way for future VLP studies to be conducted to comprehensively investigate each stage in the life cycle of the virus as well as to develop vaccine and treatment agents against CCHFV and SARS-CoV-2, and the other highly pathogenic RNA viruses, as well.

1.2 Reverse Genetics of RNA Viruses

Many of the most serious human pathogens, like influenza A virus, poliovirus, rotaviruses, dengue virus, hepatitis C virus, West Nile fever virus, yellow fever virus, and measles virus are RNA viruses, causing millions of deaths [1]. RNA viruses have been identified in recent studies as the main etiological agents responsible for most human infections (ranging from 25% to 44% of diseases in different studies) [2-5]. Both the increased contact of humans with domestic animals and wild populations, brought on by globalization, as well as the high virulence and evolutionary plasticity of RNA viruses cause viruses to find new hosts. As seen with the emergence of Human Immunodeficiency Virus (HIV), H1N1 flu, highly pathogenic H5N1 avian influenza Nipah, Hendra, Ebola, and more recently COVID-19, RNA viruses have triggered a series of pandemics originating from wildlife reservoirs, increasing the concerns on public health. [15].

There are distinct types of RNA genomes seen in RNA viruses. Some contain a non-segmented genome, whereas others have many segments, such as 2 for arenaviruses, 3 for bunyaviruses, 7-8 for influenza viruses, and 10-12 for reoviruses. Furthermore, they can be single- or double-stranded, positive-sense, negative-sense, or ambisense RNA. Positive-sense RNAs can be translated directly into protein, whereas negative sense RNAs must first be transcribed by viral proteins into positive-stranded RNA before being translated. Ambisense RNAs encode genes that run in both directions within the same genome or genome segment. In addition, there are retroviruses and hepadnaviruses that undergo both RNA and DNA phases by reverse transcription of their RNA [1].

In general terminology, forward genetics refers to the investigation of the genetic basis of a phenotype, while reverse genetics refers to the study of the effect of genetic changes on the phenotype [16]. In the context of virology, reverse genetics refers to the generation of a virus entirely from cDNA [17]. By using reverse genetics, genetic modifications is introduced directly into the complementary DNA (cDNA) to generate infectious RNA virus or virus-like particles, in order to study the function of specific gene sequences and proteins [18]. The reverse genetics system is a revolutionary tool to study the life cycles of highly pathogenic viruses, escape routes from immune responses, virus-host interactions, as well as the generation of customized viruses that

can be used as vaccines or vectors. This system allows mutational analysis to determine the molecular basis of the entire life cycle, including transcription, replication, and packaging of highly pathogenic viruses under BSL-2 conditions. As the production of vaccines and antivirals against a highly pathogenic virus first requires characterizing its life cycle, the establishment of a robust method has a critical role in the investigation of the molecular mechanisms underlying the disease. However, working with highly pathogenic viruses requires a biosafety level 3 or 4 laboratory, which restricts the virological studies.

Generating an infectious virus, or "rescuing" the virus, from modified sequences is the best comprehensive method to investigate the functions of individual sequences in viral genomes. As DNA could be delivered directly into cells to express viral genes virus, first the infectious T2 bacteriophage was rescued from DNA as early as 1957 [19]. Then, infectious clones have been developed easily for a wide variety of positive-sense RNA viruses, since their genome acts as mRNA [20]. Unlike positive-sense RNA viruses, negative-sense RNA virus genomes are inherently noninfectious due to their complementary orientation to messenger RNA. The ability to manipulate RNA virus genomes by converting viral RNA to complementary DNA (cDNA) was made possible by the discovery of reverse transcriptase in the 1970s [21], and the first successful attempt was documented for bacteriophage Qβ in 1978 [22]. In order to start viral replication, an RNA-dependent RNA polymerase is needed to transcribe negative-sense viral RNA (vRNA) into positive-sense mRNA. Thus, scientists were faced with the issue of supplying not only the vRNA, but also the nucleoprotein and viral polymerase that make up the ribonucleoprotein (RNP) complex. Therefore, in reverse genetics applications of negative RNA viruses, transfection of subgenomic cDNA into suitable cells together with a helper virus or helper plasmids is frequently used, and all of them are either constitutively or temporarily controlled by an RNA-dependent-RNA-polymerase (RdRp) such as T7, host polymerase I (Pol I) and II (Pol II) [23].

Understanding the complete virus replication cycle requires the use of full-length clone systems, which make it possible to produce infectious recombinant viruses. On the other hand, life cycle modeling systems, such as minigenome and virus-like particle (VLP) systems, can be employed to simulate the virus life cycle under BSL-2 conditions. Replication and transcription of viral genomes are modeled using

minigenome systems, whereas morphogenesis, budding, and infection of target cells are mimicked using transcriptionally and replicationally competent virus-like particles. These modeling systems greatly help researchers to understand viral elements involved in virus biology and immunology, as well as to develop therapeutics and diagnostics [7].

In this thesis, VLPs were developed for two distinct RNA viruses that served various functions. By generating VLP for Crimean Congo Hemorrhagic Fever Virus (CCHFV), a negative sense single-stranded RNA virus, it was intended to establish a mammalian cell culture model that can be utilized to study virus biology, immunity, and pathogenesis. Furthermore, VLPs that potentially be vaccine candidates for Severe Acute Respiratory Syndrome Coronavirus 2 (SARS-CoV-2), a positive sense single-stranded virus, have been produced. Thus, the contribution of VLP studies to both basic and translational research has been demonstrated by the studies conducted in this thesis for these two highly pathogenic RNA viruses.

1.3 Generation of Virus Like Particles for a Negative Sense RNA Virus, Crimean Congo Hemorrhagic Fever Virus

1.3.1 Viral hemorrhagic fever

Hemorrhagic fever viruses (HFVs) are a group of 14 enveloped, single-stranded RNA viruses from four families: *Arenaviridae, Bunyaviridae*, *Filoviridae*, and *Flaviviridae*. The term "viral hemorrhagic fever" (VHF) describes an acute febrile hemorrhagic condition caused by these viruses that affect multiple organ systems of the body and impair the general circulatory system. The effects of VHFs might range from relatively mild to potentially fatal illnesses.

Even though VHFs can be caused by viruses from several different families, all these viruses have the following features in common. Even though VHFs can be caused by viruses from several different families, they have several features in common. All these viruses employ ribonucleic acid (RNA) as their genetic material, and as a result of their rapid evolutionary adaptation, RNA viruses are a leading cause of new infectious diseases in humans. They have a protective outer coating of lipoprotein, making them more vulnerable to physical (heat, sunshine, gamma rays) and chemical (bleach, detergents, solvents) methods of elimination. They occur naturally in animal or insect

populations, called host populations, and are limited to the host's geographic range. Contact with an infected animal or insect vector results in transmission to humans. VHF outbreaks in humans can be difficult to avoid because they occur intermittently and are difficult to forecast [24].

1.3.2 Crimean-Congo Hemorrhagic Fever Virus

Crimean-Congo hemorrhagic fever (CCHF) is a tick-borne viral hemorrhagic disease, caused by the Crimean-Congo Hemorrhagic Fever Virus (CCHF) and is prevalent in more than 30 countries across a wide geographical area spanning Africa, Asia, and Eurasia. In accordance with the quality of the health system, the death rate ranges from five to eighty percent [25]. In 2019, the World Health Organization (WHO) estimated that 3 billion people were at risk of contracting the disease because of the expanding transmission of the virus by *Hyalomma* ticks. As a direct consequence of this, the case mortality rates might potentially reach up to forty percent [9].

Due to its epidemic and public health emergency of international concern (PHEIC) potential and the lack of effective therapeutics or vaccines for human or animal use, CCHF is listed among priority diseases for research and development (R&D) in emergency contexts by WHO and National Institute of Allergy and Infectious Diseases (NIH/NIAID) [26, 27]. Since 11.041 cases were reported between 2002 and 2018, CCHFV has become a growing concern threatening the public health in Türkiye [8].

1.3.3 History

In the 12th century, a Persian physician by the name of Ismail Jorjani reported a hemorrhagic disease that was brought on by a louse or tick that was parasitizing a blackbird. He referred to the condition as "kara khalak" in his book, Zakhireye Khwarazmshahi, which was published at the time [28]. Khungribta (blood taking), khunymuny (nose bleeding), and karakhalak (black death) are some of the names that CCHF has been called in Uzbekistan over the years [29, 30]. In the 16th and 17th centuries, the term "black death" was used to describe to plague in European literature [31]. There are two historical precedents for the modern definition of CCHF. The Crimean Hemorrhagic Fever (CHF) was initially documented in 1944-1945 after approximately 200 Soviet soldiers contracted the disease in Crimea [32, 33]. Then, newborn white mice were used by Chumakov and colleagues in Moscow to isolate CHFV in 1967 [34, 35]. When the virus was successfully isolated from a patient

(Drozdov) in Astrakhan using this method, it was widely used as a model strain in laboratories around the world. In 1956, a virus causing hemorrhagic fever was isolated from a patient in Congo and scientists studying hemorrhagic fever viruses, found that both Congo and Crimean Viruses were antigenically indistinguishable from each other [36, 37]. Afterward this virus was referred to CHF–Congo virus, and then it was replaced with Crimean–Congo hemorrhagic fever virus [30].

1.3.4 Virus classification, structure, and genome

Crimean Congo Hemorrhagic Fever Virus was previously classified as a member of the *Bunyaviridae* family in the *Nairovirus* genus**.** However, better classification criteria based on comparative genomics and phylogenetic analyses have been established thanks to advances in bioinformatics and sequencing technologies. New "bunya-like" species with two or more than three genome segments were discovered due to metagenomic methods and later reclassified as members of the *Bunyaviridae* family [38-41]. Consequently, the International Committee on Taxonomy of Viruses (ICTV) reorganized the *Hantavirus, Nairovirus,* and *Tospovirus* genera into families in 2016, and designated the *Bunyaviridae* family as the *Bunyavirales* order, consisting of 12 families as follows: *Arenaviridae, Cruliviridae, Fimoviridae, Hantaviridae, Leishbuviridae, Mypoviridae, Nairoviridae, Peribunyaviridae, Phasmaviridae, Phenuivirid* [42, 43]. Crimean Congo Haemorrhagic Fever Virus is now classified as a member of the genus *Orthonairovirus* of the family Nairoviridae of the order *Bunyavirales.*

Like all members of the Nairoviridae family, CCHFV has a spherical, enveloped virion about 100 nm in diameter. The viral genome consists of three single-stranded negative-sense RNA molecules called L, M, and S segments that encode structural proteins such as RNA-dependent viral RNA polymerase, glycoproteins, and nucleoproteins, respectively (Figure 1.1). Each of the 3 segments contains a single open reading frame (ORF) and highly conserved non-coding terminal complementary sequences (UCUCAAAGA at 5 ends and AGAGUUUCU at 3 ends). The non-covalent interaction between both ends forms a panhandle-like structure that provides a functional promoter region for viral polymerase binding [44-47].

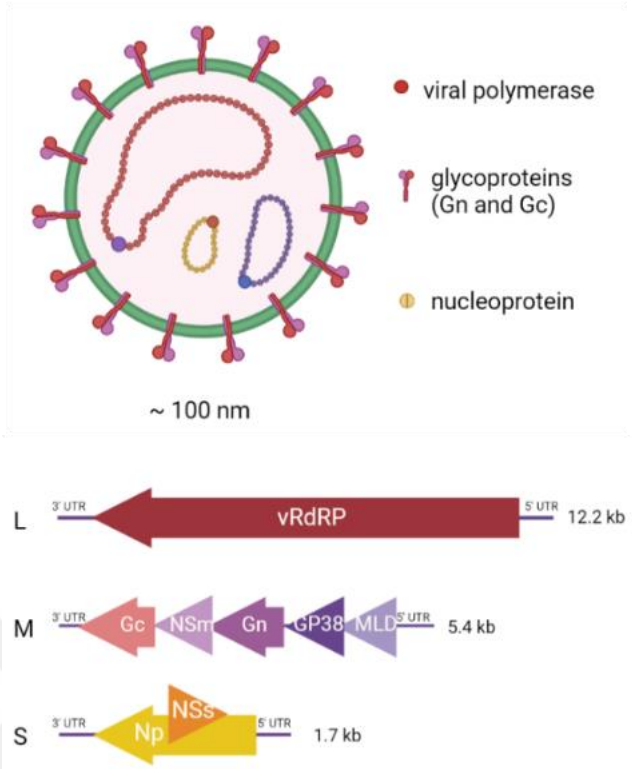

Figure 1.1 : Structure and genome organization of CCHFV. The virion is spherical and approximately 90-100 nm in diameter, consisting of three single stranded negative sense RNA genome segment encapsidated by nucleoproteins complexed with the viral RNA dependent RNA polymerase (vRdRp), which are surrounded by the lipid anchored glycoproteins (Gn and Gc). This figure is created with BioRender.com

1.3.4.1 L segment

The L segment of CCHFV is about 12.2 kb in length and encodes viral RNA-dependent RNA polymerase of 448 kDa. Genomic analysis revealed that the L segment also contains a zinc finger type C2H2 domain and a leucine zipper motif which is important for binding NP the N-terminal region of the L protein [48, 49] and a highly conserved ovarian tumor (OTU)-domain indicating that CCHFV L polyproteins may have a crucial role in viral immune evasion [50]. Viruses utilize this activity to overcome innate and adaptive cellular immunity at MHC class I and class II antigen presentation [51, 52], TLR/IL1 signaling [53], and generation of type I IFN by the cellular viral sensor retinoic acid-inducible gene I (RIG-I) [54, 55]. However, there were conflicting data in the literature about the function of the CCHFV L

segment OTU domain. Frias-Staheli et al. [53] reveal that the CCHFV L protein can deconjugate Ub and ISG-15 from cellular target proteins to evade the host's immune system [54]. In contrast, a minigenome replication experiment demonstrated that an OTU domain-containing CCHFV L protein does not exhibit autoproteolysis to generate additional protein products [56].

1.3.4.2 M Segment

The CCHFV M segment is about 5.4 kb in length and is translated into a single polypeptide of 225 kDa, then cleaved by the signal peptidase and post-transcriptionally modified in Golgi to form glycoproteins Gn (37 kDa) and Gc (75 kDa). The maturation of glycoproteins begins with cotranslational cleavage of polyprotein into the glycoprotein precursors PreGn (140 kDa) and PreGc (85 kDa), likely by signal peptidase [57, 58]. In the endoplasmic reticulum (ER)/cis-Golgi, the serine protease subtilisin-kexin isoenzyme-1/site-1-protease (SKI-1/S1P) cleaves Gn and Gc at their N termini [59, 60]. The mucin-GP38 domain is then cleaved by furin into GP38 and a mucin-like domain [57, 59, 60] (Figure 1.2). Mucin-like domains (MLD) are very variable and rich in serine, threonine, and proline amino acids; they are also strongly O glycosylated [61-63]. NSm protein is involved in CCHFV assembly and virion secretion due to an increased rate of protein trafficking through the secretory pathway with altered N-glycosylation profiles beneficial for efficient virus release, while GP85 is an essential viral factor for pre-Gc cleavage, trafficking, and Gc incorporation into particles [64].

Two glycoproteins, Gn and Gc, are embedded in the lipid bilayer of the viral envelope and are responsible for viral attachment and internalization into the host cell [65]. There is mutual dependence between the trans-Golgi secretion of Gn and Gc. The Gn is required for the transport of Gc from the ER to the Golgi due to the presence of a Golgi localization signal [66-68], and it also has a chaperone-like function for Gc folding [69]. Also, the cytoplasmic tail of Gn features a dual CCHC-type zinc finger motif, which might be responsible for viral genome packaging [44, 70]. The demonstration that only Gc-specific mAbs can eradicate the virus in vitro suggested that Gc is more important in adaptive immunity [66].

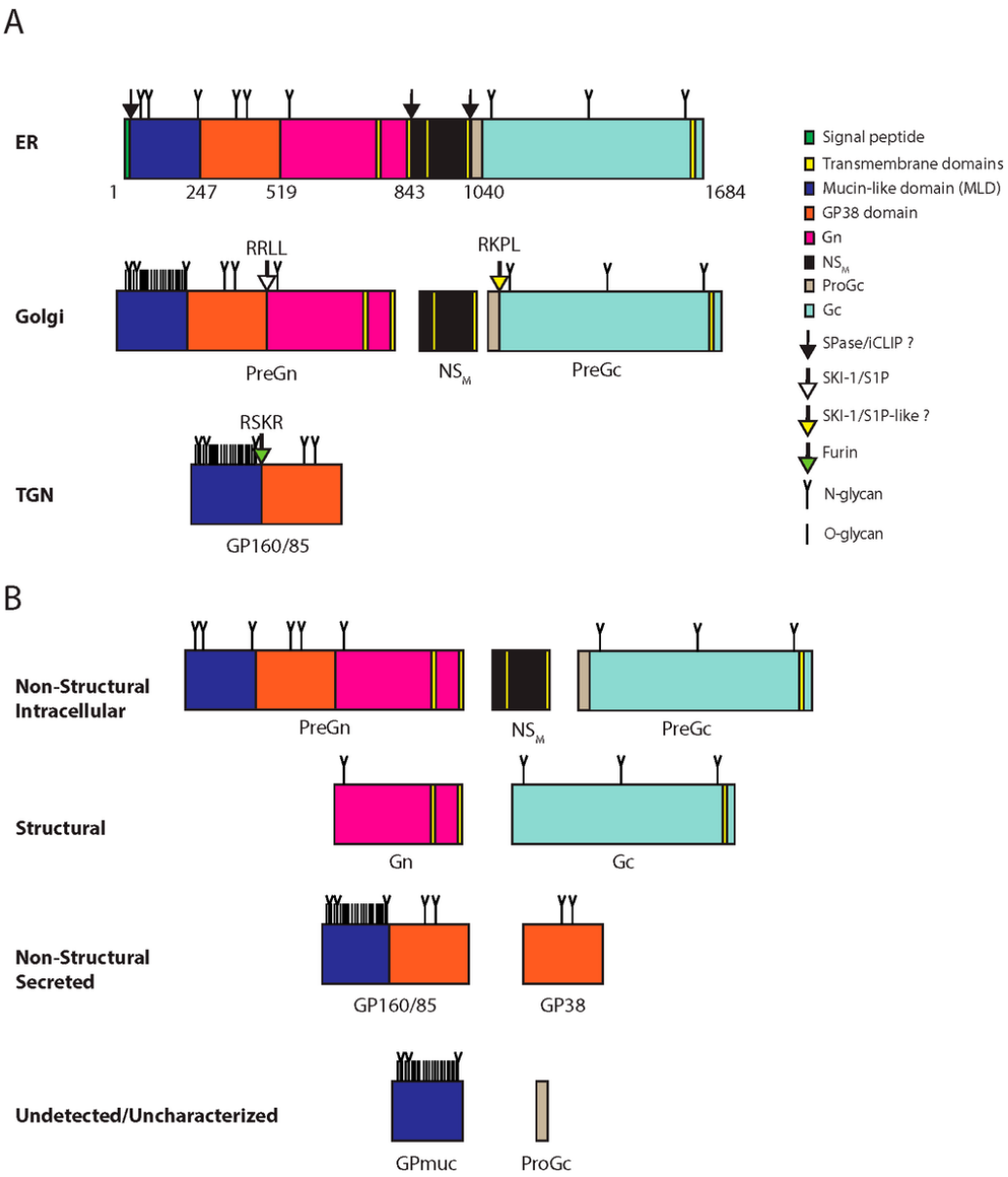

Figure 1.2 : Glycoproteins from CHF viruses, and their by-products. A) Processing of the CCHFV glycoproteins. First, GPC is expressed in the ER, where it is N-glycosylated (N-glycan). Positions of amino acids are marked by numbers. Transmembrane domains 2 and 4 of GPC are co-translationally cleaved by signal peptidase and/or intramembrane cleaving proteases. PreGn, PreGc, and NSM are produced as a result of these cleavages. The mucin-like domain of PreGn is O-glycosylated (O-glycan) in the Golgi, where it is cleaved at the RRLL motif by subtilisin kexin isozyme-1/site-1 protease (SKI-1/S1P). A protease with similar selectivity to SKI-1/SIP targets PreGc at the RKPL motif. PreGn cleavage releases an N-terminal fragment on SDS-PAGE that appears to have a total molecular weight of 160 kDa (GP160) and 85 kDa (GP85). Furin later cleaves GP160/85 in the trans-Golgi network (TGN). GPC products (B). By-products of GPC processing include intracellular (Non-structural), extracellular (Structural), secreted (Non-structural secreted), and inferred (uncharacterized) non-structural and structural component [71].

1.3.4.3 S Segment

The S segment is approximately 1.7 kb in length and encodes a 53 kDa nucleoprotein (NP). The NP structure consists of a globular domain and a prominent arm. Encapsulation of the viral segments by nucleoproteins (Np) by homo-oligomerization as pentamers and formation of a ribonucleoprotein complex together with RNA-dependent RNA polymerase (RdRp) are crucial for the initiation of viral replication and transcription in the host cell [44]. It is reported that when the caspase-3 cleavage site (DEVD motif on nucleoprotein) is disrupted during viral vRNA transcription, CCHFV polymerase activity is increased [72]. Also, a non-structural protein, NSs is encoded by the ambisense S segment. Little is known about the role of NSs in CCHFV. Inducing apoptosis by activating caspases through the permeabilization of the mitochondrial membrane is one of the reported effects of NSs [73].

All CCHFV strains share the conserved DEVD (a caspase-3 cleavage site) proteolytic cleavage site in the CCHFV nucleoprotein (Np), and recent findings showed that processing of the N protein causes a moderate effect on viral replication in mammalian cells, but while it inhibits CCHFV replication dramatically in tick cells when a mutation is introduced in the DEVD motif [74]. The DEVD motif could be the focus of an anti-infection strategy in ticks, which would help minimize the amount of time viruses are able to survive in the environment.

Actin is another molecule that Np interacts with, and this interaction allows Np to be localized around the nucleus [75]. Furthermore, it is known that viral protein interactions with actin filaments accelerate virus replication, as seen in paramyxoviruses such as Newcastle disease virus and Sendai virus [48, 76].

1.3.5 Virus life cycle

CCHFV infects host cells through its envelope glycoproteins Gn and Gc, which form a layered structure of heterodimers on the virus surface (Figure 1.3) [77-79]. It has been generally assumed, that GC is more directly involved in binding to cellular receptors and mediating fusion in endosomes. Even though the cellular receptors for CCHFV entry have not been discovered yet, Xiao and his colleagues have found that the 180-300 amino acid residues of Gc have a considerable receptor binding capability, and the human cell surface nucleolin can be a putative CCHFV host-cell receptor [80].

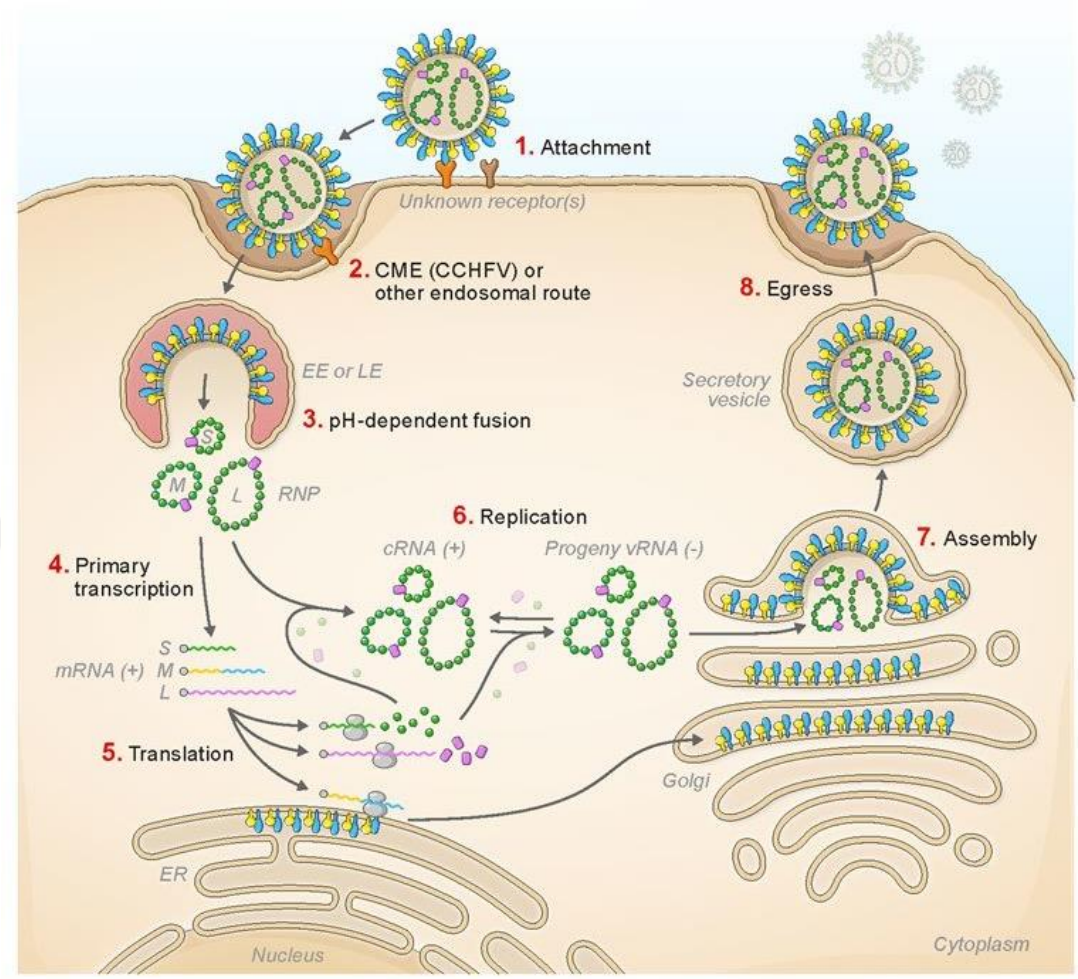

Figure 1.3 : Life cycle of nairoviruses. A) Viral attachment to surface receptor (unknown) B) Internalization through clathrin-dependent, receptor-mediated endocytosis. C) Fusion between the envelope and endosomal membranes by reduced pH in endosome D) Dissociation of the nucleocapsids and generation of mRNA and cRNA by RdRp. E) Translation of viral proteins and genomic vRNA production following new nucleocapsids formations. F) M polyprotein production in ER. G) Cleavage of polyprotein into Gn and Gc precursor forms transported to the Golgi complex H) Maturing process of glycoproteins, I) Formation of new virions. J) Virion egress [93].

Internalization of viruses occurs via clathrin- and cholesterol-dependent endocytosis, with the acidic environment of the endosome promoting dissociation of the Gn-Gc heterodimer, followed by a rearrangement of Gc into a trimer of hairpin structures to facilitate membrane fusion [81-85]. Within the first hour of infection, microtubules transport CCHFV to the cellular locations where viral transcription and replication occur [86]. Simon and colleagues discovered that virus internalization required intact microtubules and that depolymerization of microtubules inhibited progeny virus

generation. Replication begins with the synthesis of mRNA from negative sense viral RNA segment by viral polymerase in the cytoplasm [87]. Here NP plays a major role in viral replication. Encapsidation of viral RNA prevents degradation of viral RNA utilized as a template to synthesize both vRNA and capped mRNA, and interaction of NP with viral polymerase is requisite to initiate CCHFV viral replication [88]. Generally, all negative stranded RNA viruses utilize the same cap snatching mechanism for transcription through approximately 10-20 nt capped RNA fragments used as primers to start transcription of non-polyadenylated mRNA from the antisense viral RNA genome [72, 89-91]. The pentameric CCHFV NP undergoes a conformational change upon the introduction of these RNA primer sequences, resulting in the release of the free, monomeric NP. The naked vRNA is then exposed for replication or transcription, followed by the development of viral proteins [91]. Glycoproteins undergo processing and maturation in the endoplasmic reticulum (ER) and the Golgi, yielding the Gn and Gc, whereas nucleoproteins and viral polymerase are translated on free ribosomes in the cytoplasm. New CCHFV particles are thought to be assembled in the Golgi after the accumulation of nascent mature glycoproteins and genomic RNPs, followed by virion release in Golgi-derived vesicles [71]. Replication of CCHFV has been observed as early as 3 hours after infection and has been shown to peak at 24 hours [92].

1.3.6 Transmission

CCHFV is an arthropod-borne virus that causes zoonosis despite circulating in an enzootic tick–nonhuman vertebrate–tick cycle and manifesting simply as a transitory viremia [30, 44]. There are at least 31 tick species and one species of biting midge (*Culicoides* spp.) that have been identified as CCHFV reservoirs [30, 93, 94]. However, not all these reservoirs are capable of transmitting CCHFV. A blood meal from a viremic host is all that's needed to introduce the virus into a susceptible host [93]. *Hyalomma* ticks in the *Ixodidae* family are responsible for most of the CCHF transmission [95, 96]. The disease is transmitted primarily by *Hyalomma* ticks, and seven different tick species have been identified as vectors so far: *Hyalomma marginatum marginatum, Hyalomma marginatum rufipes, Hyalomma marginatum turanicum, Hyalomma anatolicum anatolicum, Dermacentor marginatus, Rhipicephalus rossicus, Amblyomma variegatum* [97]. *H. marginatum* is the most important vector for CCHFV [98] due to its widespread geographic distribution, which

extends over southern Europe, a portion of the Middle East, and Central Asia. This vector is often collected from humans and animals in endemic parts of Türkiye [99]. Transmission of CCHF occurs generally between tick and its vertebrate host in the endemic regions both transstadially (from larva to nymph and adult), and transovarially to progeny (and even in some cases to the F2 generation) [30].

Ticks of the family Ixodidae go through three distinct lifecycle stages, from larva to nymph to adult, with each stage characterized by a molt and a period of time spent feeding on a host, sometimes lasting weeks [100]. Hyalomma species have a two-host life cycle, in which they feed first on a small mammal as larvae and subsequently on non-human and/or human vertebrates as nymphs and adults (Figure 1.4) [101]. Even while CCHFV has been found in a wide variety of tick species, this does not suggest that all ticks can transmit the virus. Several parameters must be met for a tick to participate in the CCHFV tick-host-tick lifecycle. To spread the virus, the tick must pick up the virus during a blood meal. Additionally, the tick's cells must permit viral replication and transmission to another vertebrate host. Ticks only take a blood meal once throughout each of their developmental stages; therefore, the host must also retain infection through molting (horizontal transfer). Viruses can also be transovarially transmitted from one generation to the next (vertical transfer) or by adult males to females during copulation [44, 102-105]. Therefore, CCHFV infection is sustained via both horizontal and vertical paths.

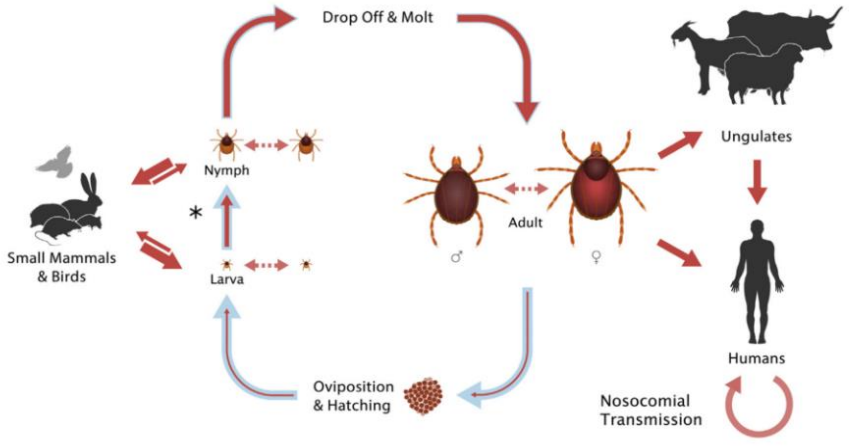

Figure 1.4 : Routes of CCHFV transmission. The transmission is marked by asterisks. Blue arrows indicate the course of the tick life cycle, while dashed arrows indicate virus spread through co-feeding. Then adult ticks take blood from large animal and after copulation virus is transmitted to eggs. Viruses can be transmitted to human by a contact with either infected animals or humans (solid red arrows). The thickness of the red arrow indicates the efficiency of transmission [106].

Tick vectors can function as a reservoir for CCHFV by the virtue of enabling asymptomatic CCHFV infection during the tick's lifecycle and allowing the virus to survive at low temperatures over winter. Even after 10 months at 4°C, *H. marginatum* was able to infect a vertebrate host and spread the virus [107]. The transmission of CCHFV exhibits a seasonal pattern, peaking mainly between May and September. The virus replicates in different host tissues, reaching the highest titers in the salivary glands and reproductive organs during the metamorphosis of ticks feeding on the host [108].

Ticks use a variety of hosts during their life cycle, but humans refer only as dead-end hosts. They are occasionally bitten by infected ticks in the enzootic areas, causing CCHF in humans. Vertebrate hosts other than humans simply suffer merely asymptomatic transitory viremia after infection. The risk of getting CCHFV is highest in people who work with or around cattle, including farmers, livestock owners and herders, abattoir employees, and veterinarians [109-112]. Direct contact with body fluids or contaminated medical equipment are the main reason for nosocomial infections and contact with tissues or fluids of a viremic animal during slaughtering is another route of transmission to humans. Occasionally, sexually transmitted cases are reported in the literature, but these cases are extremely rare [44, 113].

1.3.7 Epidemiology

As the most common tick-borne viral disease in humans, Crimean-Congo hemorrhagic fever (CCHF) is an increasing global public health threat. WHO has estimated that three billion people are at risk of contracting the disease and has identified CCHF as a priority disease for research and development due to its potential to cause major outbreaks with high fatality rates and the absence of any approved vaccines or treatments [114]. CCHF causes sporadic outbreaks with mortality rates ranging from 5 to 80% in humans [115]. Until now, virus isolation and/or disease have been reported from more than 30 countries: Africa (Democratic Republic of Congo, Uganda, Mauritania, Nigeria, South Africa, Senegal, Sudan), Asia (China, Kazakhstan, Tajikistan, Uzbekistan, Afghanistan, Pakistan, India), Europe (Russia, Bulgaria, Kosovo, Türkiye, Greece, Spain), and the Middle East (Iraq, Iran, Kuwait, Saudi Arabia, Oman, United Arab Emirates (UAE) [116].

Long-distance transmission of the CCHFV may occur through imported livestock [117] or by the movement of vectors carried by migrating birds from endemic regions. The annual spring migration of birds from southern Europe and Africa is thought to carry hundreds of thousands of *Hyalomma* ticks into or across Central Europe [118]. If enough vulnerable hosts and vectors are present, the virus may spread to a new location. Climate change, socioeconomic and anthropogenic variables may contribute to viral transmission and subsequent increases in reported cases [115, 119].

During the past twenty years, there has been a significant rise in the number of cases of CCHF in south-eastern Europe and in countries surrounding the Black Sea, like Georgia, south-western Russia, Türkiye, and Ukraine [120]. Since the first cases were reported in Türkiye in 2002, a total of 11.041 confirmed cases have been documented, with 528 deaths (4.78%) until 2018 [8].

1.3.8 Clinic manifestations and treatments

The severity of CCHF in people may vary from mild illness to one that is severe and fatal. After the incubation period typically ranges from 3-7 days followed by a tick bite, symptoms including high fever, headache, myalgia, vomiting, nausea, diarrhea and dizziness were observed usually in the prehemorrhagic stage during the first week after infection [30, 93, 109, 111, 121-123]. In most cases, the hemorrhagic phase starts between days three and five, and lasts for a couple of days [124]. In addition to gastrointestinal, gingival, cerebral, vaginal, abdominal, and urinary tract bleeding, common hemorrhagic symptoms like petechiae, conjunctivitis, and extensive cutaneous ecchymoses were reported [123]. After two weeks, severe bleeding, multi-organ dysfunction, and shock leads to the death of patients [44]. If patients can recover from CCHF, the convalescence phase typically lasts between 10 and 20 days [123]. However, the effects of the disease may remain for up to a year.

As there is currently no approved vaccine or medicine for CCHF, the primary focus of therapy is on providing patients with supportive care, involving fluid and electrolyte balance, oxygenation and hemodynamic support, and the treatment of secondary infections [125].

Ribavirin, an antiviral medication, has been shown to be effective against the virus when tested in vitro. It has been shown to limit CCHFV replication in a minigenome system [56], in virus-infected cells [126-128] in newborn mice [129], and in signal

transducer and activator of transcription 1 (STAT-1) knockout (KO) mice [130]. There was a dose-response relationship between these effects seen in vivo and in vitro [44]. Despite a lack of convincing data, detailed evaluations of ribavirin treatment showed that ribavirin is useful in CCHFV infections [131, 132].

In addition, a wide variety of immunotherapy strategies that have shown promise in treating CCHF have been documented. Intravenous immunoglobulin (IVIG) is an example of an antibody used in immunotherapy because of its anti-inflammatory effects. In addition to polyclonal and polyclonal IgG antibodies, monoclonal antibodies, which can either neutralize or not neutralize, are also available. Neutralizing antibodies like 11E7, 30F7, 8A1, 13G8 restrict the virus entry into the cell. Also, cytokine treatment like interferon 1 has been shown to stimulate ISGs, antiviral mechanisms, and to decrease virus loading. Corticosteroid medicines such as dexamethasone and methylprednisolone, which can be administered alone or in conjunction with other therapies, are another option, used in the clinic. Together, these therapies can significantly reduce the severity and fatality of the disease [133].

1.3.9 Reverse genetic applications for CCHFV

While investigations of the viral life cycle and pathogenesis have been hampered by the necessity to handle highly pathogenic bunyaviruses in high biosafety laboratories, reverse genetics systems have aided researchers in conducting these studies in lower biosafety laboratories such as BSL-2 (Figure 1.5). The minigenome and VLP systems are two of the experimental systems, designed to simulate virus partial life cycles. These models allow for the analysis of viral invasion, viral genome replication, transcription, ribonucleoprotein assembly, virion packaging, and budding activities (Table 1.1). The use of reverse genetic systems together with animal models (in mice and non-human primates) allows the examination and detection of host and viral factors that contribute to the pathogenesis of CCHF. Thus, reverse genetics techniques enable a deeper understanding of bunyaviruses and the development of vaccines as well as antiviral therapies [134].

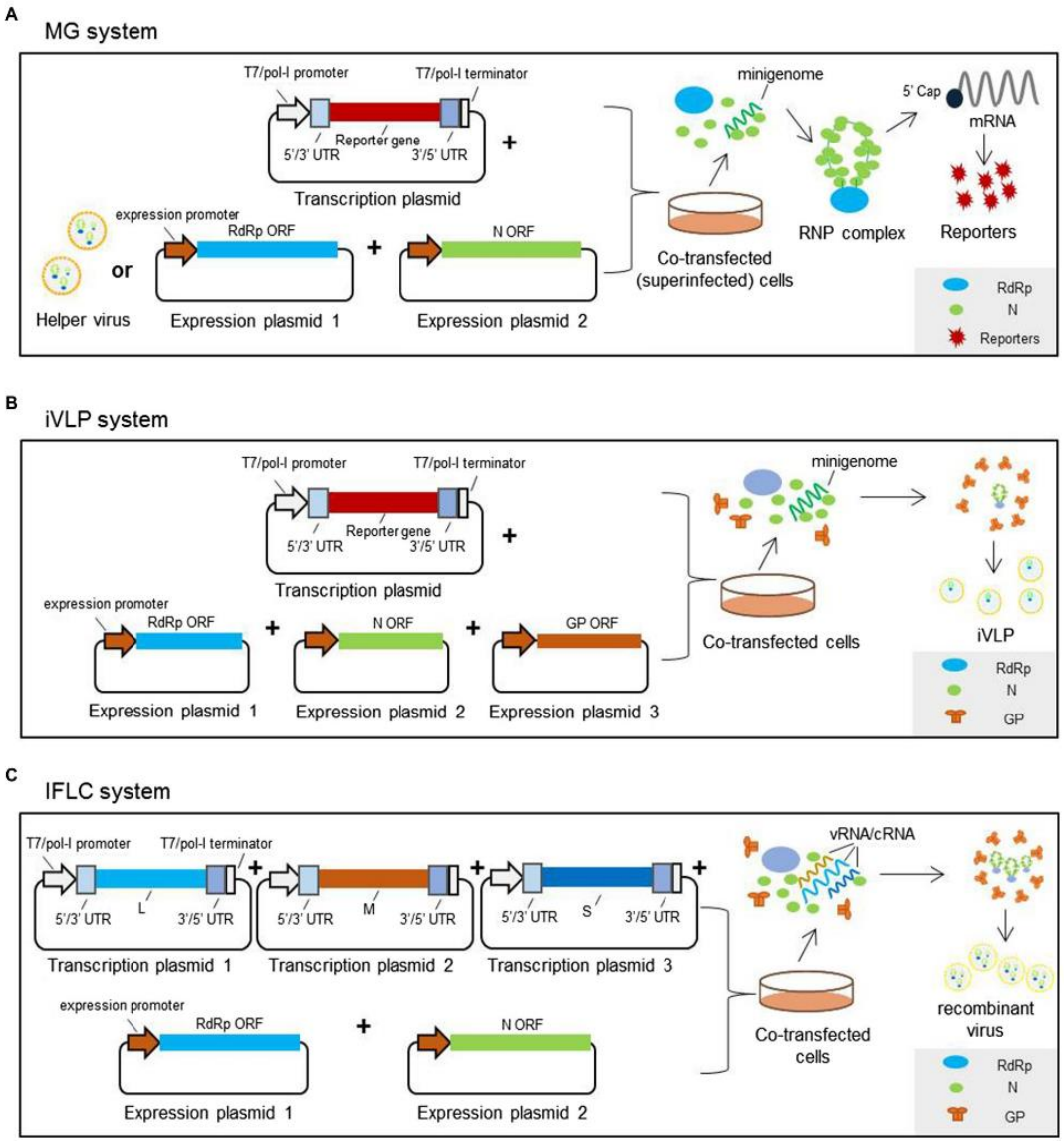

Figure 1.5 : Schematic representation of reverse genetic systems used for tri-segmented bunyaviruses. (A) A plasmid-based minigenome system is constituted by transfection of expression plasmids encoding RdRp and N, and T7 or pol-I plasmids, transcribing the virus-like RNA genome. The RdRp and NP proteins that make up the ribonucleoprotein complex are either supplied by expression plasmids containing only the ORF portions of the genes of interest or by the helper virus so that reporter proteins are expressed.(B) The infectious virus-like particle (iVLP) system is obtained by providing the expression plasmids encoding viral glycoproteins in trans in addition to the minigenome system. (C) In the infectious full-length clone (IFLC) system, cells are transfected together with plasmids that contain full-length antigenomic or genomic L, M, and S segment sequences, together with plasmids that encode proteins that form ribonucleoprotein complexes to form infectious virions[128].

Establishing an in vitro infection model such as virus-like particles through advanced molecular techniques will greatly help us to understand the life cycle of CCHFV within the cell and the relationship of viral proteins with each other. Several cell culture

models have been developed using reverse genetics methods for the *Bunyaviridae* family, including the Crimean Congo Hemorrhagic Fever Virus. First, in 1996, infectious *Bunyamwera* virus particles were generated in vitro by the transformation of only the plasmids carrying viral segments into cells, without the need for helper viruses [135]. Subsequently, different minigenome systems, developed by the replacement of the sequences encoding viral proteins with reporter genes paved the way for studies on viral transcription, replication, and packaging without the generation of any infectious viruses [136-143]. However, a complete rescue system or a non-infectious virus-like particle (VLP) system is required to examine the relationship of viral proteins to surface receptors that allow the virus to enter the host cell, viral genome encapsidation, and structural components involved in mature viral particle formation [144-147]. Because the entry of virus-like particles into the host cell, their interaction with intracellular proteins, and their budding are often similar to wild-type viruses, VLP systems allow pathogenic viruses to be studied under lower biosafety conditions [146, 148-154].

Table 1.1 : Reverse genetics studies conducted for CCHFV

Year	Title	System	Promoter	Research topic	Referrence
2022	Comparison of Crimean-Congo Hemorrhagic Fever Virus and Aigai Virus in Life Cycle Modeling Systems Reveals a Difference in L Protein Activity	tc-VLP and MG	T7	viral determinants of pathogenicity	Picken et al. [155]
2022	A screen of FDA-approved drugs with minigenome identified tigecycline as an antiviral targeting nucleoprotein of Crimean-Congo hemorrhagic fever virus	MG	T7	screening of FDA-approved compounds as an antiviral effect	Hirano et al. [156]
2020	A single mutation in Crimean-Congo hemorrhagic fever virus discovered in ticks impairs infectivity in human cells	MG VLP IFLC	T7	Zoonotic spillover effect due to a variation in the glycoprotein amino acid sequence of CCHFV	Hua et al. [157]
2020	Characterization and applications of a Crimean-Congo hemorrhagic fever virus nucleoprotein-specific Affimer: Inhibitory effects in viral replication and development of colorimetric diagnostic tests	MG	T7	viral replication and therapeutic and diagnostic applications of Affimers against CCHV	Álvarez-Rodríguez et al. [158]
2020	The interplays between Crimean-Congo hemorrhagic fever virus (CCHFV) M segment-encoded accessory proteins and structural proteins promote virus assembly and infectivity	tc-VLP and MG	T7	virus assembly and infectivity	Freites et al. [159]
2020	The Crimean-Congo Hemorrhagic Fever Virus NSm Protein is Dispensable for Growth In Vitro and Disease in Ifnar-/- Mice	IFLC and MG	T7	viral replication and pathogenesis	Welch et al. [160]
2017	Identification of broadly neutralizing monoclonal antibodies against Crimean-Congo hemorrhagic fever virus	tec-VLP and MG	T7	screening neutralizing MAbs against multiple CCHFV strains	Zivcec et al. [161]

Table 1.1 (continued): Reverse genetics studies conducted for CCHFV

Year	Title	System	Promoter	Research topic	Referrence
2017	Immunization with DNA Plasmids Coding for Crimean-Congo Hemorrhagic Fever Virus Capsid and Envelope Proteins and/or Virus-Like Particles Induces Protection and Survival in Challenged Mice	tc-VLP and MG	T7	comparation of vaccine candidate	Hinkula et al. [162]
2017	Crimean-Congo Hemorrhagic Fever Virus Suppresses Innate Immune Responses via a Ubiquitin and ISG15 Specific Protease	IFLC, tc-VLP and MG	T7	viral replication and antiviral response	Scholte et al. [163]
2015	Recovery of Recombinant Crimean Congo Hemorrhagic Fever Virus Reveals a Function for Non-structural Glycoproteins Cleavage by Furin	IFLC and MG	T7	viral glycoprotein processing and virion assembly	Bergeron et al. [164]
2015	A virus-like particle system identifies the endonuclease domain of Crimean-Congo hemorrhagic fever virus	tc-VLP and MG	T7	virus biology	Devignot et al. [89]
2013	Mini-genome rescue of Crimean-Congo hemorrhagic fever virus and research into the evolutionary patterns of its untranslated regions	MG	Pol-I and T7	virus replication and regulatory effects of UTRs on transcription	Zhao et al. [165]
2012	Structure, function, and evolution of the Crimean-Congo hemorrhagic fever virus nucleocapsid protein	MG	T7	NP structure domains involved in RNA-binding and oligomerization	Carter et al. [166]
2010	Crimean-Congo hemorrhagic fever virus-encoded ovarian tumor protease activity is dispensable for virus RNA polymerase function	MG	Pol-I and T7	Functional analysis of selected N protein residues	Bergeron et al. [167]
2003	Reverse genetics for crimean-congo hemorrhagic fever virus	IFLC and MG	Pol-I	First reverse genetic application on CCHFV	Flick et al. [139]

1.4 Generation of Virus Like Particles for a Positive Sense RNA Virus, Severe Acute Respiratory Syndrome Coronavirus 2

1.4.1 Coronaviruses and COVID-19

Coronaviruses are a large virus family that causes infections in both humans and animals such as bats, camels, cats, dogs, sheep, goats, cattle, pangolins, and civets, which can cause respiratory, enteric, hepatic, and neurological diseases of varying severity. In 1964, a Scottish virologist named June Almeida examined a sample of human nasal secretions under an electron microscope and gave the viruses the name coronaviruses because of the crown-like structure surrounding them [168, 169]. After that, human coronaviruses such as OC43, HKU1, 229E, and NL63 were identified and circulate in the population as the third most common cause of community-acquired upper respiratory tract infection. Until the turn of the millennium, coronaviruses were considered pathogens associated with only mild infections in the respiratory and gastrointestinal systems [170]. However, epidemics like that of SARS in 2002 and Middle East respiratory syndrome (MERS) in 2012 with fatality of 10% and 35%, respectively have revealed the potential of coronaviruses to cause serious illness in humans [171]. At the end of 2019, a series of highly contagious cases of severe pneumonia of unknown origin emerged in the Chinese city of Wuhan. The patients exhibited symptoms like fever, cough, dyspnea, myalgia, fatigue, anosmia, ageusia, headache, hemoptysis, and lymphopenia [172]. Thanks to modern advances in molecular biology, the viral agent underlying this condition were identified within one month after the first case and called SARS-CoV-2 due to its 79.6% sequence similarity to SARS-CoV [173]. Due to its high rate of transmission, it has caused a pandemic known as "coronavirus disease 2019" (COVID-19) within a few months, which poses a serious global threat to human health and public safety.

1.4.2 Epidemiology and transmission

World Health Organization has declared a pandemic in March 2020, with an exceeding number of 661 million cases and 6.69 million fatalities have been documented so far in 215 countries and territories [12]. In some seroprevalence studies, serum antibody titers in the United States and Europe have been interpreted to indicate that the number of people infected with SARS-CoV-2 is at least ten times higher than the number of

confirmed cases [174]. In many countries around the world, non-drug interventions such as lockdowns (including stay-at-home orders, curfews, quarantines, security cordons, and similar societal restrictions) have been implemented at various intervals for nearly two years to prevent SARS-CoV-2 transmission. Initially, it was reported that most of the patients visited the Huanan seafood market in China, but the issues regarding the origin of SARS-CoV-2 and its mode of transmission to humans are still unclear [175-181]. A wide variety of insectivorous bats belonging to the genus Rhinolophus have been studied as potential reservoirs and/or intermediate hosts of the virus since its emergence. Several studies have also implicated pangolins, minks, turtles, snakes, and even domestic animals as potential intermediate hosts for the spread of this disease [182-185]. The SARS-CoV-2 has undergone sporadic mutations and recombination events, some of which correspond to gains in fitness that have allowed the virus to spread more widely, or to escape neutralizing antibodies [186, 187]. Viral transmission between humans is thought to occur directly via respiratory particles released from coughs, sneezes, or talks of infected patients. Despite touching contaminated surfaces is not regarded as a primary route of transmission, the infection may arise indirectly through mucosal portals of entry [174]. The detection of viral RNA in related samples raises concerns about fecal-oral transmission, as well as vertical and sexual transmission, however, these modes of transmission have not been clearly proven yet [188].

1.4.3 SARS-CoV-2 phylogeny and molecular biology

The term "Coronaviruses" is referred to all viruses in the subfamily *Orthocoronavirinae* of the family *Co*ronaviridae. *Orthocoronavirinae* is divided into four genera, called *Alphacoronavirus, Betacoronavirus, Gammacoronavirus*, and *Deltacoronavirus*. The etiologic agent of COVID-19, SARS-CoV-2 is a member of the subgenus *Sarbecovirus* within the genus *Betacoronavirus*, which also includes SARS-CoV and MERS-CoV [189].

SARS-CoV-2 is an enveloped, positive sense single-stranded RNA virus, encoding a set of open reading frames (ORFs). Virus particles show a polymorphic structure with a diameter ranging from 60 to 140 nm [190]. Among the RNA viruses, the viruses with the longest genome are coronaviruses, and the genome of SARS-CoV-2 is about 30 kb. About two-thirds of the viral genome encodes the 21,291 bp long polyprotein, ORF

1a and 1b replicase/transcriptase [191]. However, due to overlapping open reading frames, viral proteases encoded in this region process polyproteins, resulting in 16 different non-structural proteins [191]. Downstream of this region, there are four genes, encoding the structural proteins S, M, N, and E [192] (Figure 1.6).

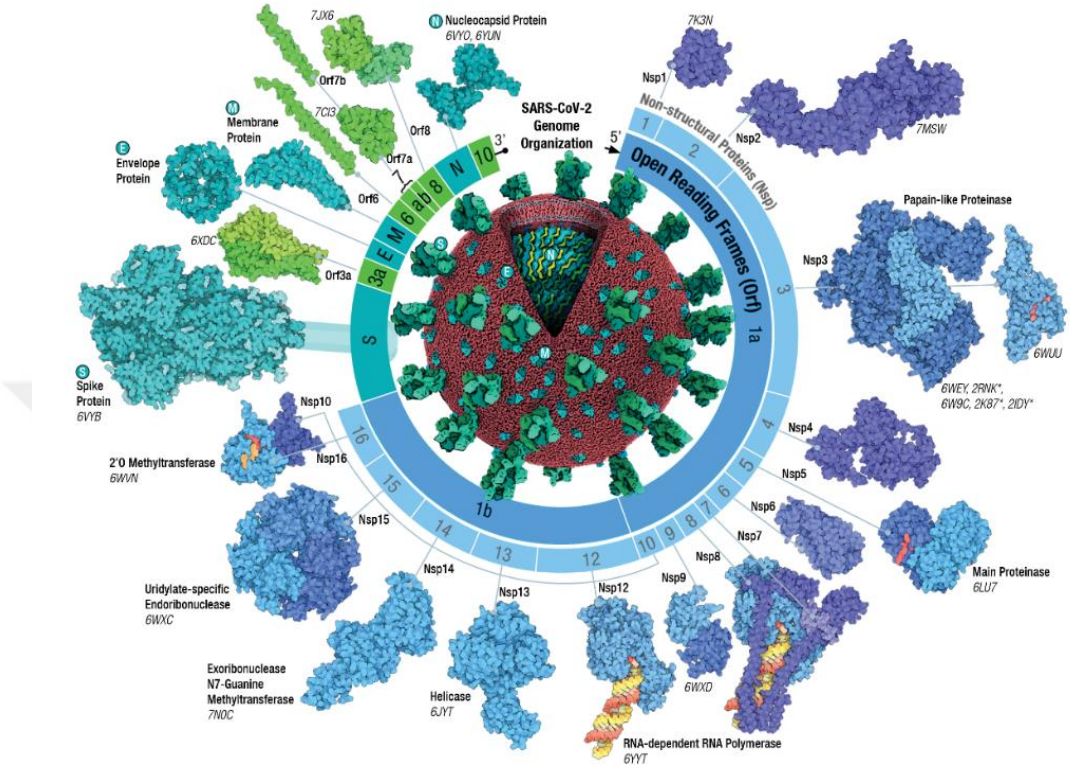

Figure 1.6 : SARS-CoV-2 Genome and Proteins [187].

The E protein has ion channel activity and is thought to be important in the formation of the mature virus particle [193]. Phosphorylated N protein binds to positive-sense viral RNA with high affinity. It also interacts with the M protein and nsp3, helping to package the viral genome into viral particles [194]. The M protein in dimer form is found abundantly in the virion and helps to maintain membrane curvature by binding to the nucleocapsid [194]. The S protein, which is found as a trimer on the virus surface, is a class I fusion protein that mediates the binding of the virus to the angiotensin-converting enzyme 2 (ACE2) receptors on the cell surface and then its uptake into endosomes.

SARS-CoV-2 utilizes two different mechanisms to enter the host cell, either by proteolytic cleavage of spike protein or by endocytosis. Furin cleavage of the polybasic region (RRAR) at the junction of the S1 and S2 subunits, which is common in betacoronaviruses other than sarbecoviruses. Then, S2' cleavage site (PSKR) within the S2 domain is cleaved by the transmembrane serine protease 2 (TMPRSS2), which

is widely expressed in epithelial cells lining the respiratory, gastrointestinal, and urogenital tracts. Membrane fusion is then triggered, and the viral DNA is released into the cytoplasm [195]. Alternatively, SARS-CoV-2 can enter cells through endocytosis. Cathepsin L (CatL), a cysteine protease can mediate the pH-dependent cleavage of the spike in the endosome [196]. According to a recent study, the licensed influenza drug amantadine inhibits CatL and protects against SARS-CoV-2 infection in vivo [197, 198]. The furin protease of the host cell cleaves the S protein into two separate polypeptides called S1 and S2, triggering viral fusion. Thus, viral RNA is released into the cytosol [193].

From the negative-stranded genomic RNA, a set of subgenomic mRNAs is transcribed, each containing a leader sequence derived from the 5'-end of the genome, encoding viral proteins. This unique mechanism, involving viral polymerase jumping from one part of the genome template to another, enables the truncated transcription of the genome. This replication ability causes high recombination, leading to evolutionary development and the prominence of coronaviruses in interspecies infections [199]. One of other important features specific to coronaviruses regarding transcription and replication is their proofreading exoribonuclease activity [200]. Besides, it has been demonstrated that the nsp14 protein has proofreading activity, therefore plays important role in controlling virus evolution [200]. Following replication and subgenomic RNA synthesis, viral structural proteins S, E, and M are transported to the endoplasmic reticulum, then to the ER-Golgi intermediate compartment, where the RNA genome is encapsidated by the nucleoprotein to form virus particles. Then, virions are transported to the cell surface and leave the cell by exocytosis (Figure 1.7) [190].

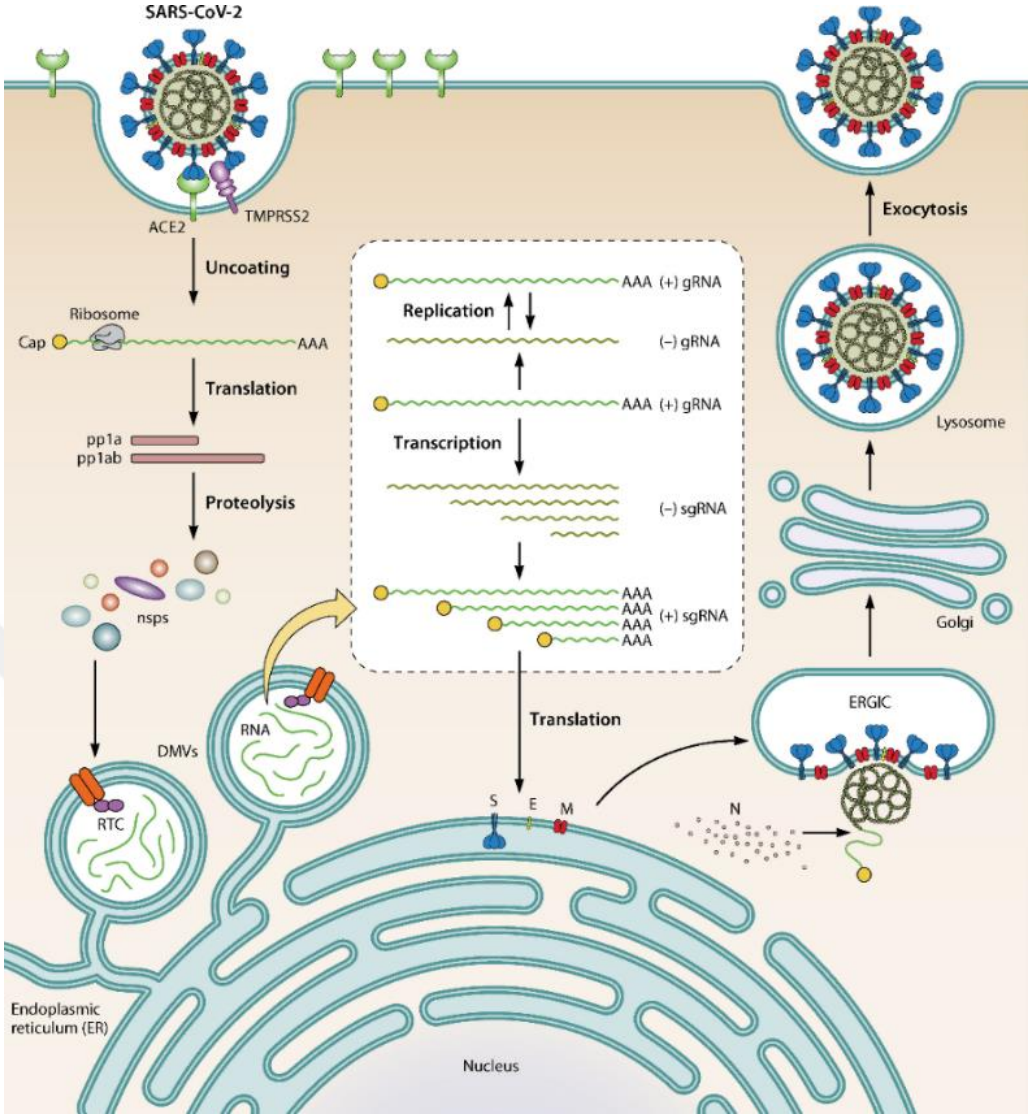

Figure 1.7 : SARS-CoV-2 life cycle. SARS-CoV-2 interacts with the ACE2 receptor, and the spike (S) protein is cleaved by TMPRSS2, after which fusion between the viral and host membranes occurs. SARS-CoV-2 can also enter host cells by endocytosis, and the S protein is then activated by endosomal cathepsins. After the viral (+) ssRNA genome is released into the host cytoplasm, it is translated and produces the polyproteins pp1a and pp1ab, which are autoproteolytically processed into the nonstructural proteins nsp1 to -16. The nsps assemble the coronavirus replicase-transcriptase complex (RTC) and remodel the membranes to form organelles for viral RNA synthesis. Viral replication and transcription occur in double-membrane vesicles (DMVs) derived from the ER. Newly synthesized viral genomic RNA is exported from the DMV interior via the pore channel and is then encapsidated by the nucleocapsid (N) protein. The nested transcribed subgenomic RNAs (sgRNAs) are translated into the structural proteins S, envelope (E), membrane (M), and N and accessory proteins. S, E, and M are anchored to the ER membrane and migrate to the virion assembly site known as the endoplasmic reticulum-Golgi intermediate compartment (ERGIC). The viral ribonucleoprotein (vRNP) complexes migrate to the ERGIC and bud into the lumen. The enveloped virion is then released from the cells via lysosomes [185].

1.4.4 Clinical manifestations, vaccines, and treatments

The pathogenesis of SARS-CoV-2-driven pneumonia is described in two phases; the early phase is identified by virus-mediated tissue damage after infection, while the late phase is characterized by the recruitment of T lymphocytes, monocytes, and neutrophils which releases cytokines such as tumor necrosis factor-α (TNF α), granulocyte-macrophage colony-stimulating factor (GM-CSF), interleukin-1 (IL-1), interleukin-6 (IL-6),), IL-1β, IL-8, IL-12 and interferon (IFN)-γ. Overactivation of the immune system that occurs in severe COVID-19 leads to a "cytokine storm," releasing large amounts of cytokines, particularly IL-6 and TNF-, into the blood, which leads to a local as well as a systemic inflammatory response [201, 202]. SARS-CoV-2, as previously said, primarily affects the respiratory system, but it can also negatively affect other critical metabolic functions in the gastrointestinal tract (GI), hepatobiliary, cardiovascular, renal, and central nervous systems. Direct viral toxicity, ischemia injury brought on by vasculitis, thrombosis, or thrombo-inflammation, immunological dysregulation, and renin-angiotensin-aldosterone system (RAAS) dysregulation may all contribute to the SARS-CoV-2-induced organ dysfunction [203].

The studies to develop a vaccine against COVID-19 was launched at an unprecedented rate as soon as the viral genome was sequenced. To date, there are 172 vaccine candidates in human clinical trials and more than 192 candidates in preclinical development worldwide according to a report by WHO in October 2022 [13]. Vaccines with varying levels of effectiveness have been designed using a variety of approaches. Due to the important role of the spike protein in the virus entry mechanism, critical parts such as the whole protein or the receptor binding domain (RBD) have been used as the main target antigen in vaccine design [204]. The use of twelve vaccine candidates that are now undergoing clinical testing has been authorized by several national regulatory agencies. The Novavax vaccine (NVX-CoV2373) was the first protein-based vaccine authorized by the European Medicines Agency (EMA), with an effectiveness rate of 89.7% [205]. MVC-COV1901, a recombinant protein vaccine created by Medigen Vaccine Biologics (Taipei, Taiwan) with an effectiveness rate of 80% to 90%, is the first COVID-19 vaccine to be approved for emergency use by Taiwan's Food and Drug Administration [206, 207]. The mRNA-based COVID-19 vaccines were revolutionized vaccine studies, as they are the first RNA vaccines

approved for clinical use The mRNA-based COVID-19 vaccines, revolutionized vaccine studies, as they are the first RNA vaccines approved for clinical use. The first of these vaccines, BNT162b2 from Pfizer-BioNTech, was approved by the WHO, then Moderna's mRNA-1273 received a second approval from the FDA for its use in emergency. The effectiveness of the mRNA vaccines to prevent covid-19 associated hospital admissions for two vaccine doses was 85% against the alpha and the delta variants, and 65% against the omicron variant while, three doses were found effective to prevent severe disease 94% against the delta variant and 86% against the omicron variant [208]. Three different adenoviral vector-based COVID-19 vaccines became prominent in clinical trials. The EMA has conditionally authorized for emergency use the ChAdOx1 nCoV-19 vaccine (AstraZeneca), which expresses the S protein with the tPA leader peptide. The EMA has conditionally authorized for emergency use the ChAdOx1 nCoV-19 vaccine (AstraZeneca), which expresses the S protein with the tPA leader peptide, while the FDA approved it. The Janssen COVID-19 vaccine (Ad26.COV2.S) expressing stabilized S protein. Additionally, The Gamaleya Research Institute in Russia used a heterologous prime-boost technique using Ad26 and Ad5 for the Sputnik V vaccine, utilizing the full-length S protein and its use was approved in more than 70 countries. The Covifenz (by Medicago), composed of recombinant spike (S) glycoprotein is the solely approved VLP-based vaccine for COVID-19 [207]. Almost half of all vaccines administered against COVID-19 worldwide consist of inactivated vaccines [209]. CoronaVac (Sinovac, China), Covaxin (Bharat Biotech, India) and Inactivated COVID-19 Vaccine (Vero Cell) (Beijing Institute of Biological Products, China) are authorized by WHO for use in emergency [210]. According to an interim analysis of the phase III study in Türkiye, the CoronaVac has a vaccine efficacy of 83.5% for the prevention of severe disease [211]. TURKOVAC (Koçak Farma, Türkiye) is another inactivated vaccine developed in Türkiye [212] and according to a recent study, TURKOVAC reduces the risk of developing COVID-19 by 49.29% compared to CoronaVac [213].

2. MATERIAL and METHODS

2.1 Generation of CCHFV VLP

2.1.1 Cell culture and virus

Baby hamster kidney-21 (BHK-21), human embryonic kidney cells (HEK293T), and african green monkey kidney epithelial cells (Vero E6) and human were grown at 37°C with 5% CO_2 in Dulbecco's modified Eagle's medium (DMEM) (Gibco™, ThermoFisher Scientific, USA), supplemented with 10% fetal bovine serum (Gibco™, ThermoFisher Scientific, USA), 100 units/ml penicillin and streptomycin (Gibco™, ThermoFisher Scientific, USA).

The formalin-inactivated PEG precipitated Crimean Congo Hemorrhagic Fever Virus Kelkit06 strain was donated by Prof. Aykut Özdarendeli, Erciyes University. The virus, employed in this thesis has been originally isolated from a serum sample of a patient from Kelkit Valley in Türkiye [30]. Briefly, all procedures with live viruses were carried out in a BSL-3 (+) Lab of Erciyes University Vaccine Research and Development Application and Research Center, Türkiye. Viruses were propagated in Vero E6 cells. Three days after infection, the viral particles, secreted into culture media were purified by using sucrose gradient ultracentrifugation and inactivated by treatment with 0.05% formaldehyde for three hours at room temperature. The formaldehyde was then removed by dialysis with phosphate-buffered saline (PBS) using a dialysis cassette with a 20K MWCO (Millipore, Bedford, MA). The protein concentration of inactivated virus was determined using the Lowry Protein Assay Kit (Thermo Fisher Scientific, Waltham, USA).

2.1.2 Antibodies and sera

Mouse monoclonal antibodies targeting CCHFV strain Ibar10200 anti-PreGn/GP38 (clones 8F10), anti-PreGc (clone 11E7), and anti-NP (clone 9D5) and were obtained from the Joel M. Dalrymple—Clarence J. Peters USAMRIID Antibody Collection

through BEI Resources, NIAID, NIH. The CCHFV-immunized rabbit and mouse sera have been kindly given by Prof. Aykut Özdarendeli.

2.1.3 Construction of plasmids

2.1.3.1 Generation of pDZ plasmids for CCHFV viral segments

The nucleotide sequences of CCHFV Kelkit06 S (1673 nt) and M (5364 nt) segments retrieved from GenBank (accession numbers: GQ337053 and GQ337054, respectively) were synthesized with flanking *Sap*I recognition sites at both ends and cloned separately by *Kpn*I and *Bam*HI enzymes into pUC19 vector (Synbio Technology USA Inc., Suzhou, China). The plasmids were propagated in One Shot™ TOP10 Chemically Competent *E. coli* (ThermoFisher Scientific, USA) cells. The pDZ plasmid was donated by Prof. Adolfo García-Sastre, Icahn School of Medicine at Mount Sinai. The viral sequences were excised by *Sap*I enzyme (New England BioLand, USA, MA) and individually ligated with *Sap*I digested pDZ vectors. The constructed plasmids (named pDZ_CCHFV_S and pDZ_CCHFV_M) were transformed into One Shot® OmniMAX™ 2 T1R *E. coli* (ThermoFisher Scientific, USA) cells. Three positive transformant colonies for each construct were selected and analyzed by restriction digestion analysis.

2.1.3.2 Generation of pcDNA3.1 plasmids for CCHFV viral proteins

The nucleotide sequences of CCHFV Kelkit06 NP, Gn, Gc and GPC ORFs were retrieved from GenBank (accession numbers: GQ337053 and GQ337054). Different primer sets were designed for each gene to be cloned into pcDNA3.1 vectors, consisting of 3EGFP (13031, Addgene), c-Flag pcDNA3 (20011, Addgene), pcDNA3-neo-cterminal-3HA (102643, Addgene) and 3.1 His C (2103, Addgene). By using these primers, the gene of interests were amplified by PCR, using pUC_S and pUC_M plasmids as templates and directionally cloned into 3.1 vectors. The constructed plasmids were transformed into XL10-Gold™ ultracompetent *E. coli* cells (Agilent, CA, USA). Three positive transformant colonies for each construct were selected and analyzed by restriction digestion analysis.

2.1.3.3 Generation of pCAGGS plasmids for CCHFV viral proteins

The nucleotide sequences of CCHFV Kelkit06 NP, Gn, Gc and GPC ORFs were retrieved from GenBank (accession numbers: GQ337053 and GQ337054). Same forward primers used to generate pcDNA 3.1 plasmids were utilized to amplify viral genes. New reverse primers were designed for each gene to be cloned into pCAGGS vectors (2042, Addgene). Downstream of stop codon the *Xho*I restriction sites were added in primer sequences for both Np and Gc, while a *Bam*HI site for Gn. The gene of interests were amplified by PCR, using pUC_S and pUC_M plazmids as templates and directionally cloned into pCAGGS vectors. The constructed plasmids were transformed into XL10-Gold™ ultracompetent *E. coli* cells (Agilent, CA, USA). Three positive transformant colonies for each construct were selected and analyzed by restriction digestion analysis.

2.1.4 2.1.4. Transfections

2.1.4.1 Transfection of pDZ plasmids

One day before transfection $5x10^5$ cells/well were seeded in 6-well plates and grown as adherent culture in DMEM supplemented with 10% fetal calf serum, and Pen-Strep (Penicillin-Streptomycin) at 37°C and 5% CO_2 in a humidified chamber so that they will be 50-70% confluent on the day of the experiment. The next day, cell culture media was removed, and the cells were incubated with DMEM including 2% FBS without Pen-Strep for two hours. Meanwhile, Polyethylenimine (PEI) (Polysciences, Germany) complexes were prepared. Briefly, 10 µl of 1 mg/ml PEI was diluted in 490 µl 150 mM NaCl, then mixed 1:1 with 2 µg plasmids (S, M, S+M or only water as negative control) in 150 mM NaCl. Cell culture media was removed and 0.5 ml DMEM without FBS and PenStrep was added to the wells. Then PEI complexes were added, and the cells were incubated for four hours at 37°C and 5% CO2 in a humidified chamber. After transformation cells were washed with DPBS (Gibco™, ThermoFisher Scientific, USA) and cultured in complete media (DMEM+ 10%FBS+PenStrep). Three days post-transfection, cell culture supernatants and pellets were collected and stored at -20 °C for further analysis.

2.1.4.2 Transfection of pcDNA 3.1 plasmids

One day before transfection $5x10^5$ cells/well were seeded in 6-well plates and grown in DMEM) supplemented with 10% fetal calf serum, and Pen-Strep at 37°C and 5% CO_2 in a humidified chamber until they reach 50-60% confluency on the day of the experiment. The next day, cell culture media was removed, and the cells were incubated with DMEM including 10% FBS with Pen-Strep. Meanwhile, Polyethyleneimine (PEI) complexes were prepared. Briefly, 6 µl of 1 mg/ml PEI was diluted in 100 µl DMEM (-), then mixed with 2 µg plasmids diluted in 65 µl DMEM (-) (1:2 ratio, 15 ng/ µl DNA: 30/ ng µl PEI). Then PEI complexes were added, and the cells were incubated for 72 hours at 37°C and 5% CO2 in a humidified chamber. Three days post-transfection, cell culture supernatants and pellets were collected and stored at -20 °C for further analysis.

2.1.4.3 Transfection of pCAGGS plasmids

One day before transfection $2x10^6$ cells/well were seeded in T75 flask and grown in DMEM supplemented with 10% fetal calf serum, and 1X Pen-Strep at 37°C and 5% CO2 in a humidified chamber until they reach 50-60% confluency on the day of the experiment. The next day, cell culture media was removed, and the cells were incubated with DMEM including 10% FBS with Pen-Strep. Meanwhile, PEI complexes were prepared. Briefly, 72 µl of 1 mg/ml PEI was diluted in 400 µl DMEM (-), then mixed with 24 µg plasmids diluted in 400 µl DMEM (-) (1:3 ratio, 60 ng/ µl DNA: 180 ng/ µl PEI). Then PEI complexes were added, and the cells were incubated for 96 hours at 37°C and 5% CO2 in a humidified chamber. Four days post-transfection, cell culture supernatants and pellets were collected and stored at -20 °C for further analysis.

2.1.5 Electroporation

The cells were washed with DPBS and resuspended in approtiate cell cultere media containing 10% FBS. The plasmids in different concentrations were mixed in 350 µl of cells (1 × 107) in a 0.4-cm cuvette by gently pipetting and incubated on ice for 10 min. The electroporations were performed in the Gene Pulser Xcell Total system, using defined protocols by its software for each cells (Bio-Rad, USA). After electroporation the cells were incubated on ice for a further 10 min and passaged to a well of 6-well

plate for the incubation at 37 °C for three days in a humidified incubator. For further analysis, cell lysates and culture supernatants were harvested.

2.1.6 Cell lysis

Transfected cells were washed two times with cold PBS and were collected by scraping followed by centrifugation at 1000 x g for 3 min. The cell pellets were lysed in lysis buffer (20 mM Tris pH7.5, 1% Triton X-100, 0.05% SDS, 0.5% Sodium Deoxycholate, 150 mM NaCl, 1mM Protease inhibitor cocktail).

2.1.7 Sucrose cushion

To analyze VLPs, culture medium of transfected cells was collected and cleared by centrifugation at 10,000 g for 10 min. Next, pre-cleared supernatant was layered on top of a 20% (w/v) sucrose cushion, added in 1/6 volume of the centrifuge tube and concentrated by ultracentrifugation at 150,000 g for 4 hours at 4°C (Beckman Coulter, Optima™ XPN, SW41 rotor, USA)

2.1.8 Transcriptional analysis of protein expression

2.1.8.1 RT-PCR

For transfection analysis of pDZ, total RNA was isolated from cells post-transfection using TRI-Reagent (BioShop, Canada) and samples were treated with DNAse I for 15 min at 37°C and then purified from DNAse I. RT-PCR is performed by the SensiFAST™ cDNA Synthesis Kit (Bioline, UK) using the Oligo d(T) primer to generate cDNA from total mRNA first, and the CCHFV S segment-specific qS reverse primer (5' TTAGATGATGTTGGCACTGGTG 3') to produce cDNA from vRNA, according to the manufacturer's instructions. Quantitative PCR were performed with qSforward (5' CATACAGGACATGGACATTGTG 3') and qSreverse (5' TTAGATGATGTTGGCACTGGTG 3') primers by using SensiFAST SYBR® No-ROX Kit (Bioline, UK).

For the analysis of the mRNA transcription ability of the vectors, RNA isolation and cDNA production from the cells transfected with different vectors were performed as decripted above Then qPCR was performed via of BlasTaq™ 2X qPCR MasterMix using different primer sets that could amplify approximately the last 130 bp of ORF sequences for each of the viral genes. The qS forward and qS reverse for Np; qM

forward (5'CAGGCTACAGAAGGATTATTGAAAGAC 3') and qM reverse (5'TTAGCCAATGTGTGTTTTTGTGGAG 3') for Gc; Primer 8 forward (5' cttggtaccGCCACCATGGTCTGCAAACGC 3') and Primer 3 reverse (5' gtggatccttaTGCAGAGGTGCTAAC 3') were used for Gn. Ct values measured by Rotor-Gene® Q (Qiagene, USA) for each gene and were normalized to the GAPDH gene used as internal control. The relative expression level was analyzed by $2^{(\Delta\Delta Ct)}$ method using the following formula:

$\Delta\Delta Ct:[(Ct_{targetgene}-Ct_{housekeeping})-(Ct_{normal}-C_{thousekeeping})]$

2.1.9 Post-translational analysis of protein expression

2.1.9.1 Western Blot

The proteins to be analyzed were separated on either by SDS-PAGE or Native-PAGE, described below.

2.1.9.2 Polyacrylamide gel electrophoresis

SDS-PAGE: The protein samples were diluted 1:1 in Laemmli buffer (4% (w/v) SDS, 10% (v/v) β-mercaptoethanol, 20% (v/v) glycerol, 0.004% (w/v) bromophenol blue, 0.125 M Tris-HCI) and heated to 95°C for 10 min unless otherwise stated. For some assays, NP and Gn samples were denatured in reducing loading buffer (5X Blue Loading Buffer, 200 mM Tris HCl pH6.8, 10% SDS, 500 mM β-mercaptoethanol and 50% glycerol) at 95°C for 5 min. Proteins were run on an 8-12% polyacrylamide gel, first at 50 V for 20 min, then at 200 V for 40 min. After electrophoresis, the gel was stained with Coomassie brilliant blue G-250 (Sigma-Aldrich, Taufkirchen, Germany).

Native-PAGE: Samples were diluted in non-reducing loading buffer (5X Blue Loading Buffer, 200 mM Tris HCl pH6.8, 20% SDS, and 50% glycerol), incubated at 50°C for 10 min and electrophoresed on 4-9% polyacrylamide gels.

Following electrophoresis, proteins were transferred to a PVDF membrane (GVS North America, Sanford, USA) immediately after methanol induction of the membrane, in transfer buffer (24 mM Tris, 192 mM glycine and 20% (v/v) methanol) either at 25 V for 7 min on semi-dry blotter (Trans-Blot Turbo, Bio-Rad, California, USA) or wet at 100 V for 90 min in Mini Trans-Blot cell (Bio-Rad, California, USA). The membrane was blocked with TBST (10 mM Tris pH 7.4, 0.9% (w/v) NaCl, and

0.05% (v/v) Tween-20) containing 5% (w/v) skim milk (Sigma-Aldrich, Taufkirchen, Germany) for two hours at room temperature and incubated with primary antibody overnight at 4°C, followed by secondary antibody incubation for one hour at room temperature. Between each step, the membrane was washed five times of 10 min using TBST and processed for chemiluminescence detection (WesternBright Sirius Chemiluminescent Detection Kit, Advansta, California, USA), according to the manufacturer's instructions. Membranes were visualized by using Fusion FX Solo imaging system (Vilber, Collégien, France).

2.1.9.3 ELISA

The 96 well microplates (Immulon 2 HB, Invitrogen, Waltham, USA) were coated overnight at 4°C with supernatant or cell lysate samples diluted in carbonate-bicarbonate buffer (pH 9.6). Then, the plates were washed four times with PBST (PBS + 0.05% (v/v) Tween 20) and blocked with PBST containing 5% (w/v) skim milk for two hours at room temperature. Plates were then incubated at 37°C for 1 hour each, first with the primary antibody and then with a corresponding HRP-conjugated secondary antibody, depending on the analytes. Between each step, the wells were washed four times with PBST. Then, TMB solution (Abcam, Cambridge, UK) were added to the wells and the plates were incubated for 20–25 min at room temperature in the dark. The reaction was stopped by adding 2N H_2SO_4 to the wells and absorbance of samples measured in iMark microplate reader (Bio-Rad, California, USA) at 450 nm. All washing steps performed using Wellwash Versa Microplate Washer (Thermo Fisher Scientific, Waltham, USA). Data were calculated by the mean of absorbance measurements obtained from duplicated samples. The cut-off value was calculated by the given formula: the mean absorbance of each negative samples + 2 SD.

2.1.10 TCA precipitation

After transfection, the cell culture medium was precipitated by the trichloroacetic acid (TCA) method. Briefly, 100% TCA was added to 1/4 of the sample and incubated on ice for 10 min. After centrifugation at 14,000 x g for 5 min, the protein pellet was washed three times with cold acetone. After all the acetone was evaporated, the proteins were boiled in 2X SDS Sample Buffer at 95 °C for 5 min and then electrophoresed.

2.2 Generation of SARS-CoV-2 VLP in *Pichia Pastoris*

2.2.1 Virus propagation

The viral strain hCoV-19/Turkey/Istanbul-BezmCoV1/2020 (GISAID accession number EPI ISL 457824) employed in this thesis have been originally isolated from nasopharyngeal swab samples taken from a 2-year-old girl who applied to Bezmialem Vakif University Hospital Clinical Microbiology Laboratory with symptoms consistent with COVID-19 [214]. The virus was propagated on Vero E6 cells in DMEM supplemented with 10% FBS, 100 U/ml penicillin, 100 μg/ml streptomycin and 1 μg/ml amphotericin B (Thermo Fisher Scientific, USA). All virus infection assays were carried out under biosafety level 3 settings in the Bezmialem Vakif University Hospital Tuberculosis Laboratory.

2.2.2 Antibodies and sera

Rabbit primary antibody cocktail prepared in final dilution of 1:4000, is composed of rabbit anti-SARS-COV-2 Spike S1 protein polyclonal antibody (Cat. A20136, ABclonal, USA), rabbit anti-SARS -COV-2 N protein monoclonal antibody (Cat. A20021, ABclonal, USA), and rabbit anti-SARS-COV-2 Envelope protein polyclonal antibody (Cat. A20199, ABclonal, USA). Also, a mouse SARS-CoV-2 total IgG positive sera were provided by Prof. Özdarendeli as a kind gift and used in the Western Blots in a dilution of 1:1000. The goat anti-mouse IgG HRP (Cat. sc2031, Santa Cruz Biotechnology, USA), and goat anti-rabbit IgG HRP (Cat. Ab97200, Abcam, UK) was used as secondary antibodies.

2.2.3 Construction of plasmids

The nucleotide sequences of Spike (S), Nucleoprotein (N) Membrane (M) and Envelope (E) genes of SARS-CoV-2 Wuhan strain, available at NCBI (NC_045512.2) were first optimized for expression in *Pichia pastoris (P. pastoris)* and then, cloned in between *Eco*RI and *Sal*I enzyme cut sites in AOX1 locus on pPICZA vector by Gene Universal® (Newark, DE, USA). The plasmids were propagated in One Shot™ TOP10 Chemically Competent *E. coli* (ThermoFisher Scientific, USA) cells. The unique *Bgl*II and *Bam*HI sites, generating compatible ends after digestion, pPICZA vector allows to construct plasmids with multiple head-to-tail expression cassettes. Based on this, expression cassettes containing each viral structural gene were cloned

into a single plasmid to generate SARS-CoV-2 VLP in *P. pastoris*. Briefly, a pPICZA plasmid containing one of the viral gene was linearized using *Bam*HI, then the other viral gene expression cassettes to be ligated head to tail were excised by the *Bgl*II - *Bam*HI double digestion and ligated with each other in vitro. The ligation mix was treated with *Bam*HI and *Bgl*II to eliminate head-to-head and tail-to-tail multimers. Finally, the multimers were ligated into *Bam*HI -linearized recombinant pPICZA. The constructed plasmids were propagated in One Shot™ TOP10 Chemically Competent *E. coli* and then, transformed into GS115, *Pichia pastoris* yeast cells (Invitrogen™ ThermoFisher Scientific, USA) and analyzed by restriction analyzes.

2.2.4 Transformation by Electroporation

Plasmids with a single expression cassette was linearized with *Sal*I restriction enzyme before transformation. The other plasmids having multimer expression cassettes were directly transformed into electrocompetent GS115 *P. pastoris* cells using Gene Pulser (Bio-Rad, USA). Briefly, an overnight culture for GS115 cells, grown at 30°C in YPD was used to inoculate 500 ml of fresh medium in a 2-liter flask with 0.1–0.5 ml of the overnight culture and then, they were grown overnight again to an OD600 to 1.3–1.5. Cells were centrifuged at 1,500 × g for 5 min at 4°C and the pellets were resuspended in 500 ml of ice-cold, sterile water. Cells were washed first with 250 ml ice-cold water, later with 20 ml of ice-cold 1 M sorbitol and resuspended in 1 ml of ice-cold 1 M sorbitol. Finally, 80 µl of competent cells were mixed with 5–10 µg of DNA (in 5–10 µl sterile water) and the mixture was transferred to an ice-cold 0.2 cm electroporation cuvette, followed by incubation on ice for 5 min. Cells were pulsed using the manufacturer's instructions for *Saccharomyces cerevisiae* (at 1.1 kV, 200 and 25 mF). After electroporation, 1 ml of ice-cold 1 M sorbitol was added to the cuvettes. The cells were then incubated at 30°C without shaking for 2 hours and spread on YPDS plates containing 100 µg/ml Zeocin™ (Invitrogen, ThermoFisher, USA). The cultures were incubated for 3-10 days at 30°C until colonies form. Positive transformants were analyzed either by PCR or restriction analysis.

2.2.5 Expression

A freshly grown single colony on a selective YPD agar plate was inoculated into 25 ml of BMGY (buffered complex glycerol medium: 1% yeast extract, 2% peptone, 100 mM, potassium phosphate pH 6.0, 1.34% YNB, 0.00004 % biotin, 1% glycerol) and

grown in a shaking incubator at 28 °C at 250 rpm until OD600 value of yeast cells reach until 2-6. Cells were then centrifuged at 3000 x g for 5 min at room temperature. To induce expression, cells were resuspended at an OD600 of 1 in 100 ml of BMMY (buffered complex methanol medium: 1% yeast extract, 2% peptone, 100 mM, potassium phosphate pH 6.0, 1.34% YNB, 0.00004 % biotin, 0.5% methanol). Every 24 hours, 100% methanol was added to the culture at a final concentration of 0.5% and 1 ml of culture sample was taken for analysis. After five days of expression, cells were harvested by centrifugation at 7000 x g for 5 min and pellets stored at -80 °C until further processing.

2.2.5.1 Cell lysis

Sample processing for small-scale expression samples: Acid-washed glass beads of 0.5 mm diameter by weight of the pellet of 1 ml expression culture were added to the pellets and then resuspended in 1 ml of lysis buffer (25 mM Phosphate Buffer, 5 mM EDTA, 0.6% Tween 20, pH 8.0). Cells were lysed by 10 cycles of 40 seconds of vortexing and 40 seconds of incubation on ice. After centrifugation for 10 min at 10,000 x g, the clear lysates and pellets were stored at -80°C for further processing.

Sample processing for large-scale expression samples: After 120 hours of expression, a pellet of 100 ml culture was dissolved in PBS, and yeast cells were mechanically lysed under high hydrostatic pressure for 15 cycles at 15,000 psi using a homegenizer (Microfluidizer M110P). After that, the cell debris was precipitated by centrifugation at 10,000 x g for 15 min. Cell lysates were centrifuged at 155,000 x g for 5 hours at 4 °C in an ultracentrifuge to precipitate VLPs, and the pellets were dissolved in 1 ml of PBS.

2.2.5.2 Western Blot

Western Blot analysis was performed with clear lysates obtained from *Pichia* expression samples. Both inactivated virus and SARS-COV-2 infected Vero cell lysate was utilized as positive control while wild-type GS115 cell lysate and uninfected Vero cell samples was used for negative control. Briefly, samples were run on a 15% SDS-polyacrylamide gel and transferred to a nitrocellulose membrane in transfer buffer (24 mM Tris, 192 mM glycine and 20% (v/v) methanol) at 25 V for 7 min on semi-dry blotter. After blocking the membrane with TBST (10 mM Tris pH 7.4, 0.9% (w/v) NaCl, and 0.05% (v/v) Tween-20) containing 5% (w/v) skim milk for two hours at

room temperature, membrane was incubated with primary antibody overnight at 4°C, followed by secondary antibody incubation for one hour at room temperature. Between each step, the membrane was washed five times of 10 min using TBST and processed for chemiluminescence detection (WesternBright Sirius Chemiluminescent Detection Kit, Advansta, California, USA), according to the manufacturer's instructions. Membranes were visualized by using Fusion FX Solo imaging system.

3. RESULTS

3.1 Studies on Plasmid-Based Virus Like Particle Models for CCHFV a negative sense RNA virus in mammalian cells

3.1.1 Studies conducted using pDZ plasmid

3.1.1.1 Construction of pDZ plasmids expressing CCHFV S and M segments

For the establishment of a plasmid based CCHFV VLP model in eukaryotic cells, a dual promoter plasmid, called pDZ was utilized in this thesis. Due to having both a human polymerase I (hPolI) promoter and a CMV promoter, vRNAs and mRNA of viral segments can be produced simultaneously by a single plasmid in transfected cells. This plasmid was first developed by Prof. García-Sastre for reverse genetic studies on the Influenza Virus, a negative sense, single-stranded and segmented RNA virus, like CCHFV [215]. With the kind permission of him, the pDZ vector was utilized to generate a non-infectious CCHFV-like particle system in mammalian cells. The S and M segments of the CCHFV Kelkit06 strain were obtained commercially, individually cloned into the pUC19 vector and were designated pUC_S and pUC_M plasmids, respectively. Following plasmid propagation, plasmids were confirmed by *Sap*I digestion analysis (Figure 3.1A). Then, the bands corresponding relative segments were isolated and ligated with *Sap*I digested pDZ plasmids. After transformation, newly constructed plasmids (named as pDZ_CCHFV_S and pDZ_CCHFV_M), three positive transformant colonies for each construct were selected and analyzed by restriction digestion analysis. For the confirmation, pDZ_CCHFV_S were digested with *Sap*I, resulting fragments of 1692 bp (indicating S segment) and of 4917 bp (vector backbone) appeared on agarose gel electrophoresis (Figure 3.1B). Analysis of pDZ_CCHFV_M plasmids were not performed with *Sap*I digestion because resulting fragments would be so close that they cannot be differed on agarose gel. Therefore, cloning of M segments were confirmed with *Bam*HI (New England BioLand, USA, MA) enzyme. In two of the three colonies analyzed, two expected bands at the 6370 bp and 3593 bp were visualized on agarose gel (Figure 3.1C). For the downstream experiments colony 1 and colony 2 were selected for S and M segment, respectively.

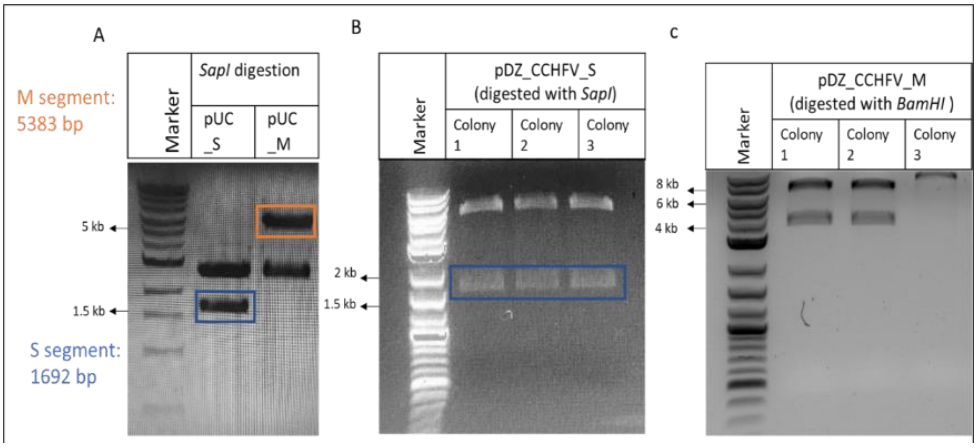

Figure 3.1 : Agarose gel electrophoresis of vectors inserted with CCHFV S and M segment. A) Confirmation of pUC_S and pUC_M plasmids by *Sap*I digestion. B) Confirmation of pDZ_CCHFV_S positive transformant colonies by *Sap*I digestion. C) Analysis of positive transformant colonies transformed with pDZ_CCHFV_M by digestion with *Bam*HI. Blue rectangles show the S segment, while the orange one shows the M segment

3.1.1.2 Transfections of pDZ plasmids into mammalian cells

Three different cell lines, BHK-21, VeroE6, and HEK293T were transfected with pDZ_CCHFV_M and pDZ_CCHFV_S plasmids either separately or together by using PEI as a transfection reagent. Three days after transfection, cell pellets were harvested, and the supernatant samples were both precipitated with trichloroacetic acid (TCA) to analyze all the protein secreted into the medium and centrifuged overnight at 21,000 x g to analyze whether VLP was budded from the transfected cells. Then, all three samples (pellets after centrifugation, TCA precipitates, and cell pellets) from each transfected cells were analyzed by Western Blot using sera of mice immunized with inactivated CCHFV (Figure 3.2). However, similar band patterns were observed in all samples, including negative control samples and any discriminative protein band could not be seen on these Western Blot images. One of the possible reasons for this situation may be that the production amount of viral proteins in transfected cells was insufficient for their detection by the Western Blot. As an alternative to Western Blot, post-transcriptional analyses were performed for the S segment using RT-PCR.

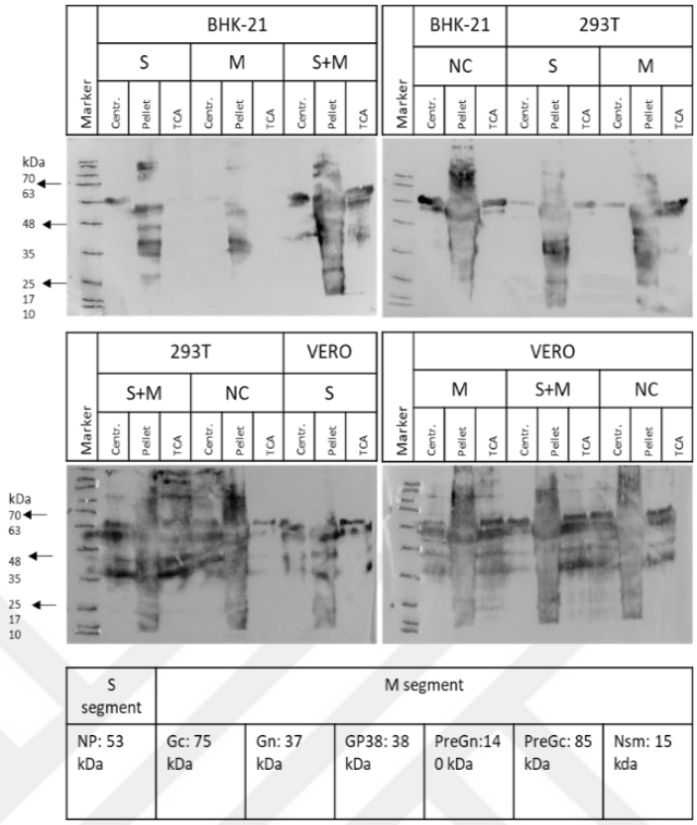

Figure 3.2 : Western Blot analysis after PEI transfection. Transfected cell supernatants and pellets analysis by Western Blot. Three different cell line (BHK-21, VeroE6, 293T) were transfected with S (pDZ_CCHFV_S), M (pDZ_CCHFV_M), or S and M. For negative control, molecular grade water instead of plasmids was used. Membranes were incubated with sera of mice immunized with inactivated CCHFV at 1:1000 dilution, then probed with goat-anti-Mouse IgG-HRP antibodies at 1:3000 dilution. Membranes were processed for chemiluminescence detection and visualized by using Fusion FX Solo imaging system (Vilber, Collégien, France). The expected protein bands after transfection from S and M segments were given under Western Blot images.

The pDZ plasmid has bidirectional dual promoters; one for human polymerase I to transcribe vRNA, and the other for human polymerase II to transcribe mRNA from viral segments. To analyze the transfection, both mRNA and vRNA transcription levels in 293T cells transfected with pDZ_CCHFV_S in different concentrations (2 and 6 µg per well) were analyzed by RT-PCR. Total RNA was isolated from all the samples tested. The cDNA reactions were set up with oligo d(T) primers to analyze the mRNA, while with gene-specific primers (qSforward) to analyze vRNA. Downstream PCRs were done with primers specific to NP gene fragment close to 3' end (Table 3.1 and Figure 3.3). However, the RT-PCR analysis clearly showed that

neither viral mRNA nor vRNA was transcribed after transfection of 293T cells with pDZ_CCHFV_S using PEI, consistent with Western Blot analysis (Table 3.2).

Figure 3.3 : Representation of partial vector map showing binding sites of primers used to analyze mRNA and vRNA levels in pDZ_CCHFV_S transfected 293T cells.

Table 3.1 : Primers used to analyze mRNA and vRNA levels in pDZ_CCHFV_S transfected 293T cells.

Template	Primers used by reverse transcriptase in first step	Primer set used by polymerase in second step
mRNA	Oligo d(T)	qSforward: 5' CATACAGGACATGGACATTGTG 3'
vRNA	qSforward	qSreverse: 5' TTAGATGATGTTGGCACTGGTG 3'

Table 3.2 : Ct values obtained from RT-PCR analysis of transfection samples.

Template used in cDNA	Ct
mRNA (isolated from 2 µg S transfected cells)	32,99
mRNA (isolated from 6 µg S transfected cells)	28,91
mRNA (negative control)	26,87
vRNA (isolated from 2 µg S transfected cells)	25,75
vRNA (isolated from 6 µg S transfected cells)	28,83
vRNA (negative control)	21,95

Considering that the problem might be caused by the transfection method, it was decided to introduce the vectors to the cells by electroporation. Electroporation was performed with Gene Pulser Xcell (Bio-Rad, USA), according to the manufacturer's recommendations. Despite using several cell-protective transfection media (like HEPES or sucrose-containing medium) and defined programs by Bio-Rad for cells, the cells were severely damaged. Therefore, further analysis with those cells couldn't be conducted.

Although various cell types and transfection methods were used to transfect the plasmids, the pDZ-based system did not yield the desired outcome in the shape of VLP. Even pDZ plasmids have been successfully used in Influenza virus reverse genetics by García-Sastre Lab (Martínez-Sobrido & García-Sastre, 2010), the pDZ-based reverse genetic system might not be suitable in the case of CCHFV.

3.1.2 Studies conducted using pCAGGS plasmid

3.1.2.1 Construction of pCAGGS plasmids expressing viral proteins

To circumvent the problem faced using pDZ in that the proteins could not be detected in WB, we decided to attempt a system that has higher transgene protein yield. To increase viral protein yield, at least to the detection limit required in the Western Blot analysis, the pDZ vector was exchanged for the pCAGGS vector, which has the same vector backbone and does not contain any human Pol I promoter and terminator regions in between human Pol II sequences. Instead of whole viral segment, only the ORF sequences encoding NP, PreGn, and PreGc proteins cloned into pCAGGS vector. To this aim, NP and Gc ORF sequences were cloned in between *Kpn*I and *Xho*I recognition sites on the vector. Because of internal cut sites of *Xho*I in Gn ORF sequence, Gn was cloned by using *Kpn*I and *Bgl*II enzymes. All constructed plasmids were transformed into chemically competent XL10 or Mach1 *E. coli* cells (ThermoFisher Scientific, USA). The three positive transformants for each were analyzed by restriction analysis. As a result, in all three colonies (1m1, 1m2, 1m3) for NP, two colonies for Gc (2m2 and 2m3), and one colony for Gn (3x1) were confirmed (Figure 3.4).

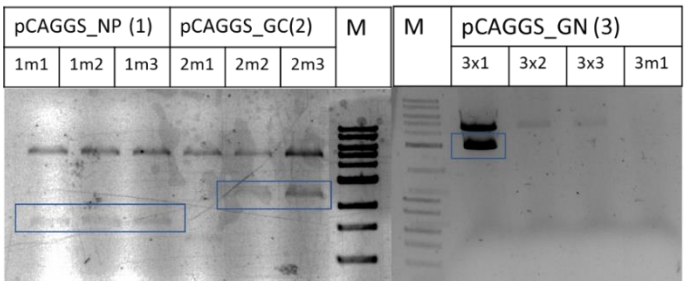

Figure 3.4 : Image of agarose gel electrophoresis, confirming constructed pCAGGS plasmids for CCHFV by restriction analysis. First number indicates genes; 1:NP, 2: Gc, 3: Gn, while last numbers for selected colonies. The character m is for Mach1 and x for XL10 cells. Blue rectangles are used to show desired bands for each gene.

3.1.2.2 Transfection analyses of pCAGGS vectors into Huh-7 cells

The constructed plasmids (pCAGGS-NP (1m1), pCAGGS-Gc (2m3), and pCAGGS-Gn (3x1) were transfected by PEI in a ratio of 1:3 into Huh-7 cells in T75 flask. After 96 h post transfection, supernatants and the cell pellets were collected separately. Supernatant samples were pelleted with sucrose cushion by ultracentrifugation. First, cell lysates were tested by Western Blot using different sera; mouse anti-NP, mouse anti-CCHFV, and rabbit anti-CCHFV sera (Figure 3.5). Here, a recombinant NP produced in another project of Dr. Doymaz was utilized as positive control and detected in all sera. Interestingly, in all mice sera, discriminative bands above 63 kDa were appeared in all NP-transfected cell lysates by comparing to negative control. Besides, significant bands at around 53 kDa in 1m1, 1m2, and in Np wells were appeared on the membrane probed with anti-CCHFV rabbit sera.

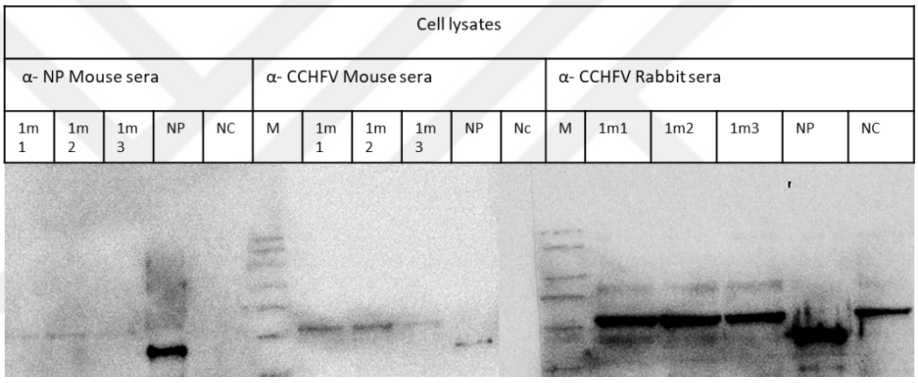

Figure 3.5 : Analysis of cell lysates transfected with different NP plasmids. Samples were probed with either NP-immunized mice sera or CCHFV-immunized mice or rabbit sera. NP is a recombinant protein produced in-house for another project and utilized here as a positive control, while mock-transfected cells were used as negative controls. Following incubation with relevant secondary antibodies conjugated with HRP, membranes were processed for chemiluminescence detection.

Additionally, all NP, Gn and GC samples were analyzed by Western Blot using specific antibodies called 9D5, 8F10, and 11E7, respectively. Samples were resuspended in 5x loading buffer without β-Mercaptoethanol. NP and Gn samples were run in 8-12 % SDS gel, while Gc samples were run in 5-9 % native gel (Figure 3.6). Again, in all NP samples, bands at about 66 kDa were detected Figure 3.6A). In Gn samples, bands were seen at above 270 kDa, around 130 kDa, in between 66 and 52 kDa and below 30 kDa in lysate (Figure 3.6B). For Gc, two different plasmids were analyzed and only in 2m3 transfected cells samples three different bands between 90 and 270 kDa were detected in cell lysate (Figure 3.6C). As a result, viral protein

expressions in transfected cell were demonstrated by Western Blot using specific antibodies.

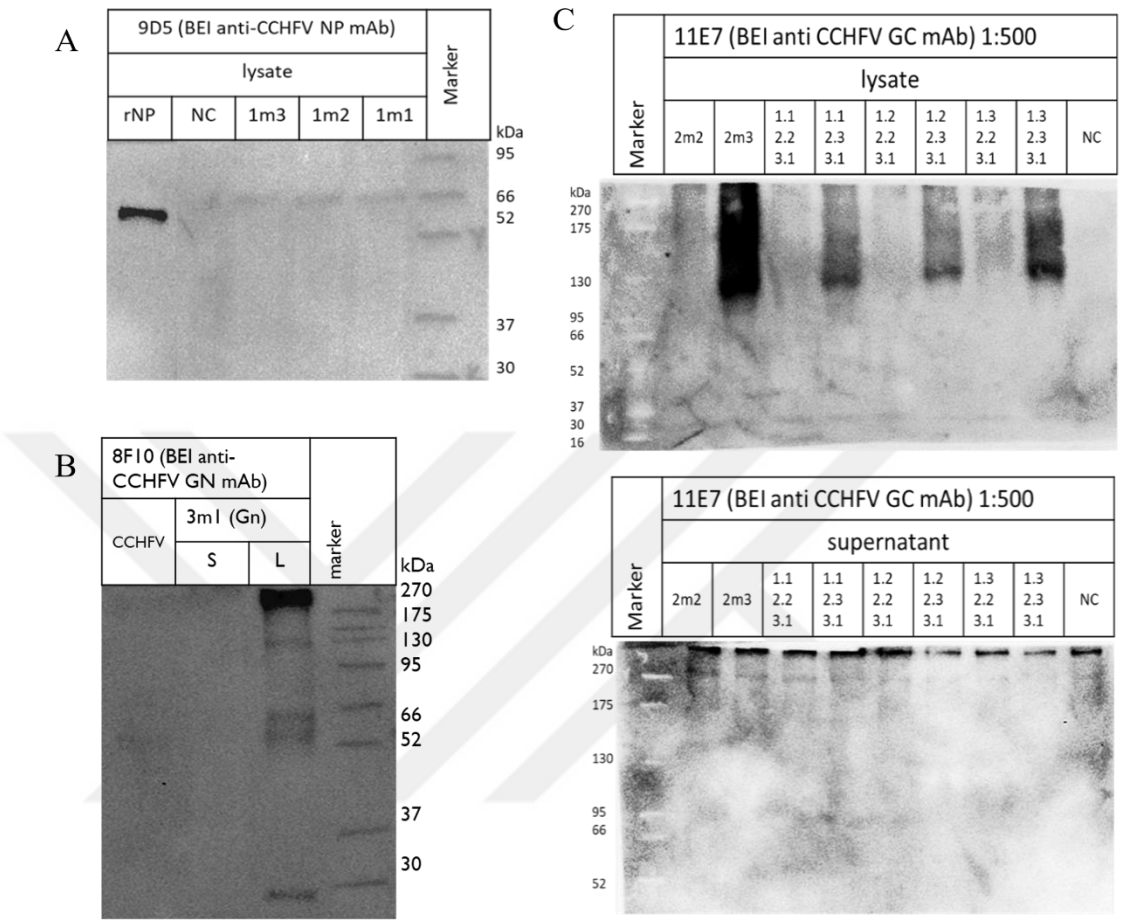

Figure 3.6 : Western Blot analysis of cells transfected with all pCAGGS plasmids containing NP, Gn, and Gc, separately. Genes were numbered as 1 for NP, 2 for Gc, and 3 for Gc. The "m" indicates the transformed bacteria called Mach1. The last numbers for colonies selected for analysis. Samples were run in NATIVE-PAGE gel and transferred onto PVDF membranes. Then the membranes were incubated with protein specific antibodies in a dilution of 1:500 (9D5, 8F10, 11E7). After incubation with goat anti Mouse IgG HRP antibodies, Membranes were processed for chemiluminescence detection.

According to the results obtained from last the Western Blot, the VLP analyzes were continued with the plasmids isolated from the colonies 1m1, 2m3, and 3x1. To demonstrate, whether these proteins can assemble to form VLP, and to increase the protein amount to be analyzed by Western Blot, plasmids were transfected into Huh-7 cells grown on T75 flasks. After 72 hours from transfection, cells were harvested by centrifugation. To analyze whether any VLP was secreted into media, supernatant samples were pelleted by sucrose cushion. Then, supernatant and clear lysate samples

were loaded onto both SDS-PAGE and NATIVE-PAGE gels. Western Blot analysis was conducted with both CCHFV-immunized rabbits (Figure 3.7) and mouse sera (Figure 3.8). Antibodies found in the sera of CCHFV-vaccinated rabbits could not capture viral proteins found neither in lysate nor in the supernatant after NATIVE-PAGE (Figure 3.7A) and smear bands with high background were observed in all samples run on an SDS-PAGE gel (Figure 3.7B).

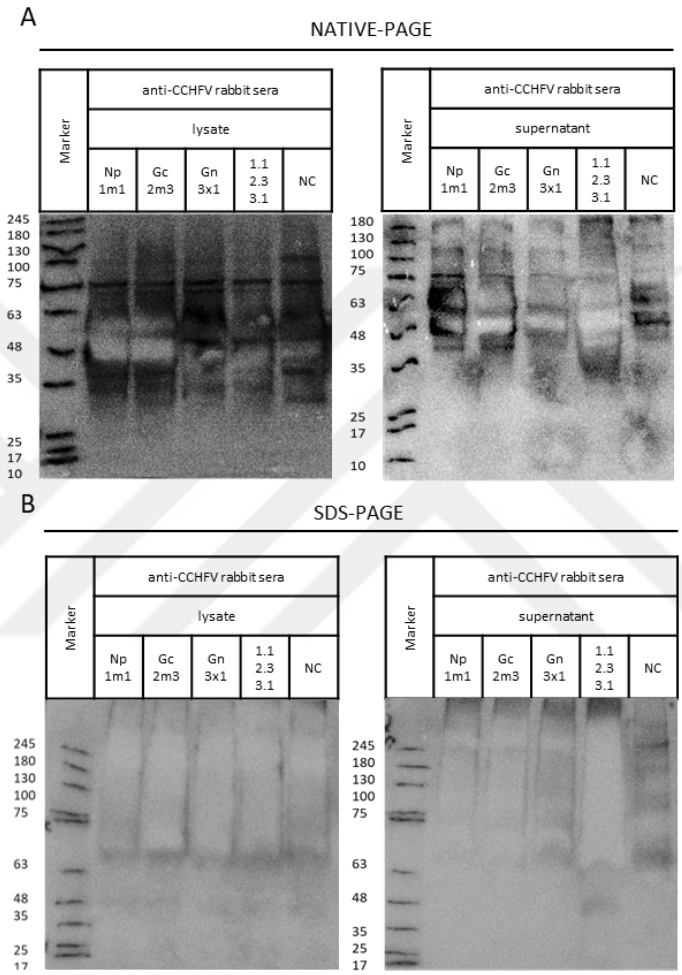

Figure 3.7 : Western Blot analysis of transfected cells with CCHFV-immunized rabbit sera. The cell samples were run in both SDS and native gel by electrophoresis. Then the gels were wet transferred to nitrocellulose membrane. Lysates (A, C) and supernatant samples after sucrose cushion (B, D) were loaded onto both NATIVE-PAGE (A, B) and SDS-PAGE (C, D). The membranes were blotted with anti-CCHFV rabbit sera at 1:3000 dilution, followed by goat anti mouse IgG HRP antibodies in a dilution of 1:5000. Membranes were processed for chemiluminescence detection.

However, using CCHFV immunized mouse serum yielded similar results in all NATIVE-PAGE samples (Figure 3.8A), while distinctive bands for all viral proteins appeared in supernatant samples run on an SDS-PAGE gel (Figure 3.8B). Accordingly, the band between 48 and 63 kDa may indicate the 53 kDa NP. While the 75 kDa Gc

protein and its 85 kDa PreGc form were prominently seen, an additional band of around 100 kDa was seen in both Gc-only and cell culture samples in which three viral proteins were transfected simultaneously. Since a band smaller than 30 kDa was also seen in the previous Western Blot analysis with Gn-specific antibody (Figure 3.6B), the band between 25 and 35 kDa was likely to be a protein produced from PreGn. Finally, viral proteins or their fragments were detected by Western Blot in cell culture media transfected with all three plasmids.

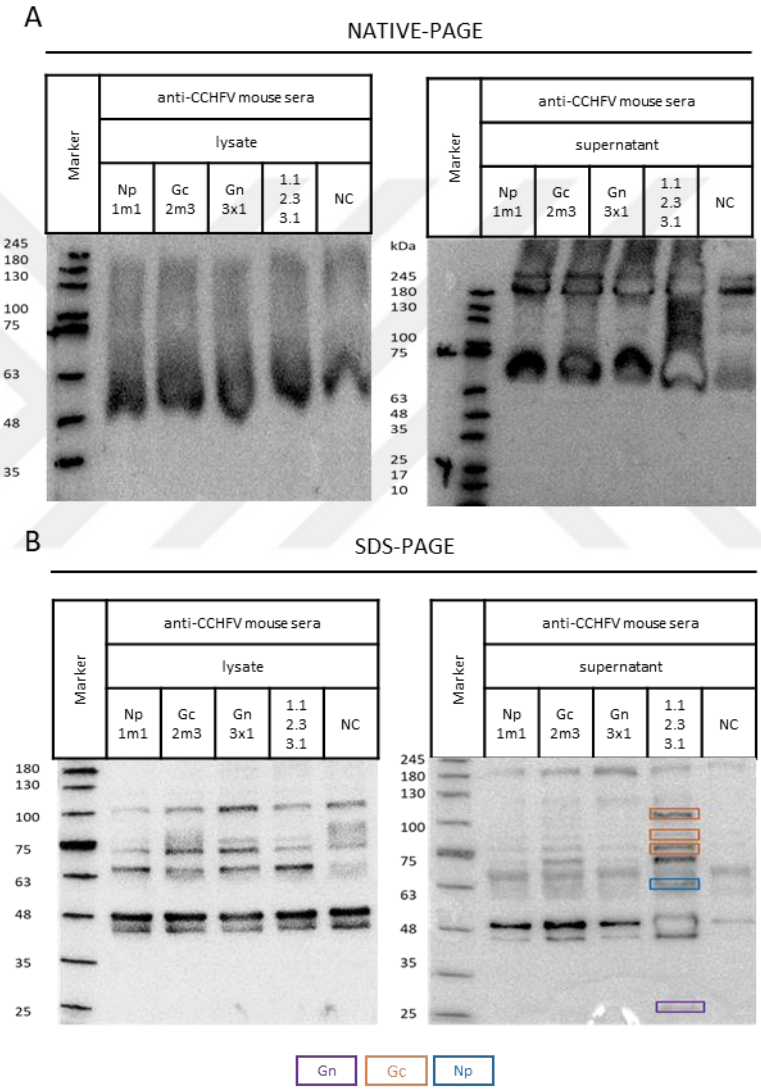

Figure 3.8 : Western Blot analysis of transfected cells with CCHFV-immunized mice sera. The cell samples were run in both SDS and native gel by electrophoresis. Then the gels were wet transferred to nitrocellulose membrane. Lysates (A, C) and supernatant samples after sucrose cushion were loaded onto both NATIVE-PAGE (A, B) and SDS-PAGE (C, D). The membranes were blotted with anti-CCHFV Mouse sera at 1:5000 dilution, followed by goat anti mouse IgG HRP antibodies in a dilution of 1:3000. Membranes were processed for chemiluminescence

Studies with pCAGGS vectors using CCHFV-specific and immunized animal sera partially showed the expression of viral proteins, but additional experiments were needed to demonstrate the proper synthesis of viral proteins. Since the desired results could not be fully achieved with pCAGGS vectors, studies were continued with pCDNA3.1 vectors, which are widely used in the production of recombinant proteins.

3.1.3 Studies conducted using pcDNA 3.1 plasmid

3.1.3.1 Construction of pcDNA3.1 plasmids to express viral proteins in transfected cells

Here, pCDNA3.1 plasmids were utilized to express proteins in mammalian cells. Unlike pDZ or pCAGGS, pcDNA3.1 plasmid has a CMV promoter instead of a CMV enhancer and chicken β-actin promoter. First, the ORF sequences encoding NP, Gn, Gc, and GPC protein regions were cloned into 3.1 vectors, separately. Four different eukaryotic expression vectors were utilized for this aim: 3EGFP (13031, Addgene), c-Flag pcDNA3 (20011, Addgene), pcDNA3-neo-cterminal-3HA (102643, Addgene) and 3.1 His C (2103, Addgene). To increase the possibilities, primers were designed to allow subcloning of viral genes amplified from pUC_S and pUC_M vectors into different pcDNA 3.1 plasmids (Table 3.3). Thus, a versatile cloning strategy has been developed that makes it possible to produce viral proteins in various forms (native proteins or FLAG- or HA-tagged or EGFP fused proteins) by cloning a single insert into different vectors. (Table 3.4).

To this aim, gene of interests were amplified by PCR using pUC_S and pUC_M plasmids as templates (Figure 3.9A). Except native NP, all amplicons were generated. To amplify the sequence to produce native NP (PCR product 25), pUC_S and PCR product 27 (NP-EGFP), produced with primer pairs 2 and 7, were used as templates. and annealing temperature optimization studies (55 ºC, 58 ºC, 60ºC) were conducted for both templates, separately. After that, NP sequences could be amplified successfully as a single band at 55 ºC and 58 ºC when pUC_S were used as template (Fig 3.9B).

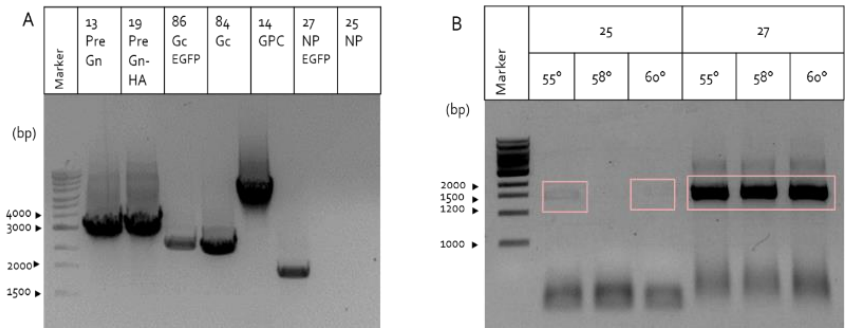

Figure 3.9 : Gel electrophoresis analysis of PCR products encoding viral genes. A. Amplification of related genes using pUC_M and pUC_S as templates. B) Annealing temperature optimizations of PCR reactions to be able to amplify native NP sequences from either pUC_S or PCR product of 27. GPC: 5090 kb, PreGc: 2228 bp, PreGn: 3028 bp, NP: 1472 bp.

Table 3.3 : Sequences of primers, which will be utilized to amplify viral genes to be cloned into pcDNA 3.1 vectors.

No.	Target Gene	Primer name	Primer sequence
1	GPC	GPC forward KpnI	cttggtaccGCCACCATGCCCACCAA
2	NP	NP forward KpnI	cttggtaccGCCACCATGGAAAACAAGATCG
3	Gn	PreGn reverse *BamHI**	gtggatccttaTGCAGAGGTGCTAAC
4	Gc	PreGC reverse *BamHI**	gtggatccttaGCCAATGTGTGTT
5	NP	NP reverse *BamHI**	gtggatccttaGATGATGTTGGC
6	Gc	PreGc-EGFP reverse XhoI	catctcgagGCCAATGTGTGTT
7	NP	NP-EGFP reverse XhoI	catctcgagGATGATGTTGGCAC
8	Gc	PreGc forward KpnI	cttggtaccGCCACCATGGTCTGCAAACGC
9	Gn	preGN-HA reverse NotI	atagtttaGCGGCCGCTGCAGAGGTG

*: After transfection with the plasmid to be generated, a stop codon was added to the sequence to produce native protein of interest in the cells.

Table 3.4 : Sequences of primers, which will be utilized to amplify viral genes to be cloned into pcDNA 3.1 vectors.

Gene	Primer sets	Plasmid	End-product
GPC	1+4	c-Flag pcDNA3 pcDNA3-neo-cterminal-3HA	GPC
		pcDNA3.1His C	HGPC
Gn	1+3	c-Flag pcDNA3 pcDNA3-neo-cterminal-3HA	Gn
		pcDNA3.1His C	HGn
	1+9	pcDNA3-neo-cterminal-3HA	Gn-HA
Gc	8+4	c-Flag pcDNA3 pcDNA3-neo-cterminal-3HA	Gc
		pcDNA3.1His C	HGc
	8+6	pcDNA 3EGFP	Gc-EGFP
NP	2+5	c-Flag pcDNA3 pcDNA3-neo-cterminal-3HA	NP
		pcDNA3.1His C	HNP
	2+7	pcDNA 3EGFP	NP-EGFP

Next, all plasmids and inserts were double digested with *Acc*651 and *Bam*HI enzymes. The plasmid backbones were recovered from the gel and ligated with target genes, separately (Figure 3.10A). Then, ligation reactions were transformed into One Shot™ TOP10 Chemically Competent *E. coli* cells. However, constructed plasmids could not be detected in any of the selected transformant colonies, indicating that ampicillin-resistant uncut plasmids were transformed dominantly (Fig 3.10B).

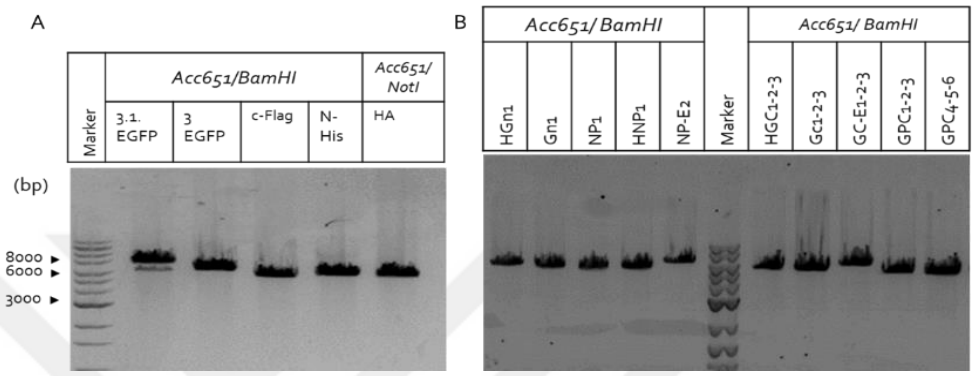

Figure 3.10 : Agarose gel electrophoresis analysis for restriction analysis with *Acc651* and *BamHI* enzymes. A) Electrophoresis of double-digested vector backbones. B) Transformation analysis of positive transformants selected for each gene. Numbers following gene names indicate nominated colony numbers.

All attempts to construct plasmids by using *Acc*65I enzyme failed since *Acc*65I enzyme is sensitive to *dam* methylation. Then, it was decided to use *KpnI*, isoschizomer of *Acc*65I, to cut plasmids. Also except of pcDNA3-neo-c-terminal-3HA, all other plasmids were excluded from the cloning strategy, because there was only one or two bases between recognition sites of *Kpn*I and *Bam*HI, which makes difficult to cut plasmids at once. However, 300 bp length fragment, appeared after electrophoresis of double digest plasmid samples enabled recovery of properly cut plasmid backbone from the agarose gel (Fig 3.11). Then, plasmid backbone was isolated from the gel and ligated with *Kpn*I and *Bam*HI digested inserts. After transformation of ligation reactions into XL10-Gold ultracompetent *E. coli* cells (Agilent, CA, USA), positive transformants were analyzed by colony PCR using gene-specific primers. Other than GPC, which encodes a full-length polyprotein of CCHFV glycoprotein, all native protein expressing vectors were generated and confirmed by PCR (Fig 3.12).

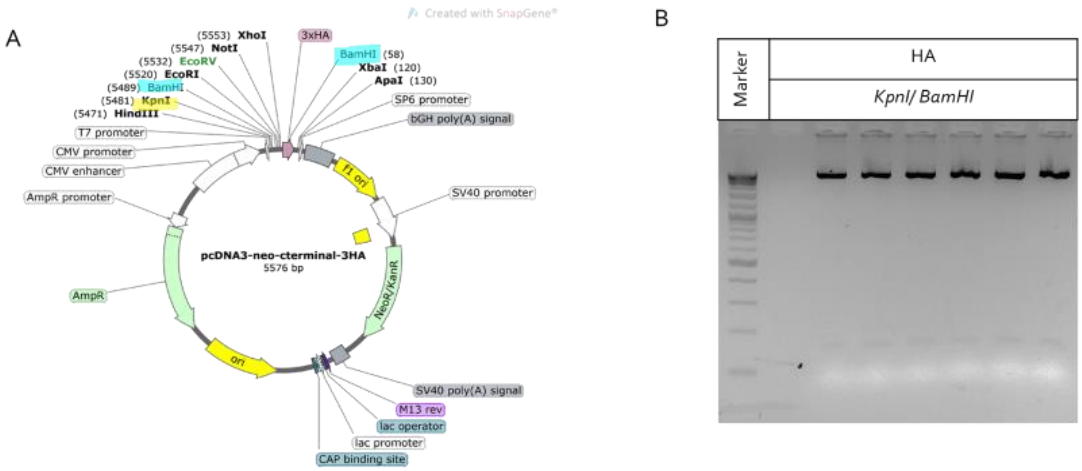

Figure 3.11 : A) The plasmid map of pcDNA3-neo-cterminal-3HA with restriction sites, highlighted. B) Agarose gel electrophoresis of the double digested vector.

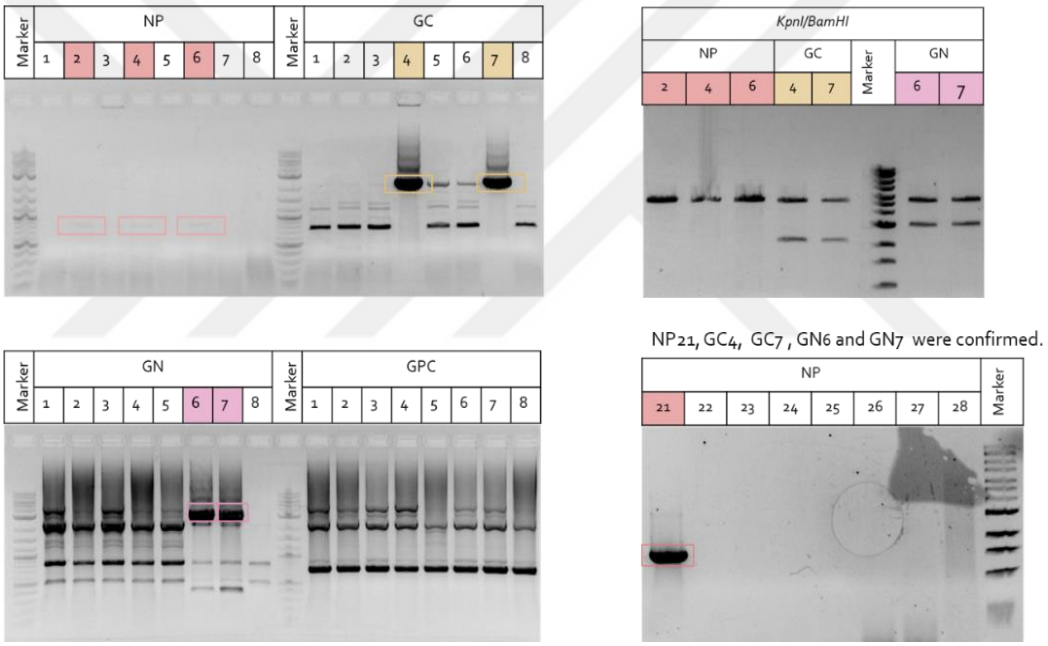

Figure 3.12 : Analysis of colony PCR products for each selected positive transformants on agarose gel. Rectangles indicate desired band appeared after PCR samples run on the gel. Red: NP, Yellow: Gc, Pink: Gn.

To visualize VLPs by fluorescent or confocal microscopy, EGFP fused gene vectors were generated. To construct the plasmids, first, NP and Gc sequences were amplified without stop codon, double digested by *Kpn*I and *Xho*I, and separately ligated into 3EGFP vector as described above. Three positive transformant colonies were selected for each and analyzed by PCR and restriction analysis (Fig 3.13).

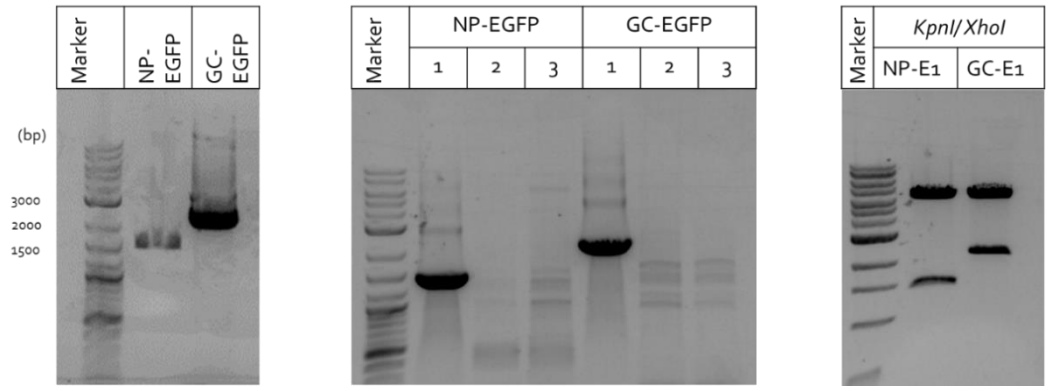

Figure 3.13 : Confirmation of NP-EGFP and GC-EGFP vector constructions by PCR, colony PCR and restriction analysis, respectively. Gc: 2228 bp, NP: 1472 bp

3.1.3.2 Transfection analyses of pcDNA 3.1 plasmids into mammalian cells

First, 293T cells were transfected with 3EFGP using PEI as a transfection reagent to test the transfection efficiency. At 48 hr post transfection, the cells were visualized under fluorescence microscope after two days (Fig 3.14).

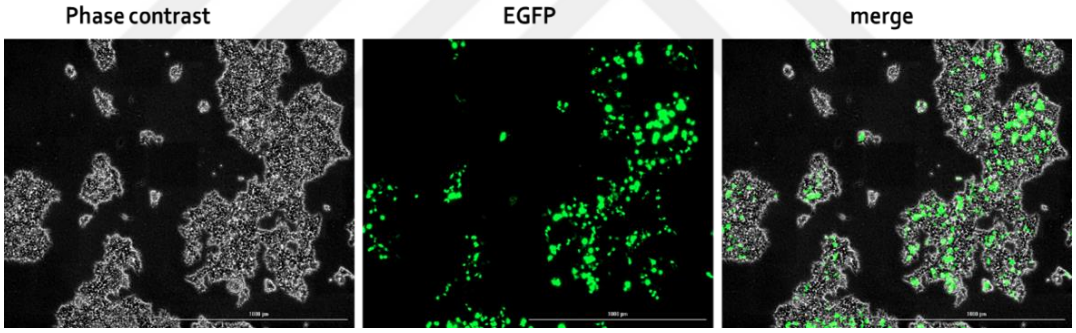

Figure 3.14 : Imaging of 293T cells transfected with pcDNA 3EGFP plasmids under fluorescence microscopy (Cytation 5, Biotek, USA).

Then, pcDNA 3.1 plasmids encoding viral genes were transfected into 293T cells in a different combination of plasmids. Also, FBS supplementation during transfection was questioned. Cell culture supernatants and pellets were collected three days post-transfection. Supernatant samples were ultracentrifuged at 150.000 g for 4 hours to analyze VLP formation. All samples were analyzed by Western Blot using inactivated CCHFV-immunized mice sera (Fig 3.16). Interestingly, similar band patterns were observed in all samples. The appearance of the same band profile in negative control samples indicated that any discriminative analyzes could not be done with these Western Blot images.

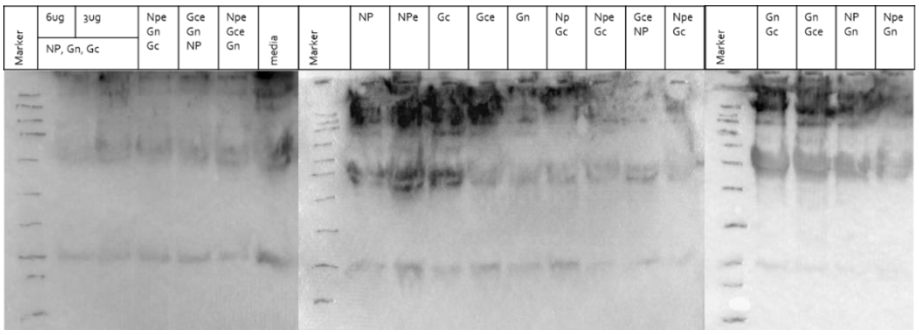

Figure 3.15 : Western Blot analysis of transfected 293T cells using mice sera immunized with inactivated CCHFV. For negative control (NC), molecular grade water instead of plasmids was used. Membranes were incubated with sera of mice immunized with inactivated CCHFV at 1:1000 dilution, then probed with goat anti Mouse IgG-HRP antibodies at 1:3000 dilution. Membranes were processed for chemiluminescence detection and visualized by using Fusion FX Solo imaging system (Vilber, Collégien, France).

Although various PEI transfection optimization studies were conducted for 293T cells, any viral protein specific signal was not detected in Western Blot analysis, indicating that 293T cells may not be suitable for this CCHFV VLP model. Besides, transfection of 293T cells were challenging because they detach easily from the plate bottom even while the plates were moved from incubator to microscope for imaging. Considering that the problem might be caused by cell lines, it was decided to introduce the vectors to the Huh-7 cells as donor cells. Transfection optimization studies were first conducted with pcDNA3 EGFP by using of a transfection reagent, PEI both in different forms (linear or branched) and in a different ratio with DNA to be transfected. Also, the effect of FBS supplementation during transfection was questioned. (Figure 3.16). Accordingly, the expression level of EGFP was found optimum in cells supplemented with FBS and transfected in a PEI (linear) to DNA ratio of 1:3.

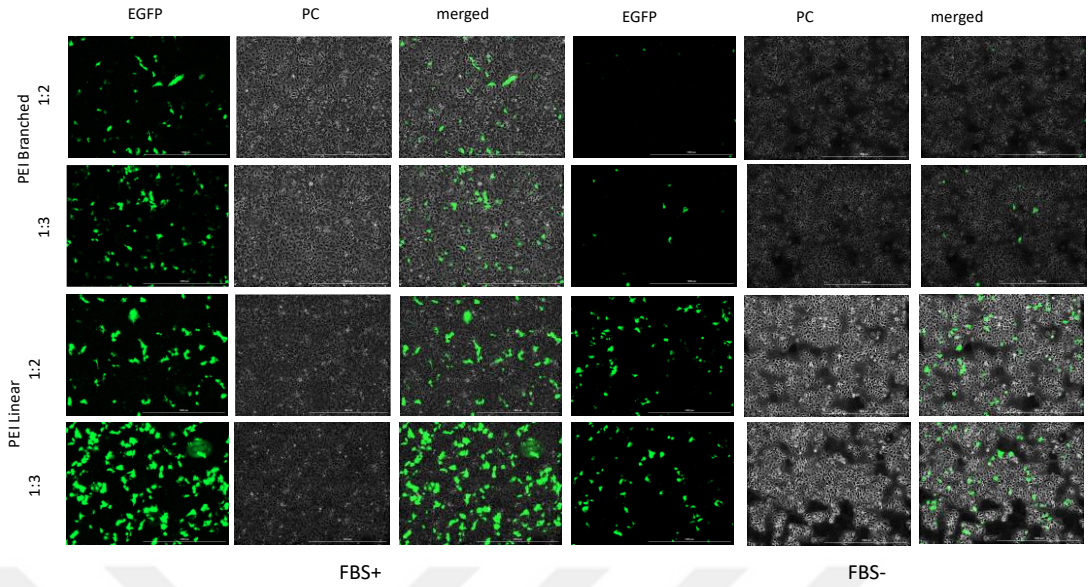

Figure 3.16 : Optimization of transfection conditions for Huh-7 cells. The effect of different factors on transfection, such as different DNA:PEI ratios (1:2 or 1:3), different forms of PEI (linear or branched), and FBS supplementation were evaluated,. Cells were transfected with 2 µg pcDNA3 EGFP and viewed under fluorescence microscopy 48 post-transfections. PC: phase contrast (Cytation 5, Biotek, USA).

Further optimizations on DNA:PEI ratio (1:2, 1:3, and 1:4) with increasing amount of DNA were performed with cells supplemented with FBS during the transfection (Figure 3.17). Although the highest fluorescent signal was visualized in cells transfected with a high concentration of PEI (1:4 ratio), its toxicity to cells has increased (Figure 3.17A), therefore, the best results were obtained from cells transfected with 3 µg DNA with a DNA:PEI ratio of 1:3, according to the RFU measurement (Figure 3.17B). According to the results achieved from these optimization studies, following experiments were performed with Huh-7 cells grown on 6-well plates and transformed with 3 µg DNA with a DNA:PEI ratio of 1:3 with FBS supplementation. The DNA amount used for the transfection was calculated proportionally depending on the type of cell culture plates utilized for each assay.

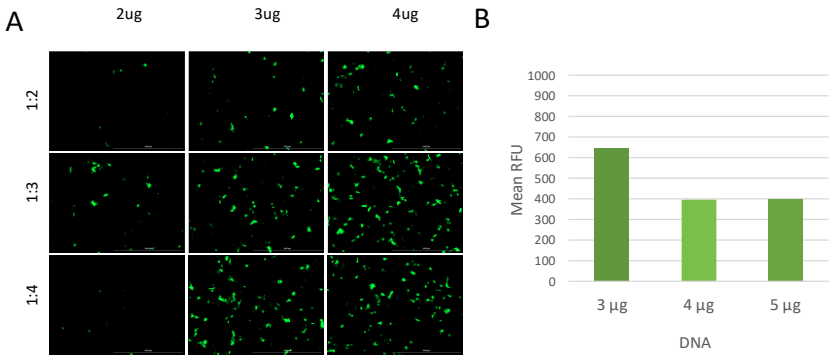

Figure 3.17 : Figure 3. 13: Optimization of transfection efficiency on Huh-7 cells according to DNA:PEI ratio and DNA amount. A) Cells were transfected with different amount of DNA (2, 3, and 4 µg pcDNA3 EGFP plasmids) in a different ratio of DNA to PEI (1:2, 1:3, and 1:4). B) Measurement of RFU in transfected cells to determine of optimum amount of DNA used in a 1:3 DNA to PEI ratio. Mean RFU were corrected for the background fluorescence and calculated by BioTek Gen5 Data Analysis Software. RFU: relative fluorescence unit. eGFP (excitation: 479 nm, emission: 520 nm).

Since the last Western Blot experiments have not been able to sufficiently show the expression of viral proteins, other techniques have been used to examine the synthesis of viral proteins. First, the fluorescent microscopy technique was used, in which Huh-7 cells were transfected with plasmids expressing Np and Gc proteins in fusion with eGFP. Fluorescence microscopy images at 48 hours post transfection showed that both proteins were successfully produced and had various subcellular localizations (Figure 3.18). While Gc was uniformly distributed across the cell surface, Np was primarily found in the perinuclear region. These different expression profiles may imply that viral proteins were expressed recombinantly and functioned properly.

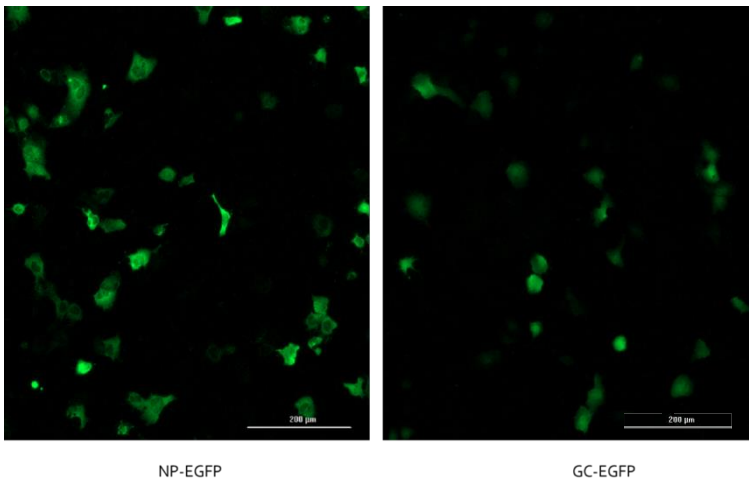

Figure 3.18 : Figure 3. 14: Visualization of differential cellular localization of NP-EGFP and GC-EGFP proteins transfected into Huh-7 cells under fluorescent microscopy.

As the presence of viral proteins was indirectly demonstrated by fluorescence microscopy, additional expression analyzes were performed to assess production. Proteins produced by pcDNA 3.1 plasmids were first analyzed by ELISA method. The supernatant samples from transfected Huh-7 cells in 96 well plates were analyzed by ELISA using CCHFV-immunized mouse and rabbit sera, and CCHFV-specific mouse mAb antibody cocktail including anti-Np (9D5), anti-Gn (8F10), and anti-Gc (11E7) primary antibodies., followed by incubation with suitable secondary antibodies for each assay (Figure 3.19).

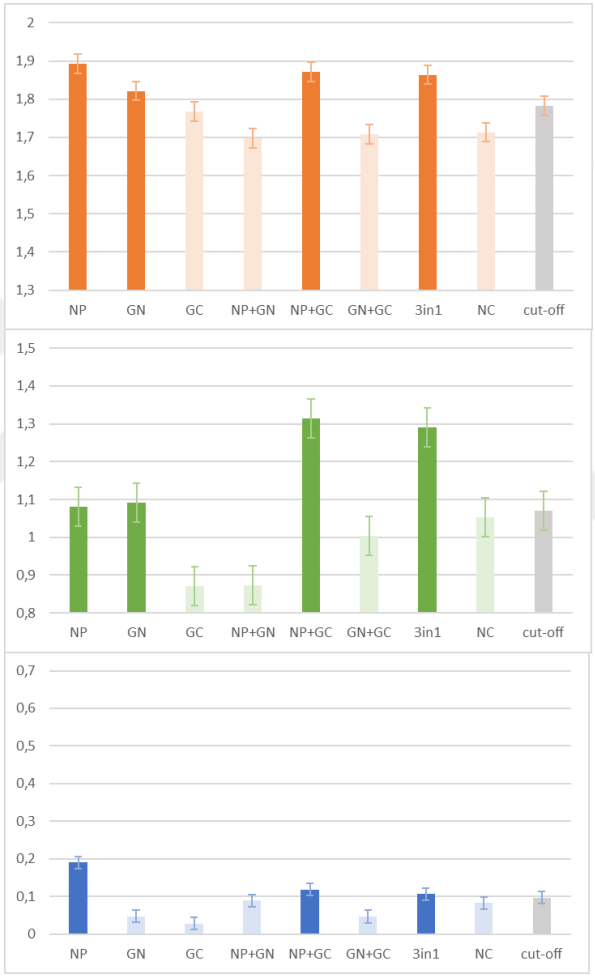

Figure 3.19 : Analysis of cell culture samples obtained from the Huh-7 cells transfected with different combination of viral plasmids, by in house ELISA tests. Plates were coated directly with samples, and the samples were probed with CCHFV-immunized mouse (orange), and rabbit sera (green), and with mouse monoclonal antibody cocktail (blue), constituted by the mixing of anti-NP(9D5), anti-Gn (8F10), and anti-Gc (11E7). The relevant HRP-conjugated secondary antibodies were utilized for detection. The absorbance of each sample was measured at 450 nm using iMark microplate reader (Bio-Rad, California, USA)

As a result, it was observed that positive samples had almost similar pattern in all tests (Figure 3. 19). All antibodies detected the viral proteins in the samples of "3in1", in which all viral plasmids were transfected simultaneously (Figure 3. 19). The reproducibility of this results suggested that CCHFV VLP might be formed via pcDNA3.1 plasmid. Interestingly, Np+Gc cell culture samples were detected positive in CCHFV-immunized animal sera. The Gn was also tested positive in all assays except specific antibody ELISA, suggesting that Gn might be able to be packed alone in the Golgi, due to its Golgi retention signal on their sequence. Additionally, Np was detected in all assays tested here, which may provide additional evidence to the previous study reporting that Np forms sphere-like structures in cytoplasmic vesicles after its expression using baculovirus expression system [216]. This analyzes showed that viral proteins were successfully expressed by using pcDNA3.1 vector and some of their combinations may contributed to form VLPs in transfected cells. To confirm viral protein production in transfected cells, further analyzes were conducted by Western Blot assays.

To overcome the detection limit problem faced with previous Western Blot analysis, here all three viral plasmids were transfected simultaneously into Huh-7 cells grown on T75 flask. The amount of plasmids were increased proportionally to cell number and the transfections were prolonged to 96 hours. Then, clear lysates and ultracentrifuged cell culture samples, run on both Native-PAGE and SDS-PAGE samples were analyzed by Western Blot using CCHFV-immunized animal sera so that, antibodies found in these sera may be able to recognize confirmational and linear epitopes on antigens. Besides, mock transfected cell samples as negative controls were loaded onto same gels (Figure 3.20). As results, when the membranes were incubated with CCHFV-immunized mice sera after SDS-PAGE, pre-Gc (85 kDa) and Gc (75 kDa) were detected in the lysates while similar bands around 130 kDa and 245 kDa for Gn were appeared in cell culture supernatant samples, referring to the Figure 3.6, in which the same bands were visualized in Gn transfected cell lysate (Figure 3.20A). Meanwhile, Np (53 kDa) proteins were detected both in lysate and supernatant samples, when they transferred to the membrane after Native-PAGE (Figure 3.20B). Finally, all three proteins Np, Gn, and Gc were recognized by the antibodies found in the CCHFV-immunized rabbit sera (Figure 3.20C). Accordingly, these results

indicated that viral proteins were successfully expressed via pcDNA3.1 plasmids in Huh-7 cells.

A final analysis was carried out to investigate the underlying cause of the problem encountered in viral protein production. Successful transfection of the eGFP-expressing plasmid used in transfection optimization suggests that the problem was not due to transfection. However, even if plasmid DNAs enter the cell, they may not be transcribed. The pDZ and pCAGGS plasmids have the chicken beta actin promoter with the CMV enhancer, while the pcDNA 3.1 vectors have the CMV promoter. Therefore, differences in transcription abilities are likely to be observed.

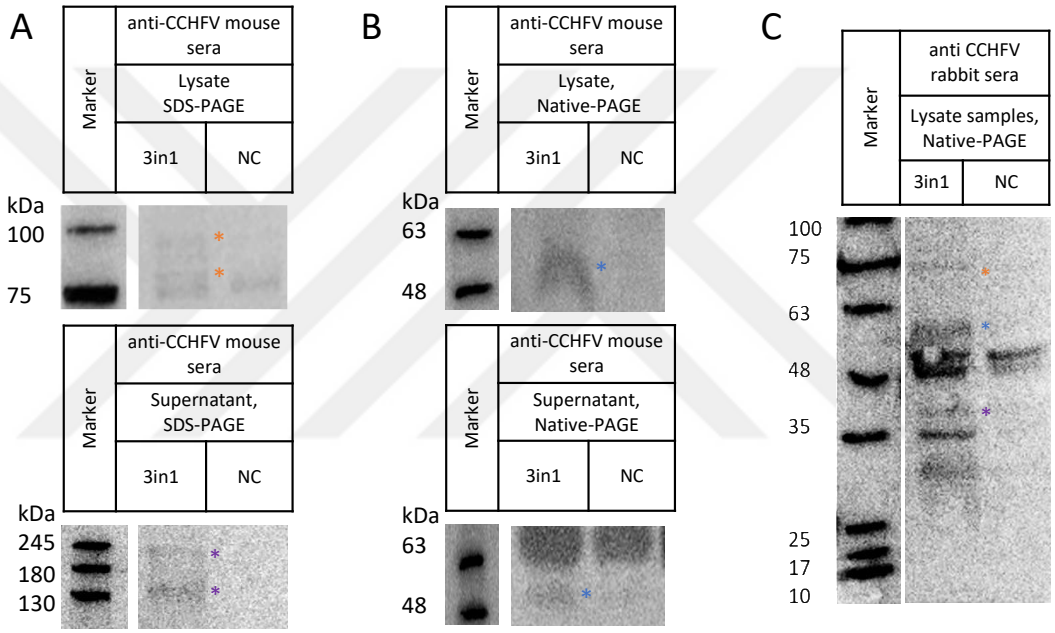

Figure 3.20 : Western Blot analysis of viral proteins in Huh-7 cells, transfected with all plasmids together. Lysate and supernatant samples analyzed using CCHFV-immunized mouse sera were either dissolved on SDS-PAGE (A) or on Native-PAGE (B), while lysate proteins dissolved on Native-PAGE were analyzed using CCHFV- immunized rabbit sera (C).

To test the mRNA transcript levels of each vector after transfection, Huh-7 cells were transfected with the related plasmids carrying all three genes in separate vectors. All mRNA was then isolated, and qPCR was performed using specific primers to amplify approximately the last 130 bases of each gene. Accordingly, the CMV promoter was more able to transcribe the mRNAs of the CCHFV viral genes compared to the chicken beta actin promoter (Figure 3.21). Both immunological and fluorescent microscopy analyzes with pcDNA 3.1 plasmids confirmed this information. Although not as high as pcDNA 3.1 ($4x10^5$), approximately $3x10^4$ times higher viral mRNA transcription

was observed in other expression systems compared to housekeeping gene, GAPDH (Figure 3.21). As a result, both the relatively low level of transcription and the lack of an optimized sequence of encoding viral genes may have prevented the production of viral proteins in amounts that could be detected by Western Blot method. However, due to the strong transcription capability of the CMV promoter, it was speculated that this problem may have been circumvented with the pcDNA 3.1 vector.

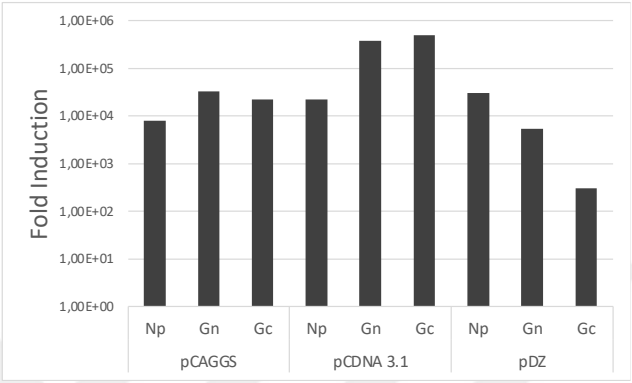

Figure 3.21 : Post-transcriptional analysis of viral mRNAs generated in different expression systems by RT-PCR. Using GAPDH as an internal control, data were normalized to the control cell value which was set to be 1. The relative gene expression levels were measured using the 2−ΔΔCT method.

In conclusion, the results obtained from the preliminary studies required for CCHAV VLP production in this thesis show that viral proteins of CCHFV Kelkit 06 strain can be produced in Huh-7 cells using pcDNA 3.1 plasmid. Although ELISA results imply that various viral protein combinations produce different VLP compositions, further studies were needed to confirm the results obtained in this thesis.

3.1.4 Designing of an unique minigenome plasmid for CCHFV

To study viral replication and transcription, as well as entry, assembly, and budding of CCHFV, a transcriptionally competent VLP model is required. To achieve this goal, a minigenome plasmid is needed to be packaged into the VLP, such as the CCHFV segment. With a unique strategy, an ambisense minigenome plasmid was so designed that may transcribe vRNA in VLP forming donor cells without using any viral polymerases. The minigenome plasmid named as the 7miniC plasmid was produced by insertion of the vRNA coding cassette into the pTWIST CMV Puro vector and was commercially available from Twist Bioscience (CA, USA). In this ambisense vRNA coding cassette, a reporter gene in positive polarity was located between the antisense 3'UTR and 5'UTR sequences of the CCHFV L segments and downstream of the T7

promoter region was encoded and two additional UTR sequences (NEO UTR2 and NEO UTR 3) in sense orientation were inserted upstream of the reporter gene to increase its expression. According to a recent article, this UTR combination has enabled 200 times higher GFP protein production in contrast to control plasmid which does not have any additional UTRs [217]. To generate synthetic RNAs with a precise 3′ end, the hepatitis delta virus ribozyme (HDVR) sequence was added to the final nucleotide of the viral genome. (Figure 3.22). After transfection of vRNA-like in vitro transcripts together with viral protein encoding plasmids into donor cells, viral proteins may pack it during VLP formation and VLPs can be released into cell culture media. Upon its attachment on other naive cell membrane, minigenome RNA can be released into the cytoplasm and the reporter gene can be expressed in indicator cell.

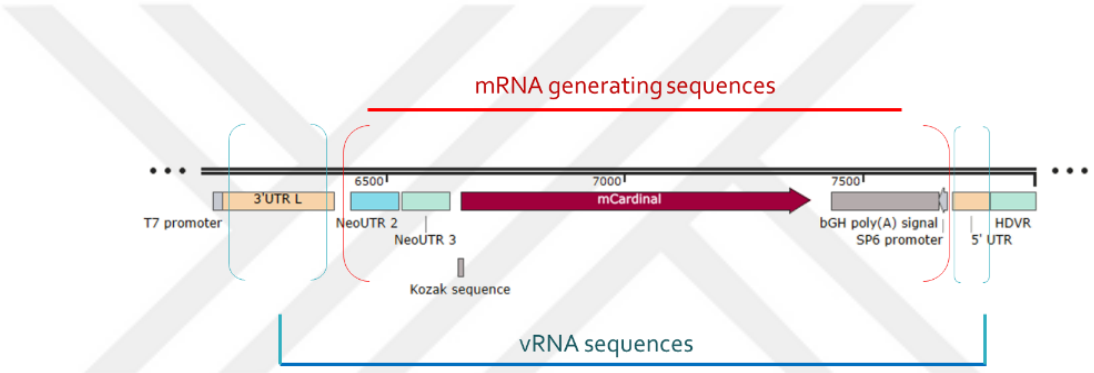

Figure 3.22 : Partial vector map showing the ambisense vRNA-encoding cassette in 7miniC plasmid. The mRNA generating sequence, in which ORF of reporter gene together with the regulatory sequences, recognized by human protein translation system was inserted between negative sense viral UTR sequences, providing viral genome packaging signal.

To demonstrate proof of concept, in vitro transcribed minigenome RNA transcripts, carrying either mCardinal (7miniC) or eGFP (7miniE) as reporter gene were transfected into Huh-7 cells using Lipofectamine or PEI. The expression of reporter gene was visualized by laser scanning confocal microscopy (Figure 3.23).

In this study, a unique ambisense minigenome system was developed for CCHFV. Unlike existing systems, the fact that this new minigenome system does not require additional helper virus or viral RNP complex has brought an innovative approach for CCHFV reverse studies.

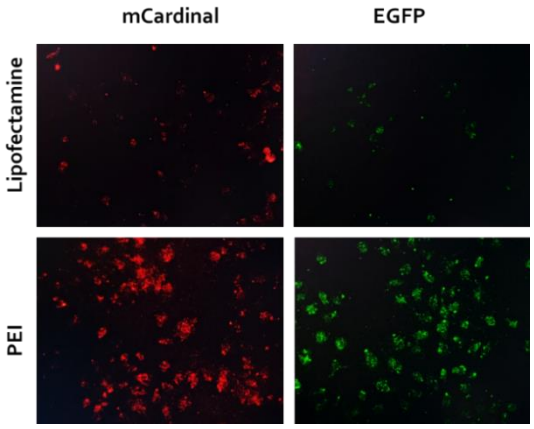

Figure 3.23 : Confocal laser scanning microscopy (CLSM) images of Huh-7 cells transfected with 7miniC (red) and 7miniE (green) *in vitro* transcripts using PEI or lipofectamine at 6 hours post-transfection.

Within the scope of this thesis, extensive studies on viral protein expression have been carried out to develop a VLP that will enable us to better understand CCHFV, a highly pathogenic and increasing prevalence virus. BSL-4 facilities are a requirement to study such pathogens as there are no approved treatments. In this sense, the development of a safe models that simulate the virus infection particularly such as replication competent VLPs has a vital role in virology. In this thesis, various studies have been carried out to ensure proper expression of viral proteins of CCHFV Kelkit 06 strain in mammalian cells, which will lead to the development of such a VLP model. In addition, the inclusion of the newly developed minigenome system in future VLP studies will pave the way for studies on both the life cycle of CCHF and the development of antiviral treatment methods.

3.2 Studies on Plasmid-Based Virus Like Particles for SARS-CoV-2 a positive sense RNA virus in *P. pastoris*

3.2.1 Designing of plasmids for VLP-based vaccine candidates for SARS-CoV-2

In addition to basic virological research, the other objective of this thesis was to demonstrate one of the reverse genetic applications in the field of translational biotechnology. For this purpose, it was aimed to demonstrate the importance of reverse genetics, utilized in studies to generate treatment agents. To this aim, VLP-based vaccine candidates were designed for SARS-CoV-2 virus, one of the positive RNA viruses that recently caused the COVID-19 pandemic. The SARS-CoV-2 structural

genes were commercially optimized according to *P. pastoris* expression system, were cloned into pPICZA vector, and were confirmed by restriction analyzes using *Bgl*II and *Bam*HI (Figure 3.24).

Due to the prediction that the minimum protein content to form a VLP structure is M and E proteins, and the antigenic properties of S and N proteins, four different SARS-CoV-2 VLPs plasmids, called SEM, SEN, SENM and ENM according to encoded genes, were designed (Figure 3. 25).

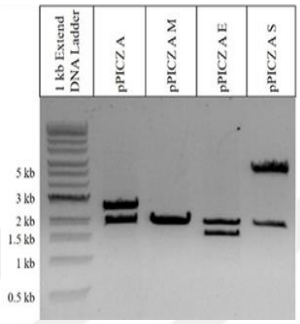

Figure 3.24 : Conformation analysis of SARS-CoV-2 plasmids on agarose gel electrophoresis

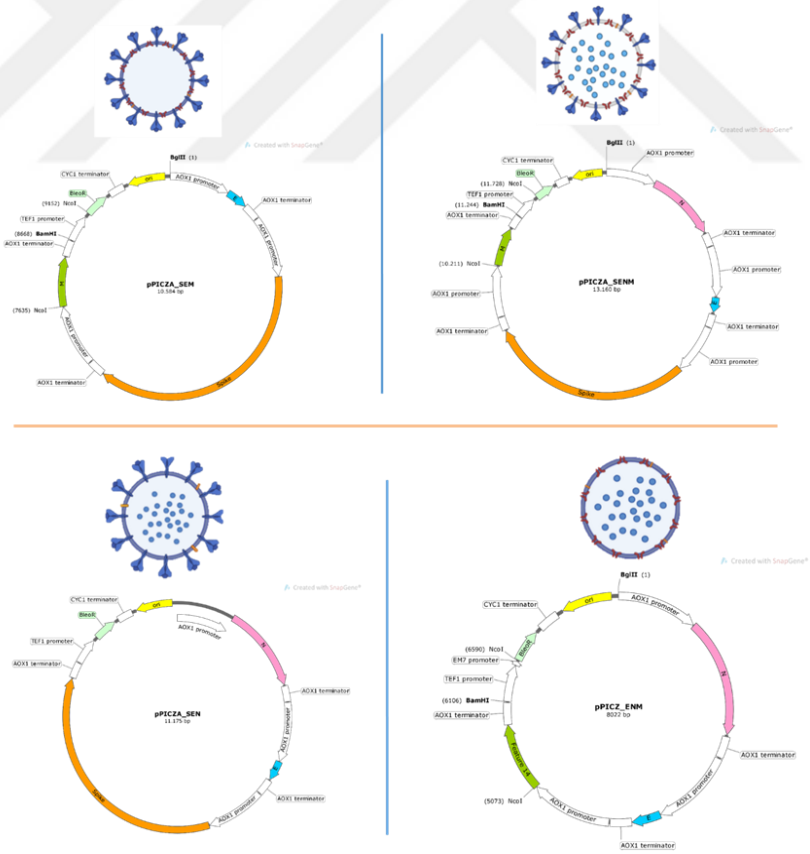

Figure 3.25 : The plasmids map and the resulting SARS-CoV-2 VLP structures consisting of different combinations of spike, envelope, membrane and nucleocapsid proteins. The plasmids were named according to the coronavirus genes they carry.

To produce these VLP by transformation of a single plasmid encoding multiple expression cassettes for each the viral genes; first, the gene of interest was inserted into the vector between *Eco*RI and *Sal*I sites. The resulting expression cassette (the AOX1 locus plus a viral gene) was flanked on the upstream side by *Bgl*II site and on the downstream by *Bam*HI enzyme recognition sites on the pPICZA plasmid. This expression cassette was excised with *Bgl*II and *Bam*HI and then, reinserted at the BamHI site of other expression cassette to create a tandem repeat of the cassette. The reinsertion process can be repeated to generate a series of vectors that contain multiple expression cassettes. Additionally, *Nco*I enzyme was utilized to be able to generate some of the VLP plasmid constructs, in order to overcome internal cut sites problem, appeared on sequences of newly constructed plasmids (Figure 3.26).

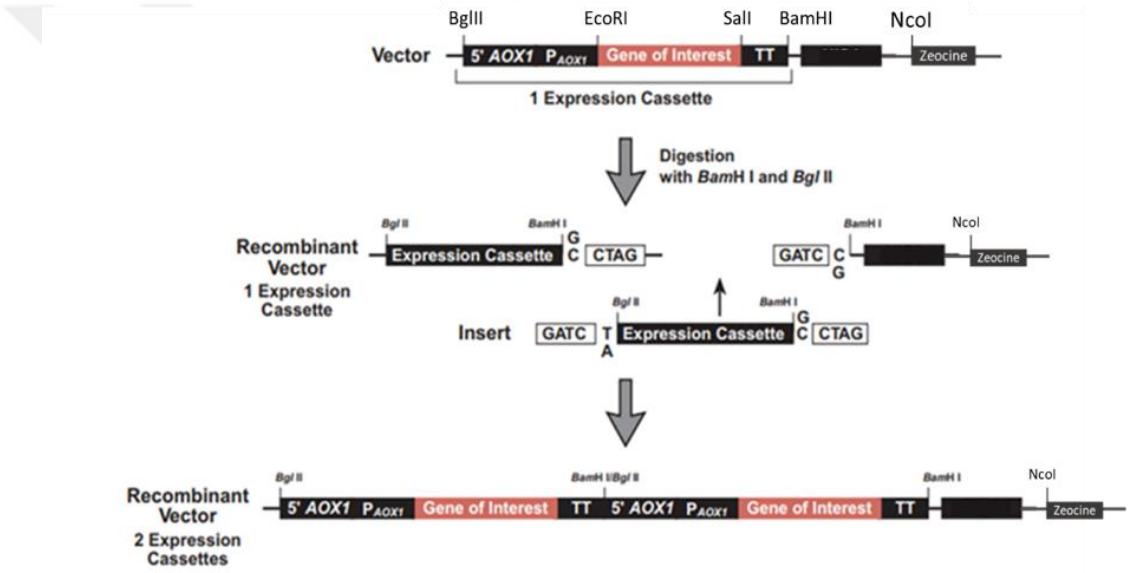

Figure 3.26 : Generation of multiple expression cassettes in a single vector prior to transformation into yeast cells.

In order to generate SEM and SEN plasmids, first a SE plasmid were generated by ligation of the *Bgl*II and *Nco*I digested pPICZA_S plasmid with the *Bam*HI and *Nco*I digested pPICZA_E plasmid. Subsequently, the resulting pPICZA_SE plasmid (8599 bp) was cut with *Bgl*II and *Nco*I and ligated with the *Bam*HI and *Nco*I digested pPICZA_N plasmid. At the end of these procedures, the pPICZA_SEN plasmid with a size of 11,175 bp was generated (Figure 3.27).

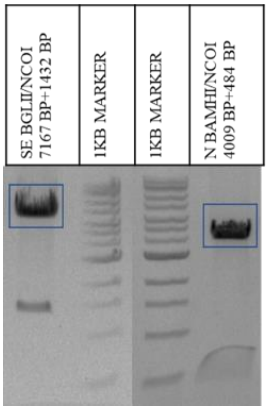

Figure 3.27 : Construction of the SARS-CoV-2 VLP forming pPICZA_SEN plasmid. Blue rectangles are used to mark digested DNA fragments to be ligated to construct the plasmid.

For pPICZA_SEM; plasmid pPICZA_SE was linearized with *Bam*HI and ligated with *Bgl*II and *Bam*HI digested pPICZA_M. At the end of these processes, the pPICZA_SEM plasmid with a size of 10,584 bp was generated. (Figure 3.28). The subcloned plasmids, pPICZA_SEN an pPICZA_SEM, were transformed into Top10 *E. coli* cells and conformational analysis were performed by using *Eco*RI and *Sal*I restriction enzymes (Figure 3.29).

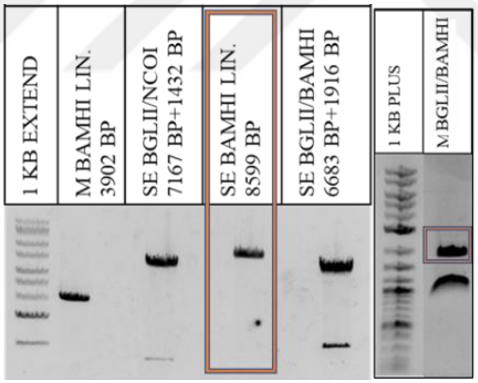

Figure 3.28 : Construction of the SARS-CoV-2 VLP forming pPICZA_SEM plasmid. Orange rectangles are used to mark digested DNA fragments to be ligated to construct the plasmid.

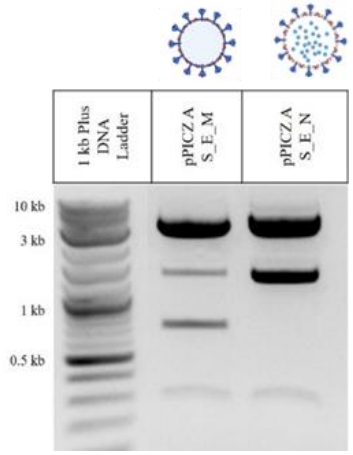

Figure 3.29 : Confirmation of the constructed plasmids, pPICZA_SEM and pPICZA_SEN with restriction analysis using *Eco*RI and *Sal*I. Lane 1: 1 kb Plus DNA Ladder, Lane 2: 10584 bp pPICZA SEM (3834 bp Spike + 3221 bp vector fragment + 1304 bp AOX promoter +AOX terminator + 681 bp Membrane + 240 bp Envelope), Lane 3: 11175 bp pPICZA SEN (3834 bp Spike + 3221 bp vector fragment + 1304 bp AOX promoter /AOX terminator + 1272 bp Nucleocapsid + 240 bp Envelope).

In addition, two different plasmids were developed to produce VLP constructs containing full structural proteins of SARS-CoV-2, called SENM and the other VLP without Spike protein, so called ENM VLPs. First, the plasmid pPICZA_SENM, was generated by the ligation of BamHI linearized pPICZA_SEN plasmids with BglII and BamHI digested pPICZA_M. (Figure 3.30).

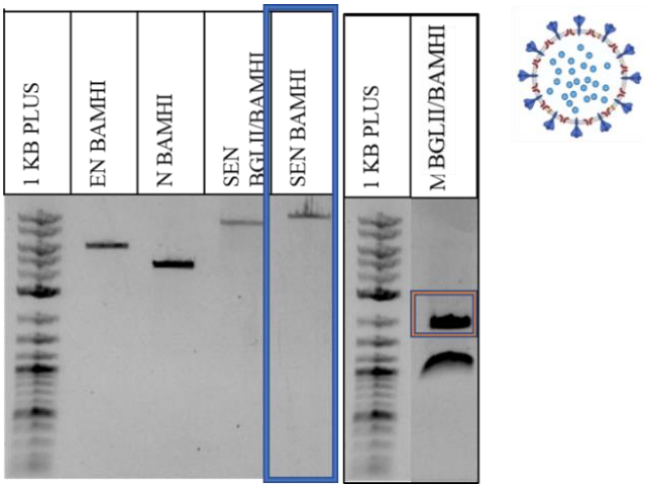

Figure 3.30 : Construction of the SARS-CoV-2 VLP forming pPICZA_SENM plasmid. Orange and blue rectangles are used to mark digested DNA fragments to be ligated to construct the plasmid.

Following transformation into Top10 *E. coli* cells, plasmids were isolated from a positive transformant and analyzed and confirmed by restriction enzymes, *Bam*HI and *Nco*I in a comparison with an early confirmed pPICZA_SEM plasmid. Comparative

analysis of SENM and SEM plasmids showed the molecular weight difference caused by the nucleoprotein expression cassette (2576 bp) on agarose gel (Figure 3.31).

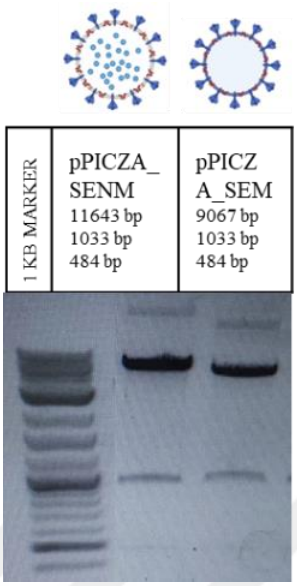

Figure 3.31 : Confirmation of the pPICZA_SENM in comparison with pPICZA_SEM by restriction analysis using *Bam*HI and *NcoI*. Lane 1: 1 kb Plus DNA Ladder, Lane 2: pPICZA_SENM (11643 bp Spike, Envelope and Nucleoprotein expression cassettes+ 1033 bp Membrane + 484 vector fragment), Lane 3: pPICZA SEM (9067 bp Spike and Envelope expression cassettes + 1033 bp Membrane + 484 vector fragment).

In addition, another plasmid was created to form the ENM VLP construct without the Spike protein. For this purpose, firstly, pPICZA_E was cut with *Bgl*II/*Nco*I and ligated with *Bam*HI/*Nco*I disested pPICZA_N. The resulting 6029 bp pPICZA_EN plasmid was then linearized with *Bam*HI, and the expression cassette of M flanked with *Bgl*II and *Bam*HI enzymes was subcloned into pPICZA_EN plasmid. Following these steps, the 8022 bp length plasmid pPICZA_ENM was generated (figure 3.32) and confirmed by both restriction digestions with either *Bgl*II and *Bam*HI or *Eco*RI and *Sal*I enzymes, and PCR analysis using primers amplifying E (240 bp) and M (681 bp) genes (Figure 3.33).

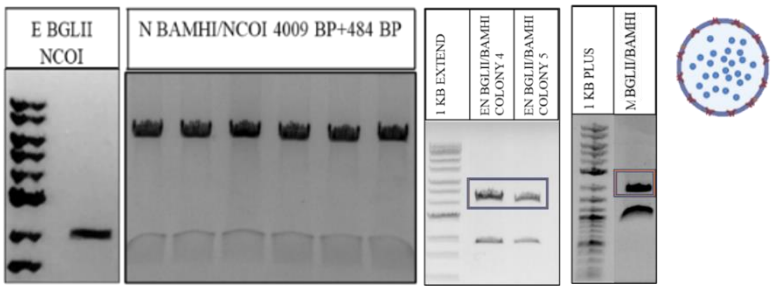

Figure 3.32 : Construction of the SARS-CoV-2 VLP forming pPICZA_ENM plasmid. Orange and blue rectangles are used to mark digested DNA fragments to be ligated to construct the plasmid.

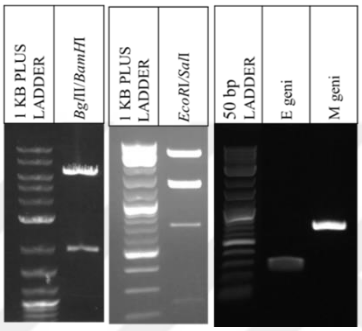

Figure 3.33 : Confirmation analyzes of the pPICZA_ENM plasmid by double-digestion using *Bgl*II and *Bam*HI and *Eco*RI and *Sal*I, and by PCRs, which specific to detect envelope (E) and membrane (M) genes of SARS-CoV-2.

3.2.2 Transformation of SARS-CoV-2 VLP forming plasmids into yeast cells

All subcloned plasmids were first propagated in Top10 *E. coli* cells and then transformed into *P. pastoris* GS115 strain yeast cells by electroporation. Positive transformants were analyzed by either PCRs or restriction analyzes (Figure 3.34). The pPICZA_SEM and pPICZA_ENM transformed yeast cells were analyzed by PCR using primers targeting the E and M genes, while the primers targeting the N gene were utilized in SEN samples. Accordingly, 2 out of 10 colonies (colony number 4 and 7) for SEM; 4 out of 10 colonies (colony number 2, 4, 6, 8, and 9) for ENM; and 3 out of 9 colonies (colony number 2, 4, and 6) for SEN were tested positive (Figure 3.34). The colonies transformed with pPICZA_SENM were analyzed by double digestion using both *Eco*RI-*Sal*I, and *Bam*HI-*Nco*I, resulting in 8 out of 9 colonies confirmed (Figure 3.34). Additionally, all plasmids were confirmed once again by *Bgl*II digestion (Figure 3.35).

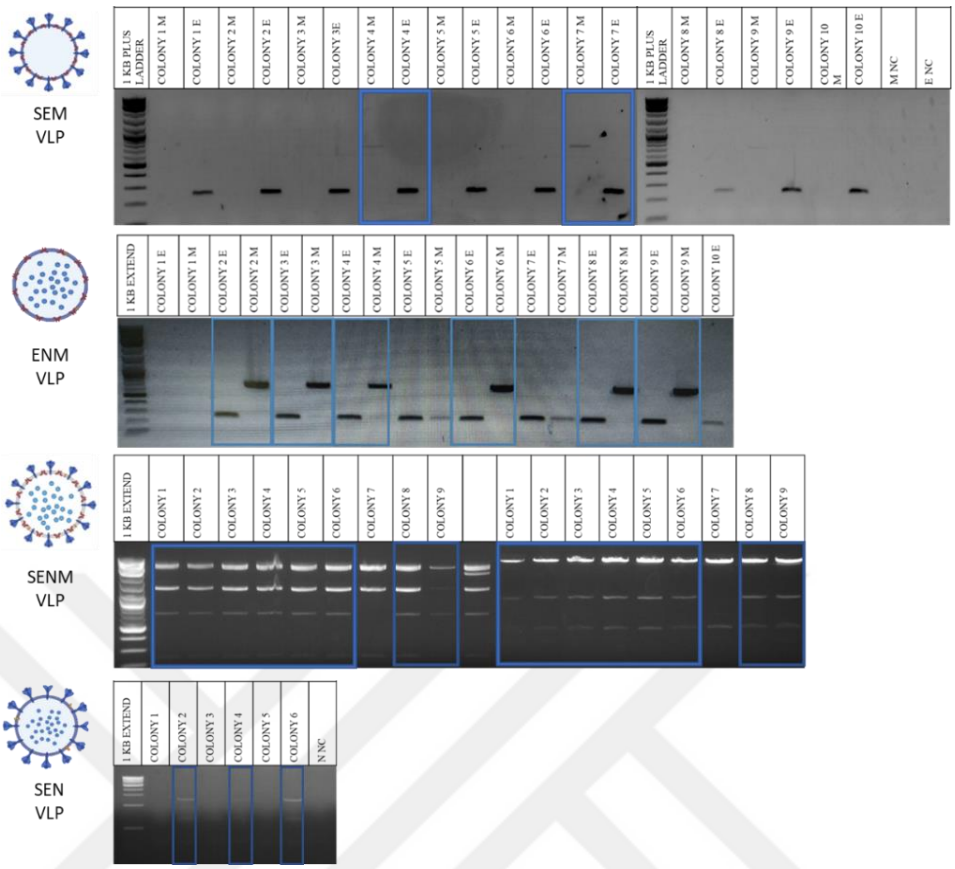

Figure 3.34 : Agarose gel electoropheresis analyzes of GS115 cells selected after transformation with SARS-CoV-2 VLP plasmids. Positive transformant colonies transfected with SEM, ENM and SEN VLP plasmids were analyzed by PCR while SENM VLP samples by double digestion using both *Eco*RI-*Sal*I (left), and *Bam*HI-*Nco*I (right). After PCRs, the considered band lengths are 240 bp for E; 681 bp for M; 1362 bp for N. The corresponding bands after EcoRI-SalI digestion were 3834 bp, 3221 bp, 1272 bp, 1334 bp, 681 bp, 240 bp, while 11643 bp, 1033 bp, 484 bp after BamHI-NcoI digestion. Blue rectangles indicate the correct bands appeared on the gel.

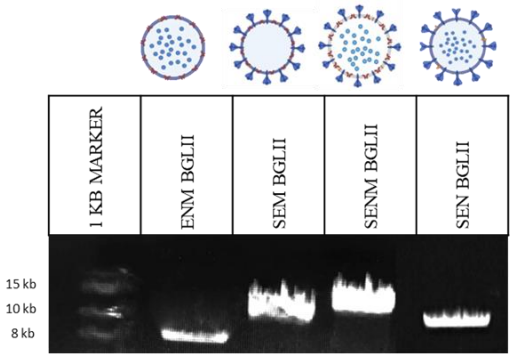

Figure 3.35 : Confirmation of constructed plasmids encoding multimer expression cassettes to generate different SARS-CoV-2 VLPs. Plasmids were linearized with *Bgl*II enzyme and loaded on agarose gel. Lane 1: 1 kb DNA Ladder, Lane 2: pPICZA_ENM (8022 bp), Lane 3: pPICZA_SEM (10584 bp), Lane 4: pPICZA_SENM (13160 bp), Lane 4: pPICZA_SEN (1175 bp)

3.2.3 Expression of different VLP constructs in *P. pastoris* GS115 strain

To produce different VLP constructs, initially one colony from each recombinant GS115 strains were cultured at 28°C with daily methanol induction. Expression was terminated after five days, and the cells were collected by centrifugation. One milliliter cell culture from each were taken for analysis. Cell pellets were lysed with glass beads. Western Blot analysis was performed with clear lysates. Purified inactivated virus sample by ultracentrifuge precipitation of both SARS-COV-2 infected cell lysate and infected cell medium was used as positive control. Vero cell lysate uninfected with wild-type GS115 cell lysate was used for negative control. Rabbit primary antibody cocktail as primary antibody (rabbit anti-SARS-COV-2 Spike S1 protein monoclonal antibody, rabbit anti-SARS-COV-2 N protein monoclonal antibody and rabbit anti-SARS-COV-2 Envelope protein polyclonal antibody, each diluted 1:4000) was used. According to the chemiluminescent imaging results, significant bands were seen between 41-53 kDa level, which corresponds to the N protein (46.6 kDa), in both the positive control samples and the ENM VLP sample. Besides, same bands were also detected in other VLP structures including the N protein. However, only the band indicating spike protein was seen in the inactive virus sample (Figure 3.36). These results might be explained by low amount of antigen in samples which cannot be detected by Western Blot.

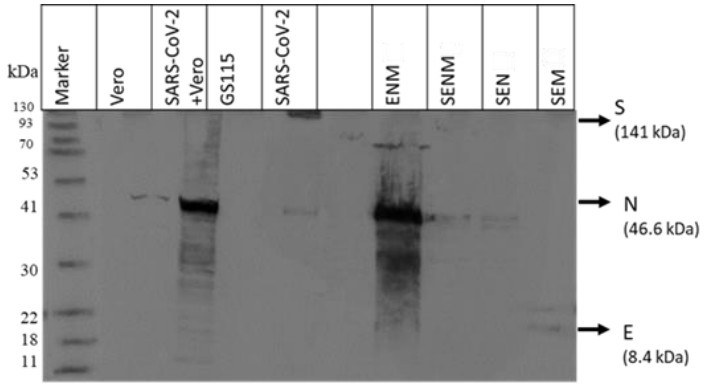

Figure 3.36 : Small-scale expression analysis of different recombinant GS115 strains transformed with VLP plasmids by Western Blot, in which proteins were transferred to nitrocellulose membrane and incubated with rabbit primary antibody cocktail containing anti-S1, anti-N, anti-E antibodies.

In order to overcome the detection limit problem in western blot, it was decided to analyze all culture pellets. Also, expression was repeated with different colonies. For this purpose, 100 ml expression pellets were dissolved in PBS and yeast cells were mechanically lysed using a homogenizer under high hydrostatic pressure. Then, the

samples were centrifuged, and cellular debris was removed from the lysate. To precipitate VLPs, clear lysates were centrifuged at 150.000 g for 4 hours on 20% sucrose cushion and the resulting pellets were dissolved with 1 ml of PBS. Western blot analysis was repeated using rabbit primary antibody cocktail under the same conditions (Figure 3. 37). In this experiment with more concentrated samples compared to the previous one, N protein (46.6 kDa) could be detected in SEN and SARS-CoV-2 virus-infected cell lysates. However, the N-specific antibodies could not bind to the proteins found in other VLP samples and even in wild-type virus sample. The S proteins were appeared only in virus samples and a very faint band indicating M were detected only in virus infected Vero cell lysate sample (Figure 3. 37).

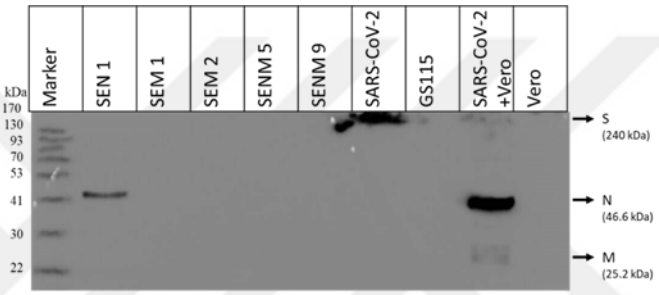

Figure 3.37 : Large-scale expression analysis of different recombinant GS115 strains transformed with VLP plasmids by Western Blot, in which proteins were transferred to nitrocellulose membrane and incubated with rabbit primary antibody cocktail containing anti-S1, anti-N, anti-E antibodies

Since rabbit monoclonal antibody sera and SEM and SENM proteins could not be visualized, Western Blot was repeated using SARS-COV-2 IgG positive human serum diluted 1:10,000, which we used in our previous study [214]. When human serum was used to probe antigens, bands at the level of the spike protein (141 kDa) were observed in all VLP samples containing spike protein. While bands showing nucleoprotein protein (46.6 kDa) were detected in SEN and SENM samples, bands were observed at the membrane protein level (25.2 kDa) in both SEM and SENM samples (Figure 3.38).

Finally, ENM samples were analyzed by Western Blot using mouse sera immunized with SARS-CoV-2 and all viral antigens both in ENM sample and in SARS-CoV-2 virion sample were successfully captured by mouse antibodies (Figure 3.39).

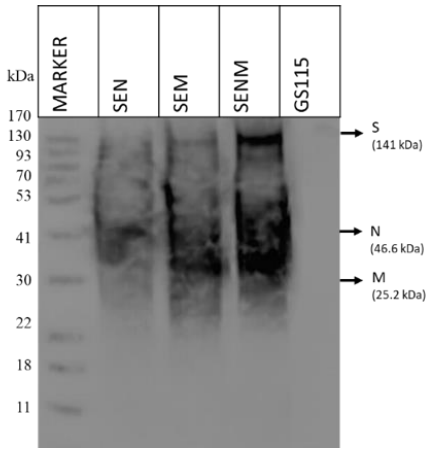

Figure 3.38 : Western Blot analysis of SARS-CoV-2 VLP antigens after expression in GS115 cells.

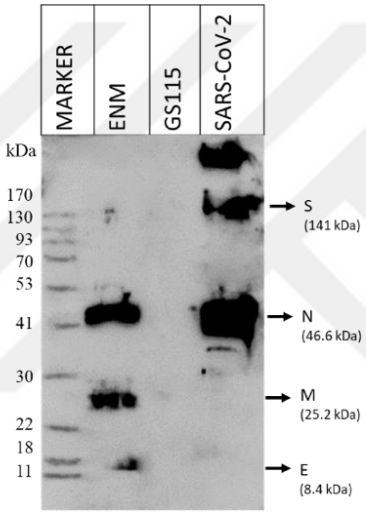

Figure 3.39 : Confirmation of ENM VLP production in GS115 cells.

4. DISCUSSION and CONCLUSIONS

4.1 CCHFV VLP studies representing applications of reverse genetics on a negative sense RNA virus

Studies on CCHFV are generally considered to be challenging owing to high risk of transmission, the need for BSL-4 facilities, lack of suitable animal models, difficulties in establishing highly productive infections in cell cultures and indistinct cytopathic effect in cells. Therefore, information on virus biology, immunology, and pathology especially afforded by individual proteins, will be valuable contribution to field of CCHFV virology. In the present thesis, different mammalian cell culture models were tested to generate a plasmid based VLP system for CCHFV, which may further facilitate studies on virus life cycle, discovery of new therapeutics, and on development of diagnostic tools. Various plasmids, employing distinct eukaryotic expression systems were constructed to express the viral proteins of CCHFV Kelkit 06 strain in mammalian cells.

Initially, viral proteins were subcloned into an ambisense plasmid, called pDZ, which was successfully used earlier in the influenza virus reverse genetics system [215]. In order to generate viral mRNA, a DNA copy of the viral gene was inserted between the RNA polymerase II promoter and the poly-A signal. Meantime, the RNA polymerase I promoter and terminator sequences, responsible for the transcription of viral RNA on the negative strand were placed in reverse orientation at both ends. By the virtue of its bidirectional promoters, both viral RNA and mRNA synthesis are facilitated in transfected cells with a single vector, reducing the number of plasmids required to generate an infectious influenza virus from 17 to 8 plasmids [218]. This method has led to significant improvements in reverse genetic studies for negative sense RNA viruses. Therefore, in the context of CCHFV VLP generation studies, conducted for this thesis, pDZ plasmid was first utilized to clone S and M segment sequences of CCHFV Kelkit 06 strain, separately. Then, the plasmids were transfected into CCHFV permissive cell lines, like BHK-21, HEK293T, and Vero E6, which have been widely

used in CCHFV studies [219]. However, despite the transfection of various combinations of plasmids into different cells, pDZ plasmid was not capable of driving sufficient production of viral protein yield in this model (see Figure 3. 2). Therefore, studies were continued using different alternative vectors.

The pCAGGS vector has been frequently used in various CCHFV studies and has enabled the expression of viral proteins in mammalian cells [64, 67, 220-222]. Therefore, pCAGGS plasmid was preferred as an expression vector to circumvent the problem with the recombinant protein production. To simplify protein expression, UTR regions, the Pol I promoter and its terminator sequences on the vector were discarded, and only the Pol II-driven plasmid known as pCAGGS was used to get viral proteins expressed in transfected cells. Also, instead of whole viral segments, ORF regions of NP, PreGn and PreGc were subcloned into individual pCAGGS plasmids. However, although the Western Blot results revealed that virus specific antibodies captured the proteins in transgene transfected cells, the uncertainty about the band profile appeared on the images raised some hesitation that the recombinant proteins may have been expressed differently comparing to their native forms (Figure 3. 4-8). Thus, another expression plasmid, called pcDNA3.1 plasmids were employed to produce recombinant proteins properly. Fluorescent microscopy images revealed that eGFP displayed various intracellular signals depending on the viral protein with which it was fused. When eGFP was expressed as a fusion with NP, it fluoresced in the perinuclear region, while a diffuse fluorescent light throughout the cytoplasm was noticed when it was fused with Gc (Figure 3.19). In the literature, CCHFV NP has been reported to localize the perinuclear region of infected cells [86, 223, 224] and Gc requires Gn for its transition to the Golgi [67]. In accordance with the information in the literature, fluorescence microscopy assay provided the first data suggesting that pcDNA 3.1 plasmids are capable of efficiently producing Np and Gc proteins. Immunological analysis of viral proteins by Western Blot demonstrated that all viral proteins were expressed properly in Huh-7 cells using the pcDNA 3.1 plasmid (Figure 3. 21). Furthermore, cell culture samples were examined using ELISA, and samples in which all three proteins were co-transfected were recognized by both specific antibodies and antibodies found in CCHFV-immunized animal sera. In addition, transfection samples involving only NP or a combination of NP and Gc were also recognized by most of the antibodies tested (Figure 3. 20). According to current

knowledge, the nucleoproteins of Dengue virus-2 and of Hepatitis C virus (HCV) can self-assemble into virus-like particles [16, 20]. Furthermore, Wang et al. (2011) reported that CCHFV NP form sphere-like structures that vary in morphology and size, ranging from 40 nm to 160 nm in diameter, within cytoplasmic vesicles of NP-transfected insect cells [216]. These findings suggested that further research was required to determine the minimal protein content needed for CCHFV VLP.

Reverse-genetics systems are valuable tools for understanding RNA virus replication cycles. Instead of using full-length clones, life cycle modeling systems like minigenome and transcription and replication competent VLP systems can be utilized to simulate various stages of the virus life cycle out of containment facilities. Replication and transcription of viral genomes can be modeled using minigenome systems, whereas morphogenesis, budding, and infection can be modeled on VLP systems that are capable of transcription and replication [7]. In 1989, Palese et al. established the first minigenome system to modify Influenza A virus with the assistance of a helper virus [225]. Later, Pattnaik and Wertz et al. developed the plasmid-based minigenome system for investigating the structure-function interactions of viral proteins and RNA replication [226, 227]. For bunyaviruses, Dunn et al. produced the first MG system utilizing the T7 promoter and BUNV S segment [228]; since then, minigenome systems have been extensively employed to understand the biology of viral proteins involved in the replication, transcription and pathogenesis of viruses [134]. One of the main studies of this thesis was to generate a minigenome system that could be integrated into the CCHFV VLP system. Several minigenome systems have been developed for bunyaviruses [7]. Like arenaviruses, the viral polymerase and NP are minimum required components for a proper genome replication and transcription in bunyaviruses[229] . However, due to the difficulty of cloning CCHFV viral polymerase gene, which is 12 kb in length, a unique minigenome system was designed that could simultaneously generate a single RNA that possesses the features of both vRNA of CCHFV and mRNA of a reporter gene, without the aid of any viral RNP complexes. Unlike existing systems, this system requires neither T7 expressing cells, Pol I, nor viral polymerase. This minigenome cassette has ambisense character since an mRNA cassette in sense orientation was flanked by antisense viral UTR sequences on the same strand. Similarly to the previously reported Lassa virus minigenome system [230], a study

found that the signal-to-noise ratio was significantly improved by transfecting *in vitro* synthesized minigenome RNA rather than plasmid DNA utilizing either T7 or Pol I polymerases [56]. On the other hand, VLP production independent of a permanently T7 polymerase expressing cells (like BSR-T7/5) might provide versatility in CCHFV studies with various cells, as well. For this reason, the minigenome RNA used in this study was synthesized *in vitro* using T7 polymerase. Confocal microscopy images showing the expression of reporter genes in Huh-7 cells transfected with *in vitro* transcribed minigenome RNA conceptually proved that this system allows the generation of reporter proteins without any viral RNP complexes, which are generally required for most minigenome systems (Figure 3.24). As a result, this system might enable one to scrutinize a steps of the viral life cycle, such as virion assembly, genome packaging, and cell entry mechanisms, when the viral structural proteins provided *in trans.*

Already, various VLP systems have been developed for bunyaviruses. In 2006, the first *Bunyamwera Orthobunyavirus* (BUNV) VLPs were successfully developed, allowing researchers to assess the involvement of nonstructural proteins in virus assembly and morphogenesis [231]. At the same year, another VLP system for the Uukuniemi virus (UUKV) was developed, and it was shown that, RNP complexes are dispensable for particle formation and minigenome packaging did not make significant changes in morphology of the virus [232]. Next, another VLP system was reported that transcriptions of Rift Valley Fever Virus (RVFV) was inhibited by MxA, a human interferon-derived protein [233]. First CCHFV VLP system, known as the transcription and entry competent virus-like particle (tc-VLP) system, was developed in 2015 by Devignot et al. [89]. With this system, the endonuclease domain was identified around 693. position of amino acid sequence of the CCHFV L protein [89]. Later, the role of furin cleavage during glycoprotein maturation and virus replication [164], function of viral OTU proteases during infection [50] , and the effect of glycoprotein sequence variance on virus infectivity using a tick strain [157] were studied in the same system. Furthermore, in an interferon alpha receptor knockout mouse model, the combination of CCHFV tc-VLP and a specific DNA vaccination has been shown to provide 100% protection in mice [162]. Recent research using the tc-VLP technology has shown the significance of CCHFV GP38 and NSm in particle assembly and infectivity [64].

The invaluable contribution of reverse genetic studies to the biology of negative sense RNA viruses are demonstrated during the last several decades of research. A tremendous amount of information on the biology of many highly pathogenic RNA viruses has been garnered by research involving VLP systems, particularly with the integration of minigenomes. To combat CCHFV effectively which poses a significant threat to the health of billions of people, it is important to conduct studies on characterization of biological, immunological, and pathogenic features of the virus in a safe manner. The purpose of the current thesis was to develop such model. Here, experiments utilizing different expression vectors were conducted to generate a VLP systems for CCHFV and studies with pcDNA 3.1 plasmid have shown that viral proteins were sufficiently produced. Viral protein expressions were evidenced in tests involving immunological and expression methods. Additionally, a viral RNP complex-independent ambisense minigenome system was developed for future studies, aiming to generate cell-entry competent and transcriptionally active VLPs for CCHFV Kelkit 06 strain. However, the model was not sufficiently driving the production of VLPs by which some of the virological questions could be addressed. It appears that optimization of the model is required. For this aim, utilization of codon optimized gene segments, alternative cell lines and more sensitive detection methods such as quantitative RT-PCR are planned. Nevertheless, the expression studies in the thesis have contributed valuable information to the literature on the development of VLP systems in CCHFV. It is believed that the data generated in this project will pave the way for future comprehensive studies investigating each stage in the life cycle of the virus and as well as developing diagnostic, protective, and therapeutic agents against CCHFV.

4.2 SARS-CoV-2 VLP studies representing applications of reverse genetics on a positive sense RNA virus

In this section of the thesis, four SARS-CoV-2 VLP candidates were developed by different combinations of viral structural proteins expressed in yeasts. The minimum molecular requirement for SARS-CoV-2 virions to assemble and exit the cell efficiently is not yet fully known. There is approximately 79.5% genomic homology between SARS-CoV and SARS-CoV-2, [234]. The reports in the literature show that SARS-CoV VLP formation is dependent on M and E proteins or M and N proteins

[235-237]. In the paper published by Xu et al., M and E proteins were shown to be required for SARS-CoV-2 VLPs to assemble and release from the cell. However, it has been noted that for efficient production and release of VLPs by transfected Vero E6 cells, both the E and N proteins must be co-expressed with the M protein [238]. In addition, the antigenic properties of Spike and N proteins and that they are indispensable elements of vaccine studies have been shown with SARS virus [239-241]. In this thesis, four different VLPs (SEM, SEN, SENM, and ENM) were aimed to be generated since the antigenic structues of S and N proteins are needed for a successful vaccine candidate and the minimum proteins that can form the VLP structure are M and E. Spike protein included D614G mutation, which was a more common form of S (as reported to be in circulation in 2020 [242]. Addtionally, two proline mutations at the C-terminus of the S2 domain were added to the sequence to increase expression and stability of S [243].

Heterologous proteins are increasingly manufactured in biological expression systems. Yeasts are also commonly employed in the pharmaceutical and biotech industries to produce vaccines or drugs. *Pitchia pastoris* expression system is widely used as a cost-effective and reliable way of producing eucaryotic proteins recombinantly. *Pichia pastoris* is a eukaryotic organism that can be easily manipulated similar to prokaryotic expression model of *E. coli* or eukaryotic *Saccharomyces cerevisiae* but possesses many of the benefits of higher eukaryotic expression systems, including protein processing, protein folding, and posttranslational modifications. When compared to alternative eukaryotic expression systems like baculovirus or mammalian tissue culture, it typically yields higher expression levels. It also benefits from molecular and genetic modifications in the same ways that *Saccharomyces* does, but heterologous protein expression levels are 10- to 100-fold higher. Moreover, stable cell lines can be made by inserting linearized foreign DNA into a chromosome via cross recombination events. Because of these advantageous characteristics, *Pichia* serves as an extremely useful system for the protein expression industry [14].

Virus-like particles (VLPs) are multimeric nanoparticles composed entirely of viral structural proteins and are devoid of any genetic material. Virus-like particles are regarded as subunit vaccines and are referred as one of the most ideal human vaccines as they provide completely safe form of protection since the vaccine formulations composed of VLPs contains no foreign genetic material (DNA/RNA). Furthermore,

when compared to other subunit vaccines, VLP has several advantages, including morphological similarity to the source viruses, a frequently repeated immunogenic surface structure, comparable mechanism of entry into the cell to that of the source virus, and significant protective immunity induced. It has been shown that VLPs are acting like self-adjuvant due to repeated antigenic structures on their surfaces and can potently stimulate both humoral and cellular arms of the immune system [10].

Recent developments in biomedical engineering have led to the widespread use of VLP-based vaccinations for the treatment of infectious diseases. The hepatitis B virus VLP, composed of hepatitis B virus surface antigen (HBsAg) was first detected in human plasma, then used as a vaccine. This vaccine is in use since 1968 and is the forerunner of the VLP vaccines. Later, in 1981, the HBV VLP vaccine was produced recombinantly while still preserving its virological and immunological characteristics, received FDA approval, and has been widely used for more than 40 years under trade names such as Engerix-B®, Recombivax HB®, Heplisav®, Heberbiovac-HB®, Euvax-B®, Hepavax-Gene® [11]. Additionally, prophylactic VLP vaccines such as bivalent, quadrivalent, and 9-valent human papilloma virus vaccines (Gardasil®, Cervarix®), hepatitis E virus vaccine (Hecolin®), and anti-malarial vaccine (Mosquirix^{TM}) demonstrate the safety and efficacy of VLP vaccinations [244-246]. Moreover, hundreds of antiviral vaccines based on VLPs, ranging from influenza to dengue virus, are currently either approved by an official authority like FDA, EMA or WHO or in various stages of development in clinical trials [247-249].

The global spread of the 2019 coronavirus disease caused by severe acute respiratory syndrome coronavirus 2 (SARS-CoV-2) infection has prompted the deployment of urgent preventive countermeasures. As SARS-CoV-2 continues to evolve and new variants of concern (VOC) arise, immunization becomes more important than ever. Vaccines against SARS-CoV-2 now available can be classified as either inactivated, live attenuated, viral vectors, protein subunits, RNA, DNA, or virus-like particle (VLP). A novel mRNA-based vaccination platform has been launched, and billions of vaccine doses have been administered around the world in response to the urgency of the pandemic and considerable preliminary data have been generated on these formulations. Further infrastructure is being built to facilitate the production of improved and safer vaccines. Virus-like particle-based vaccines are one of them, and

as of December 2022, seven SARS-CoV-2 VLP vaccines are in development [13]. One of them is the SpyBiotech/SIIPL VLP-based COVID-19 vaccine, for which yeasts were used as hosts. The VLP element of the vaccine consists of the HBV surface antigen, which is extensively used in many authorized vaccines. Here, the SARS-CoV-2 RBD antigen was attached to the HbsAg protein via Spytag/Spycatcher technology. HbsAg is the homologous antigen used in recombinant HBV vaccinations, prompting the body to generate protective antibodies, on the other hand, is employed as a carrier for heterologous antigens in VLP platforms used to develop vaccines against different diseases [250]. Another vaccine was developed by Medicago in collaboration with GlaxoSmithKline (GSK). It is a plant based VLP vaccine. This COVID-19 vaccine was produced by the expression of a stabilized prefusion form of SARS-CoV-2 spike protein fused with the transmembrane domain and cytoplasmic tail of influenza hemagglutinin in *Nicotiana benthamiana*, which serves as the expression system for the VLPs, a frequently used plant expression system to manufacture biopharmaceuticals [250-252]. Thirdly, the VBI technology employs enveloped VLPs (eVLPs) that contain the murine leukemia virus (MLV) Gag proteins, that incorporates a modified and optimized prefusion form of SARS-CoV-2 spike protein [250]. In ABNCoV2 vaccine study, the clinical trials are continuing at Radboud University Medical Center in the Netherlands. In ABNCoV2 Vaccine study, RBD antigen was expressed in a fusion with Catcher in insect cells and attached to the spontaneously represented Tag peptide on the surface of preassembled capsid-like particles (CLPs) in *E. coli* [250]. Another VLP vaccine study is utilizing RBD as the antigen (Yantai Patronus Biotech Co., Ltd), but details of the study are not made public yet. The other vaccine was developed by Scientific and Technological Research Council of Türkiye (TUBITAK). One of the key differences between this and other VLP-based COVID vaccines in clinical phase is that VLP contains all four structural proteins of SARS-CoV-2 (S, E, M, and N) [250, 253].

Unlike the aforementioned clinical studies with VLPs containing only spikes or all structural proteins, our study focused on the production of different VLPs by combining viral proteins. Considering that cost-effective manufacturing is critical in the development of vaccines for mass production, *P. pastoris* expression system was chosen to produce target antigens at lower production costs than other eukaryotic systems (such as mammalian, insect, and plant) while maintaining

their immunogenicity. Thus, recombinant yeast cell lines that constitutively produce different SARS-CoV-2 VLPs were generated. Further immunological characterizations of these recombinant VLPs are required to demonstrate their potential as vaccines against COVID-19. The strategies that were employed in this part of the thesis might lead to additional vaccine studies to be developed in our laboratory against a number of different viral diseases.

5. CONCLUSIONS AND RECOMMENDATIONS

Within the scope of this thesis, extensive studies on viral protein expression have been carried out to develop VLPs that will enable us to better understand CCHFV, a highly pathogenic and increasingly prevalent virus. Our studies demonstrated that viral proteins were produced best via pcDNA 3.1 plasmid in Huh-7 cells and the expression was confirmed by immunological and molecular methods. Although ELISA results imply that various viral protein combinations produce different VLP compositions, further studies are needed to support the results obtained in this thesis. Low protein production in pDZ and pCAGGS plasmids based expression systems may be due to relatively low mRNA transcription levels and the lack of optimized sequence of genes encoding viral genes. As another objective of this thesis was to form a viral RNP complex-independent ambisense minigenome system to generate transcriptionally and entry-competent VLP for CCHFV Kelkit 06 strain. For this aim, the expression studies in the thesis contributed valuable information in the development of VLP systems. This information might pave the way for future studies to be conducted to comprehensively investigate each stage in the life cycle of the virus and as well as to develop vaccine and treatment agents against CCHFV.

In addition, plasmids were generated for SARS-CoV-2 to allow production of four different VLP (SEM, SEN, SENM and ENM)-based vaccine candidates in *P. pastoris*. These plasmids were constructed by sequentially cloning different combinations of viral expression cassettes. These studies might also be followed an exemplary study showing the usage of VLP systems in translational biotechnology may provide data to the clinical studies examining the immunogenicity and safety of vaccine candidates in future.

In conclusions, the experiments conducted in this thesis have shown expression and detection of immunologically significant viral antigenic proteins from CCHFV and SARS CoV-2, two of the most serious human viral pathogens of our time, in eukaryotic cells. These studies have established a critical infrastructure at our laboratory which

will be imperative in future studies. It appears that for generation and demonstration of vast quantities and commercially meaningful VLPs from plasmid based expression systems, further optimizations are needed. It should be underlined that to address the questions on the biology and immunology of these viruses through VLP and minigenome approaches, these optimizations such as exhaustive trials with different expression models, optimization of sequences, transfection systems and stable expressions should be undertaken.

6. REFERENCES

1. Bridgen, A. (2012). Introduction. *Reverse Genetics of RNA Viruses* pp. 1-23):
2. Binder, S., Levitt, A. M., Sacks, J. J. and Hughes, J. M. (1999). Emerging infectious diseases: public health issues for the 21st century. *Science*, *284*(5418), 1311-1313.
3. Jones, K. E., Patel, N. G., Levy, M. A., Storeygard, A., Balk, D., Gittleman, J. L., et al. (2008). Global trends in emerging infectious diseases. *Nature*, *451*(7181), 990-993.
4. Morens, D. M., Folkers, G. K. and Fauci, A. S. (2004). The challenge of emerging and re-emerging infectious diseases. *Nature*, *430*(6996), 242-249.
5. Woolhouse, M. E. and Gowtage-Sequeria, S. (2005). Host range and emerging and reemerging pathogens. *Emerg Infect Dis*, *11*(12), 1842-1847.
6. Ma, D. Y. and Suthar, M. S. (2015). Mechanisms of innate immune evasion in re-emerging RNA viruses. *Current opinion in virology*, *12*, 26-37.
7. Hoenen, T., Groseth, A., de Kok-Mercado, F., Kuhn, J. H. and Wahl-Jensen, V. (2011). Minigenomes, transcription and replication competent virus-like particles and beyond: reverse genetics systems for filoviruses and other negative stranded hemorrhagic fever viruses. *Antiviral research*, *91*(2), 195-208.
8. Müdürlüğü, T. H. S. G. KIRIM KONGO KANAMALI ATEŞİ (Hekimlere Yönelik). (2020). Retrieved 04.12.2022, from *https://hsgm.saglik.gov.tr/depo/birimler/zoonotik-vektorel-hastaliklar-db/zoonotik-hastaliklar/1-KKKA/7-Sunumlar/KKKA_Sunum_Hekimlere_Ynelik08.04.2020.pdf*
9. Karaaslan, E., Çetin, N. S., Kalkan-Yazıcı, M., Hasanoğlu, S., Karakeçili, F., Özdarendeli, A., et al. (2021). Immune responses in multiple hosts to Nucleocapsid Protein (NP) of Crimean-Congo Hemorrhagic Fever Virus (CCHFV). *PLoS Negl Trop Dis*, *15*(12), e0009973.
10. Chroboczek, J., Szurgot, I. and Szolajska, E. (2014). Virus-like particles as vaccine. *Acta Biochim Pol*, *61*(3), 531-539.
11. Mulder, A. M., Carragher, B., Towne, V., Meng, Y., Wang, Y., Dieter, L., et al. (2012). Toolbox for non-intrusive structural and functional analysis of recombinant VLP based vaccines: a case study with hepatitis B vaccine. *PloS one*, *7*(4), e33235.
12. University, J. H. COVID-19 Content Portal. Retrieved 03.01.2023, from *https://systems.jhu.edu/research/public-health/ncov/*
13. WHO. COVID-19 vaccine tracker and landscape. (2022). WHO; Retrieved 18.12.2022, from *https://www.who.int/publications/m/item/draft-landscape-of-covid-19-candidate-vaccines*
14. Invitrogen. User Manual: Multi-Copy Pichia Expression Kit (2010). Retrieved 18.12.2022, from *https://tools.thermofisher.com/content/sfs/manuals/pichmulti_man.pdf*

15. Carrasco-Hernandez, R., Jácome, R., López Vidal, Y. and Ponce de León, S. (2017). Are RNA Viruses Candidate Agents for the Next Global Pandemic? A Review. *ILAR Journal*, *58*(3), 343-358.
16. Desselberger, U. (2017). Reverse genetics of rotavirus. *Proceedings of the National Academy of Sciences of the United States of America*, *114*(9), 2106-2108.
17. Neumann, G. and Kawaoka, Y. (2004). Reverse genetics systems for the generation of segmented negative-sense RNA viruses entirely from cloned cDNA. *Current topics in microbiology and immunology*, *283*, 43-60.
18. Bridgen, A. (2012). *Reverse Genetics of RNA Viruses*. Wiley-Blackwell. 408 p.
19. Fraser, D., Mahler, H. R., Shug, A. L. and Thomas, C. A. (1957). THE INFECTION OF SUB-CELLULAR ESCHERICHIA COLI, STRAIN B, WITH A DNA PREPARATION FROM T2 BACTERIOPHAGE. *Proceedings of the National Academy of Sciences of the United States of America*, *43*(11), 939-947.
20. Boyer, J. C. and Haenni, A. L. (1994). Infectious transcripts and cDNA clones of RNA viruses. *Virology*, *198*(2), 415-426.
21. Coffin, J. M. and Fan, H. (2016). The Discovery of Reverse Transcriptase. *Annu Rev Virol*, *3*(1), 29-51.
22. Taniguchi, T., Palmieri, M. and Weissmann, C. (1978). Qβ DNA-containing hybrid plasmids giving rise to Qβ phage formation in the bacterial host. *Nature*, *274*(5668), 223-228.
23. Stobart, C. C. and Moore, M. L. (2014). RNA virus reverse genetics and vaccine design. *Viruses*, *6*(7), 2531-2550.
24. What are VHFs? : Centers for Disease Control and Prevention, National Center for Emerging and Zoonotic Infectious Diseases (NCEZID), Division of High-Consequence Pathogens and Pathology (DHCPP), Viral Special Pathogens Branch (VSPB); Retrieved 19.09.2022, from *https://www.cdc.gov/vhf/about.html#:~:text=Viral%20hemorrhagic%20fevers%20(VHFs)%20are,to%20function%20on%20its%20own*
25. Blair, P. W., Kuhn, J. H., Pecor, D. B., Apanaskevich, D. A., Kortepeter, M. G., Cardile, A. P., et al. (2019). An Emerging Biothreat: Crimean-Congo Hemorrhagic Fever Virus in Southern and Western Asia. *Am J Trop Med Hyg*, *100*(1), 16-23.
26. World Health Organization, W. Prioritizing diseases for research and development in emergency contexts. Retrieved 04.12.2022, from *https://www.who.int/activities/prioritizing-diseases-for-research-and-development-in-emergency-contexts*
27. Sorvillo, T. E., Rodriguez, S. E., Hudson, P., Carey, M., Rodriguez, L. L., Spiropoulou, C. F., et al. (2020). Towards a Sustainable One Health Approach to Crimean-Congo Hemorrhagic Fever Prevention: Focus Areas and Gaps in Knowledge. *Trop Med Infect Dis*, *5*(3).
28. Keshtkar-Jahromi, M., Sajadi, M. M., Ansari, H., Mardani, M. and Holakouie-Naieni, K. (2013). Crimean-Congo hemorrhagic fever in Iran. *Antiviral research*, *100*(1), 20-28.
29. Chumakov, M. P. (1974). On 30 years of investigation of Crimean hemorrhagic fever *Tr Inst Polio Virusn Entsefalitov Akad Med Nauk SSSR*
, (22), 5-18.

30. Hoogstraal, H. (1979). The epidemiology of tick-borne Crimean-Congo hemorrhagic fever in Asia, Europe, and Africa. *Journal of medical entomology*, *15*(4), 307-417.
31. Dols, M. W. (1977). *The Black Death in the Middle East : by Michael W. Dols*. Princeton University Press; 1977. 390 pp. p.
32. Chumakov, M. P. (1947). A new virus disease—Crimean hemorrhagic fever. *Nov Med* (4), 9-11.
33. Chumakov, M. P. (1945). A new tick-borne virus disease - Crimean hemorrhagic fever. pp. 13–45.
34. Chumakov, M. P., Butenko, A. M., Shalunova, N. V., Mart'ianova, L. I., Smirnova, S. E., Bashkirtsev Iu, N., et al. (1968). [New data on the viral agent of Crimean hemorrhagic fever]. *Voprosy virusologii*, *13*(3), 377.
35. Butenko, A. M., Chumakov, M.P., Bashkirtsev, V.N., Zavodova, T.I., and Tkachenko, E. A., Rubin, S.G., Stolbov, D.N. (1968). Isolation and investigation of Astrakhan strain ("Drozdov") of Crimean hemorrhagic fever virus and data on serodiagnosis of this infection. *Nauchn Sess Inst Polio Virus Ensefalitis*, (3), 88-90 (in Russian; in English, NAMRU83-T866).
36. Simpson, D. I., Knight, E. M., Courtois, G., Williams, M. C., Weinbren, M. P. and Kibukamusoke, J. W. (1967). Congo virus: a hitherto undescribed virus occurring in Africa. I. Human isolations--clinical notes. *East African medical journal*, *44*(2), 86-92.
37. Woodall, J. P., Williams, M.C., Simpson, D.I.H. (1967). Congo virus: a hitherto undescribed virus occurring in Africa. II. Identification studies. *East Afr Med J* (44), 93-98.
38. Li, C. X., Shi, M., Tian, J. H., Lin, X. D., Kang, Y. J., Chen, L. J., et al. (2015). Unprecedented genomic diversity of RNA viruses in arthropods reveals the ancestry of negative-sense RNA viruses. *Elife*, *4*.
39. Tokarz, R., Williams, S. H., Sameroff, S., Sanchez Leon, M., Jain, K. and Lipkin, W. I. (2014). Virome analysis of Amblyomma americanum, Dermacentor variabilis, and Ixodes scapularis ticks reveals novel highly divergent vertebrate and invertebrate viruses. *J Virol*, *88*(19), 11480-11492.
40. Elbeaino, T., Digiaro, M. and Martelli, G. P. (2009). Complete nucleotide sequence of four RNA segments of fig mosaic virus. *Arch Virol*, *154*(11), 1719-1727.
41. van Poelwijk, F., Prins, M. and Goldbach, R. (1997). Completion of the impatiens necrotic spot virus genome sequence and genetic comparison of the L proteins within the family Bunyaviridae. *J Gen Virol*, *78 (Pt 3)*, 543-546.
42. The ICTV Bunyaviridae Study Group, T. I. E. S. G., The ICTV Tenuivirus Study Group, Junglen, Sandra Create a new order, Bunyavirales, to accommodate nine families (eight new, one
renamed) comprising thirteen genera. online; 2016.
43. Abudurexiti, A., Adkins, S., Alioto, D., Alkhovsky, S. V., Avšič-Županc, T., Ballinger, M. J., et al. (2019). Taxonomy of the order Bunyavirales: update 2019. *Arch Virol*, *164*(7), 1949-1965.
44. Bente, D. A., Forrester, N. L., Watts, D. M., McAuley, A. J., Whitehouse, C. A. and Bray, M. (2013). Crimean-Congo hemorrhagic fever: history, epidemiology, pathogenesis, clinical syndrome and genetic diversity. *Antiviral research*, *100*(1), 159-189.
45. Clerex-Van Haaster, C. M., Clerex, J. P., Ushijima, H., Akashi, H., Fuller, F. and Bishop, D. H. (1982). The 3' terminal RNA sequences of bunyaviruses and

nairoviruses (Bunyaviridae): evidence of end sequence generic differences within the virus family. *J Gen Virol, 61 (Pt 2)*, 289-292.
46. Morikawa, S., Saijo, M. and Kurane, I. (2007). Recent progress in molecular biology of Crimean-Congo hemorrhagic fever. *Comparative immunology, microbiology and infectious diseases, 30*(5-6), 375-389.
47. Marriott, A. C. and Nuttall, P. A. (1996). Large RNA segment of Dugbe nairovirus encodes the putative RNA polymerase. *J Gen Virol, 77 (Pt 8)*, 1775-1780.
48. Macleod, J. M. L., Marmor, H., García-Sastre, A. and Frias-Staheli, N. (2015). Mapping of the interaction domains of the Crimean-Congo hemorrhagic fever virus nucleocapsid protein. *J Gen Virol, 96*(Pt 3), 524-537.
49. Honig, J. E., Osborne, J. C. and Nichol, S. T. (2004). Crimean-Congo hemorrhagic fever virus genome L RNA segment and encoded protein. *Virology, 321*(1), 29-35.
50. Scholte, F. E. M., Zivcec, M., Dzimianski, J. V., Deaton, M. K., Spengler, J. R., Welch, S. R., et al. (2017). Crimean-Congo Hemorrhagic Fever Virus Suppresses Innate Immune Responses via a Ubiquitin and ISG15 Specific Protease. *Cell Rep, 20*(10), 2396-2407.
51. Loureiro, J. and Ploegh, H. L. (2006). Antigen presentation and the ubiquitin-proteasome system in host-pathogen interactions. *Advances in immunology, 92*, 225-305.
52. Shin, J. S., Ebersold, M., Pypaert, M., Delamarre, L., Hartley, A. and Mellman, I. (2006). Surface expression of MHC class II in dendritic cells is controlled by regulated ubiquitination. *Nature, 444*(7115), 115-118.
53. Chen, Z. J. (2005). Ubiquitin signalling in the NF-kappaB pathway. *Nature cell biology, 7*(8), 758-765.
54. Frias-Staheli, N., Giannakopoulos, N. V., Kikkert, M., Taylor, S. L., Bridgen, A., Paragas, J., et al. (2007). Ovarian tumor domain-containing viral proteases evade ubiquitin- and ISG15-dependent innate immune responses. *Cell host & microbe, 2*(6), 404-416.
55. Gack, M. U., Shin, Y. C., Joo, C. H., Urano, T., Liang, C., Sun, L., et al. (2007). TRIM25 RING-finger E3 ubiquitin ligase is essential for RIG-I-mediated antiviral activity. *Nature, 446*(7138), 916-920.
56. Bergeron, E., Albarino, C. G., Khristova, M. L. and Nichol, S. T. (2010). Crimean-Congo hemorrhagic fever virus-encoded ovarian tumor protease activity is dispensable for virus RNA polymerase function. *Journal of virology, 84*(1), 216-226.
57. Bergeron, E., Vincent, M. J. and Nichol, S. T. (2007). Crimean-Congo hemorrhagic fever virus glycoprotein processing by the endoprotease SKI-1/S1P is critical for virus infectivity. *Journal of virology, 81*(23), 13271-13276.
58. Altamura, L. A., Bertolotti-Ciarlet, A., Teigler, J., Paragas, J., Schmaljohn, C. S. and Doms, R. W. (2007). Identification of a novel C-terminal cleavage of Crimean-Congo hemorrhagic fever virus PreGN that leads to generation of an NSM protein. *Journal of virology, 81*(12), 6632-6642.
59. Vincent, M. J., Sanchez, A. J., Erickson, B. R., Basak, A., Chretien, M., Seidah, N. G., et al. (2003). Crimean-Congo Hemorrhagic Fever Virus Glycoprotein Proteolytic Processing by Subtilase SKI-1. *Journal of virology, 77*(16), 8640-8649.
60. Sanchez, A. J., Vincent, M. J., Erickson, B. R. and Nichol, S. T. (2006). Crimean-congo hemorrhagic fever virus glycoprotein precursor is cleaved by

Furin-like and SKI-1 proteases to generate a novel 38-kilodalton glycoprotein. *Journal of virology*, *80*(1), 514-525.
61. Jeffers, S. A., Sanders, D. A. and Sanchez, A. (2002). Covalent modifications of the ebola virus glycoprotein. *Journal of virology*, *76*(24), 12463-12472.
62. Simmons, G., Wool-Lewis, R. J., Baribaud, F., Netter, R. C. and Bates, P. (2002). Ebola virus glycoproteins induce global surface protein down-modulation and loss of cell adherence. *Journal of virology*, *76*(5), 2518-2528.
63. Sullivan, N. J., Peterson, M., Yang, Z. Y., Kong, W. P., Duckers, H., Nabel, E., et al. (2005). Ebola virus glycoprotein toxicity is mediated by a dynamin-dependent protein-trafficking pathway. *Journal of virology*, *79*(1), 547-553.
64. Freitas, N., Enguehard, M., Denolly, S., Levy, C., Neveu, G., Lerolle, S., et al. (2020). The interplays between Crimean-Congo hemorrhagic fever virus (CCHFV) M segment-encoded accessory proteins and structural proteins promote virus assembly and infectivity. *PLoS pathogens*, *16*(9), e1008850.
65. Mishra, A. K., Hellert, J., Freitas, N., Guardado-Calvo, P., Haouz, A., Fels, J. M., et al. (2022). Structural basis of synergistic neutralization of Crimean-Congo hemorrhagic fever virus by human antibodies. *Science*, *375*(6576), 104-109.
66. Bertolotti-Ciarlet, A., Smith, J., Strecker, K., Paragas, J., Altamura, L. A., McFalls, J. M., et al. (2005). Cellular localization and antigenic characterization of crimean-congo hemorrhagic fever virus glycoproteins. *Journal of virology*, *79*(10), 6152-6161.
67. Haferkamp, S., Fernando, L., Schwarz, T. F., Feldmann, H. and Flick, R. (2005). Intracellular localization of Crimean-Congo Hemorrhagic Fever (CCHF) virus glycoproteins. *Virology journal*, *2*, 42.
68. Andersson, C. (2013) *Virus-host interactions: Entry and replication of crimean-congo hemorrhagic fever virus* (Master). Stockholm: Karolinska Institutet.
69. Shi, X., van Mierlo, J. T., French, A. and Elliott, R. M. (2010). Visualizing the replication cycle of bunyamwera orthobunyavirus expressing fluorescent protein-tagged Gc glycoprotein. *Journal of virology*, *84*(17), 8460-8469.
70. Estrada, D. F. and De Guzman, R. N. (2011). Structural Characterization of the Crimean-Congo Hemorrhagic Fever Virus Gn Tail Provides Insight into Virus Assembly. *The Journal of biological chemistry*, *286*(24), 21678-21686.
71. Zivcec, M., Scholte, F. E., Spiropoulou, C. F., Spengler, J. R. and Bergeron, É. (2016). Molecular Insights into Crimean-Congo Hemorrhagic Fever Virus. *Viruses*, *8*(4), 106.
72. Wang, Y., Dutta, S., Karlberg, H., Devignot, S., Weber, F., Hao, Q., et al. (2012). Structure of Crimean-Congo hemorrhagic fever virus nucleoprotein: superhelical homo-oligomers and the role of caspase-3 cleavage. *Journal of virology*, *86*(22), 12294-12303.
73. Carter, S. D., Surtees, R., Walter, C. T., Ariza, A., Bergeron, E., Nichol, S. T., et al. (2012). Structure, function, and evolution of the Crimean-Congo hemorrhagic fever virus nucleocapsid protein. *Journal of virology*, *86*(20), 10914-10923.
74. Salata, C., Monteil, V., Karlberg, H., Celestino, M., Devignot, S., Leijon, M., et al. (2018). The DEVD motif of Crimean-Congo hemorrhagic fever virus nucleoprotein is essential for viral replication in tick cells. *Emerg Microbes Infect*, *7*(1), 190.

75. Andersson, I., Simon, M., Lundkvist, A., Nilsson, M., Holmstrom, A., Elgh, F., et al. (2004). Role of actin filaments in targeting of Crimean Congo hemorrhagic fever virus nucleocapsid protein to perinuclear regions of mammalian cells. *Journal of medical virology*, *72*(1), 83-93.
76. Taylor, M. P., Koyuncu, O. O. and Enquist, L. W. (2011). Subversion of the actin cytoskeleton during viral infection. *Nature reviews Microbiology*, *9*(6), 427-439.
77. Guardado-Calvo, P. and Rey, F. A. (2017). The Envelope Proteins of the Bunyavirales. *Adv Virus Res*, *98*, 83-118.
78. Hulswit, R. J. G., Paesen, G. C., Bowden, T. A. and Shi, X. (2021). Recent Advances in Bunyavirus Glycoprotein Research: Precursor Processing, Receptor Binding and Structure. *Viruses*, *13*(2).
79. Nairoviridae Retrieved 05.12.2022, from *https://www.researchgate.net/figure/Nairoviridae-Lifecycle-of-nairoviruses-1-Virion-attachment-2-virion-uptake-3_fig3_343863181*
80. Xiao, X., Feng, Y., Zhu, Z. and Dimitrov, D. S. (2011). Identification of a putative Crimean-Congo hemorrhagic fever virus entry factor. *Biochemical and biophysical research communications*, *411*(2), 253-258.
81. Mishra, A. K., Hellert, J., Freitas, N., Guardado-Calvo, P., Haouz, A., Fels, J. M., et al. (2022). Structural basis of synergistic neutralization of Crimean-Congo hemorrhagic fever virus by human antibodies. *Science*, *375*(6576), 104-109.
82. Albornoz, A., Hoffmann, A. B., Lozach, P. Y. and Tischler, N. D. (2016). Early Bunyavirus-Host Cell Interactions. *Viruses*, *8*(5).
83. Gonzalez-Scarano, F., Pobjecky, N. and Nathanson, N. (1984). La Crosse bunyavirus can mediate pH-dependent fusion from without. *Virology*, *132*(1), 222-225.
84. Simon, M., Johansson, C. and Mirazimi, A. (2009). Crimean-Congo hemorrhagic fever virus entry and replication is clathrin-, pH- and cholesterol-dependent. *J Gen Virol*, *90*(Pt 1), 210-215.
85. Marsh, M. and Helenius, A. (2006). Virus entry: open sesame. *Cell*, *124*(4), 729-740.
86. Simon, M., Johansson, C., Lundkvist, A. and Mirazimi, A. (2009). Microtubule-dependent and microtubule-independent steps in Crimean-Congo hemorrhagic fever virus replication cycle. *Virology*, *385*(2), 313-322.
87. Schmaljohn CS, N. S. (2007). Bunyaviridae. In H.P. Knipe DM, (Ed.). *Fields Virology* (5th ed. USA: Lippincott Williams and Wilkins.
88. Kraus A. A and A., M. (2010). Molecular Biology and Pathogenesis of Crimean–Congo Hemorrhagic Fever Virus. *Future Virology*, *5*(4), 469-479.
89. Devignot, S., Bergeron, E., Nichol, S., Mirazimi, A. and Weber, F. (2015). A Virus-Like Particle System Identifies the Endonuclease Domain of Crimean-Congo Hemorrhagic Fever Virus. *Journal of virology*, *89*(11), 5957-5967.
90. Reguera, J., Weber, F. and Cusack, S. (2010). Bunyaviridae RNA polymerases (L-protein) have an N-terminal, influenza-like endonuclease domain, essential for viral cap-dependent transcription. *PLoS pathogens*, *6*(9), e1001101.
91. Holm, T., Kopicki, J. D., Busch, C., Olschewski, S., Rosenthal, M., Uetrecht, C., et al. (2018). Biochemical and structural studies reveal differences and commonalities among cap-snatching endonucleases from segmented negative-strand RNA viruses. *The Journal of biological chemistry*, *293*(51), 19686-19698.

92. Moroso, M., Verlhac, P., Ferraris, O., Rozières, A., Carbonnelle, C., Mély, S., et al. (2020). Crimean-Congo hemorrhagic fever virus replication imposes hyper-lipidation of MAP1LC3 in epithelial cells. *Autophagy*, *16*(10), 1858-1870.
93. Whitehouse, C. A. (2004). Crimean-Congo hemorrhagic fever. *Antiviral research*, *64*(3), 145-160.
94. Tahmasebi, F., Ghiasi, S. M., Mostafavi, E., Moradi, M., Piazak, N., Mozafari, A., et al. (2010). Molecular epidemiology of Crimean- Congo hemorrhagic fever virus genome isolated from ticks of Hamadan province of Iran. *Journal of vector borne diseases*, *47*(4), 211-216.
95. Deyde, V. M., Khristova, M. L., Rollin, P. E., Ksiazek, T. G. and Nichol, S. T. (2006). Crimean-Congo hemorrhagic fever virus genomics and global diversity. *Journal of virology*, *80*(17), 8834-8842.
96. Bell-Sakyi, L., Kohl, A., Bente, D. A. and Fazakerley, J. K. (2012). Tick Cell Lines for Study of Crimean-Congo Hemorrhagic Fever Virus and Other Arboviruses. *Vector Borne and Zoonotic Diseases*, *12*(9), 769-781.
97. Kırım-Kongo Kanamalı Ateşi. T.C. Tarım Ve Orman Bakanlığı İzmir Bornova Veteriner Kontrol Enstitüsü Retrieved 05.12.2022, from *https://vetkontrol.tarimorman.gov.tr/bornova/Menu/82/Kirim-Kongo-Kanamali-Atesi*
98. Gargili, A., Thangamani, S. and Bente, D. (2013). Influence of laboratory animal hosts on the life cycle of Hyalomma marginatum and implications for an in vivo transmission model for Crimean-Congo hemorrhagic fever virus. *Frontiers in cellular and infection microbiology*, *3*, 39.
99. Ozdarendeli, A., Canakoglu, N., Berber, E., Aydin, K., Tonbak, S., Ertek, M., et al. (2010). The complete genome analysis of Crimean-Congo hemorrhagic fever virus isolated in Turkey. *Virus research*, *147*(2), 288-293.
100. Estrada-Peña, A. and de la Fuente, J. (2014). The ecology of ticks and epidemiology of tick-borne viral diseases. *Antiviral research*, *108*, 104-128.
101. Randolph, S. E. and Rogers, D. J. (2007). Ecology of Tick-Borne Disease and the Role of Climate. In O. Ergonul, C.A. Whitehouse, (Eds.), *Crimean-Congo Hemorrhagic Fever: A Global Perspective* pp. 167-186). Dordrecht: Springer Netherlands.
102. Dohm, D. J., Logan, T. M., Linthicum, K. J., Rossi, C. A. and Turell, M. J. (1996). Transmission of Crimean-Congo Hemorrhagic Fever Virus by Hyalomma impeltatum (Acari: Ixodidae) after Experimental Infection. *Journal of medical entomology*, *33*(5), 848-851.
103. Gordon, S. W., Linthicum, K. J. and Moulton, J. R. (1993). Transmission of Crimean-Congo hemorrhagic fever virus in two species of Hyalomma ticks from infected adults to cofeeding immature forms. *American Journal of Tropical Medicine and Hygiene*, *48*(4), 576-580.
104. Gonzalez, J. P., Camicas, J. L., Cornet, J. P., Faye, O. and Wilson, M. L. (1992). Sexual and transovarian transmission of Crimean-Congo haemorrhagic fever virus in Hyalomma truncatum ticks. *Research in Virology*, *143*, 23-28.
105. Logan, T. M., Linthicum, K. J., Bailey, C. L., Watts, D. M., Dohm, D. J. and Moulton, J. R. (1990). Replication of Crimean-Congo Hemorrhagic Fever Virus in Four Species of Ixodid Ticks (Acari) Infected Experimentally. *Journal of medical entomology*, *27*(4), 537-542.
106. Gargılı, A., Estrada-Peña, A., Spengler, J. R., Lukashev, A. N., Nuttall, P. A. and Bente, D. A. (2017). The role of ticks in the maintenance and transmission

of Crimean-Congo hemorrhagic fever virus: A review of published field and laboratory studies. *Antiviral research*, *144*, 93–119.

107. Turell, M. J. (2007). Role of Ticks in the Transmission of Crimean-Congo Hemorrhagic Fever Virus. In O. Ergonul, C.A. Whitehouse, (Eds.), *Crimean-Congo Hemorrhagic Fever: A Global Perspective* pp. 143-154). Dordrecht: Springer Netherlands.
108. Dickson, D. L. and Turell, M. J. (1992). Replication and Tissue Tropisms of Crimean-Congo Hemorrhagic Fever Virus in Experimentally Infected Adult Hyalomma truncatum (Acari: Ixodidae). *Journal of medical entomology*, *29*(5), 767-773.
109. Karti, S. S., Odabasi, Z., Korten, V., Yilmaz, M., Sonmez, M., Rahmet Caylan, E. A., Necmi Eren, Iftihar Koksal, Ercument Ovali, Bobbie R. Erickson, and Martin J. Vincent, S. T. N., James A. Comer, Pierre E. Rollin, and Thomas G. Ksiazek. (2004). Crimean-Congo Hemorrhagic Fever in Turkey. *Emerging Infectious Diseases*, *10*(8), 1379–1384.
110. Ahmeti, S. and Raka, L. (2006). Crimean-Congo haemorrhagic fever in Kosova : a fatal case report. *Virology journal*, *3*, 85.
111. Bakir, M., Ugurlu, M., Dokuzoguz, B., Bodur, H., Tasyaran, M. A. and Vahaboglu, H. (2005). Crimean-Congo haemorrhagic fever outbreak in Middle Anatolia: a multicentre study of clinical features and outcome measures. *Journal of medical microbiology*, *54*(Pt 4), 385-389.
112. Ergonul, O., Celikbas, A., Dokuzoguz, B., Eren, S., Baykam, N. and Esener, H. (2004). Characteristics of patients with Crimean-Congo hemorrhagic fever in a recent outbreak in Turkey and impact of oral ribavirin therapy. *Clinical infectious diseases : an official publication of the Infectious Diseases Society of America*, *39*(2), 284-287.
113. Ergonul, O. and Battal, I. (2014). Potential sexual transmission of Crimean-Congo hemorrhagic fever infection. *Jpn J Infect Dis*, *67*(2), 137-138.
114. Organization, W. H. Introduction to Crimean-Congo Haemorrhagic Fever. Retrieved 05.12.2022, from *https://www.who.int/publications/i/item/introduction-to-crimean-congo-haemorrhaigc-fever*
115. Bhowmick, S., Kasi, K. K., Gethmann, J., Fischer, S., Conraths, F. J., Sokolov, I. M., et al. (2022). Ticks on the Run: A Mathematical Model of Crimean-Congo Haemorrhagic Fever (CCHF)—Key Factors for Transmission. *Epidemiologia*, *3*(1), 116-134.
116. Al-Abri, S. S., Abaidani, I. A., Fazlalipour, M., Mostafavi, E., Leblebicioglu, H., Pshenichnaya, N., et al. (2017). Current status of Crimean-Congo haemorrhagic fever in the World Health Organization Eastern Mediterranean Region: issues, challenges, and future directions. *International journal of infectious diseases : IJID : official publication of the International Society for Infectious Diseases*, *58*, 82-89.
117. Jameson, L. J. and Medlock, J. M. (2009). Results of HPA tick surveillance in Great Britain. *Veterinary Record*, *165*(5), 154-154.
118. Chitimia-Dobler, L., Schaper, S., Rieß, R., Bitterwolf, K., Frangoulidis, D., Bestehorn, M., et al. (2019). Imported Hyalomma ticks in Germany in 2018. *Parasites & Vectors*, *12*(1), 134.
119. Spengler, J. R., Bergeron, É. and Spiropoulou, C. F. (2019). Crimean-Congo hemorrhagic fever and expansion from endemic regions. *Current opinion in virology*, *34*, 70-78.

120. Monsalve-Arteaga, L., Alonso-Sardón, M., Muñoz Bellido, J. L., Vicente Santiago, M. B., Vieira Lista, M. C., López Abán, J., et al. (2020). Seroprevalence of Crimean-Congo hemorrhagic fever in humans in the World Health Organization European region: A systematic review. *PLoS Negl Trop Dis*, *14*(3), e0008094.
121. Ergonul, O. (2012). Crimean-Congo hemorrhagic fever virus: new outbreaks, new discoveries. *Current opinion in virology*, *2*(2), 215-220.
122. Schwarz, T. F., Nsanze, H. and Ameen, A. M. (1997). Clinical features of Crimean-Congo haemorrhagic fever in the United Arab Emirates. *Infection*, *25*(6), 364-367.
123. Swanepoel, R., Gill, D. E., Shepherd, A. J., Leman, P. A., Mynhardt, J. H. and Harvey, S. (1989). The clinical pathology of Crimean-Congo hemorrhagic fever. *Reviews of infectious diseases*, *11 Suppl 4*, S794-800.
124. Ergonul, O., Tuncbilek, S., Baykam, N., Celikbas, A. and Dokuzoguz, B. (2006). Evaluation of serum levels of interleukin (IL)-6, IL-10, and tumor necrosis factor-alpha in patients with Crimean-Congo hemorrhagic fever. *The Journal of infectious diseases*, *193*(7), 941-944.
125. Centers for Disease Control and Prevention, C. Crimean-Congo Hemorrhagic Fever (CCHF). from *https://www.cdc.gov/vhf/crimean-congo/treatment/index.html#:~:text=Treatment%20for%20CCHF%20is%20primarily,to%20the%20antiviral%20drug%20ribavirin.).*
126. Huggins, J. W. (1989). Prospects for treatment of viral hemorrhagic fevers with ribavirin, a broad-spectrum antiviral drug. *Reviews of infectious diseases*, *11 Suppl 4*, S750-761.
127. Watts, D. M., Ussery, M. A., Nash, D. and Peters, C. J. (1989). Inhibition of Crimean-Congo hemorrhagic fever viral infectivity yields in vitro by ribavirin. *The American journal of tropical medicine and hygiene*, *41*(5), 581-585.
128. Paragas, J., Whitehouse, C. A., Endy, T. P. and Bray, M. (2004). A simple assay for determining antiviral activity against Crimean-Congo hemorrhagic fever virus. *Antiviral research*, *62*(1), 21-25.
129. Tignor, G. H. and Hanham, C. A. (1993). Ribavirin efficacy in an in vivo model of Crimean-Congo hemorrhagic fever virus (CCHF) infection. *Antiviral research*, *22*(4), 309-325.
130. Bente, D. A., Alimonti, J. B., Shieh, W. J., Camus, G., Stroher, U., Zaki, S., et al. (2010). Pathogenesis and immune response of Crimean-Congo hemorrhagic fever virus in a STAT-1 knockout mouse model. *Journal of virology*, *84*(21), 11089-11100.
131. Keshtkar-Jahromi, M., Kuhn, J. H., Christova, I., Bradfute, S. B., Jahrling, P. B. and Bavari, S. (2011). Crimean-Congo hemorrhagic fever: current and future prospects of vaccines and therapies. *Antiviral research*, *90*(2), 85-92.
132. Soares-Weiser, K., Thomas, S., Thomson, G. and Garner, P. (2010). Ribavirin for Crimean-Congo hemorrhagic fever: systematic review and meta-analysis. *BMC infectious diseases*, *10*, 207.
133. Gholizadeh, O., Jafari, M. M., Zoobinparan, R., Yasamineh, S., Tabatabaie, R., Akbarzadeh, S., et al. (2022). Recent advances in treatment Crimean–Congo hemorrhagic fever virus: A concise overview. *Microbial Pathogenesis*, *169*, 105657.
134. Ren, F., Shen, S., Wang, Q., Wei, G., Huang, C., Wang, H., et al. (2021). Recent Advances in Bunyavirus Reverse Genetics Research: Systems

Development, Applications, and Future Perspectives. *Frontiers in microbiology*, *12*.
135. Bridgen, A. and Elliott, R. M. (1996). Rescue of a segmented negative-strand RNA virus entirely from cloned complementary DNAs. *Proc Natl Acad Sci U S A*, *93*(26), 15400-15404.
136. Barr, J. N., Elliott, R. M., Dunn, E. F. and Wertz, G. W. (2003). Segment-specific terminal sequences of Bunyamwera bunyavirus regulate genome replication. *Virology*, *311*(2), 326-338.
137. Elliott, R. M., Blakqori, G., van Knippenberg, I. C., Koudriakova, E., Li, P., McLees, A., et al. (2013). Establishment of a reverse genetics system for Schmallenberg virus, a newly emerged orthobunyavirus in Europe. *J Gen Virol*, *94*(Pt 4), 851-859.
138. Flick, K., Katz, A., Overby, A., Feldmann, H., Pettersson, R. F. and Flick, R. (2004). Functional analysis of the noncoding regions of the Uukuniemi virus (Bunyaviridae) RNA segments. *J Virol*, *78*(21), 11726-11738.
139. Flick, R., Flick, K., Feldmann, H. and Elgh, F. (2003). Reverse genetics for crimean-congo hemorrhagic fever virus. *Journal of virology*, *77*(10), 5997-6006.
140. Ikegami, T., Peters, C. J. and Makino, S. (2005). Rift valley fever virus nonstructural protein NSs promotes viral RNA replication and transcription in a minigenome system. *J Virol*, *79*(9), 5606-5615.
141. Ikegami, T., Won, S., Peters, C. J. and Makino, S. (2006). Rescue of infectious rift valley fever virus entirely from cDNA, analysis of virus lacking the NSs gene, and expression of a foreign gene. *J Virol*, *80*(6), 2933-2940.
142. Kohl, A., Lowen, A. C., Léonard, V. H. J. and Elliott, R. M. (2006). Genetic elements regulating packaging of the Bunyamwera orthobunyavirus genome. *J Gen Virol*, *87*(Pt 1), 177-187.
143. Takenaka-Uema, A., Sugiura, K., Bangphoomi, N., Shioda, C., Uchida, K., Kato, K., et al. (2016). Development of an improved reverse genetics system for Akabane bunyavirus. *J Virol Methods*, *232*, 16-20.
144. Eichler, R., Strecker, T., Kolesnikova, L., ter Meulen, J., Weissenhorn, W., Becker, S., et al. (2004). Characterization of the Lassa virus matrix protein Z: electron microscopic study of virus-like particles and interaction with the nucleoprotein (NP). *Virus Res*, *100*(2), 249-255.
145. Gómez-Puertas, P., Albo, C., Pérez-Pastrana, E., Vivo, A. and Portela, A. (2000). Influenza virus matrix protein is the major driving force in virus budding. *J Virol*, *74*(24), 11538-11547.
146. Strecker, T., Eichler, R., Meulen, J., Weissenhorn, W., Dieter Klenk, H., Garten, W., et al. (2003). Lassa virus Z protein is a matrix protein and sufficient for the release of virus-like particles [corrected]. *J Virol*, *77*(19), 10700-10705.
147. Watanabe, T., Watanabe, S., Neumann, G., Kida, H. and Kawaoka, Y. (2002). Immunogenicity and protective efficacy of replication-incompetent influenza virus-like particles. *J Virol*, *76*(2), 767-773.
148. Ako-Adjei, D., Johnson, M. C. and Vogt, V. M. (2005). The retroviral capsid domain dictates virion size, morphology, and coassembly of gag into virus-like particles. *J Virol*, *79*(21), 13463-13472.
149. Hsieh, P. K., Chang, S. C., Huang, C. C., Lee, T. T., Hsiao, C. W., Kou, Y. H., et al. (2005). Assembly of severe acute respiratory syndrome coronavirus RNA packaging signal into virus-like particles is nucleocapsid dependent. *J Virol*, *79*(22), 13848-13855.

150. Lee, K. J., Perez, M., Pinschewer, D. D. and de la Torre, J. C. (2002). Identification of the lymphocytic choriomeningitis virus (LCMV) proteins required to rescue LCMV RNA analogs into LCMV-like particles. *J Virol*, *76*(12), 6393-6397.
151. Li, P. P., Naknanishi, A., Tran, M. A., Ishizu, K., Kawano, M., Phillips, M., et al. (2003). Importance of Vp1 calcium-binding residues in assembly, cell entry, and nuclear entry of simian virus 40. *J Virol*, *77*(13), 7527-7538.
152. Licata, J. M., Johnson, R. F., Han, Z. and Harty, R. N. (2004). Contribution of ebola virus glycoprotein, nucleoprotein, and VP24 to budding of VP40 virus-like particles. *J Virol*, *78*(14), 7344-7351.
153. Schmitt, A. P., Leser, G. P., Waning, D. L. and Lamb, R. A. (2002). Requirements for budding of paramyxovirus simian virus 5 virus-like particles. *J Virol*, *76*(8), 3952-3964.
154. Watanabe, S., Watanabe, T., Noda, T., Takada, A., Feldmann, H., Jasenosky, L. D., et al. (2004). Production of novel ebola virus-like particles from cDNAs: an alternative to ebola virus generation by reverse genetics. *J Virol*, *78*(2), 999-1005.
155. Pickin, M. J., Devignot, S., Weber, F. and Groschup, M. H. (2022). Comparison of Crimean-Congo Hemorrhagic Fever Virus and Aigai Virus in Life Cycle Modeling Systems Reveals a Difference in L Protein Activity. *Journal of virology*, *96*(13), e00599-00522.
156. Hirano, M., Sakurai, Y., Urata, S., Kurosaki, Y., Yasuda, J. and Yoshii, K. (2022). A screen of FDA-approved drugs with minigenome identified tigecycline as an antiviral targeting nucleoprotein of Crimean-Congo hemorrhagic fever virus. *Antiviral research*, *200*, 105276.
157. Hua, B. L., Scholte, F. E., Ohlendorf, V., Kopp, A., Marklewitz, M., Drosten, C., et al. (2020). A single mutation in Crimean-Congo hemorrhagic fever virus discovered in ticks impairs infectivity in human cells. *Elife*, *9*.
158. Álvarez-Rodríguez, B., Tiede, C., Hoste, A. C. R., Surtees, R. A., Trinh, C. H., Slack, G. S., et al. (2020). Characterization and applications of a Crimean-Congo hemorrhagic fever virus nucleoprotein-specific Affimer: Inhibitory effects in viral replication and development of colorimetric diagnostic tests. *PLOS Neglected Tropical Diseases*, *14*(6), e0008364.
159. Freitas, N., Enguehard, M., Denolly, S., Levy, C., Neveu, G., Lerolle, S., et al. (2020). The interplays between Crimean-Congo hemorrhagic fever virus (CCHFV) M segment-encoded accessory proteins and structural proteins promote virus assembly and infectivity. *PLoS pathogens*, *16*(9), e1008850.
160. Welch, S. R., Scholte, F. E. M., Spengler, J. R., Ritter, J. M., Coleman-McCray, J. D., Harmon, J. R., et al. (2020). The Crimean-Congo Hemorrhagic Fever Virus NSm Protein Is Dispensable for Growth In Vitro and Disease in Ifnar-/- Mice. *Microorganisms*, *8*(5), 775.
161. Zivcec, M., Guerrero, L. I. W., Albariño, C. G., Bergeron, É., Nichol, S. T. and Spiropoulou, C. F. (2017). Identification of broadly neutralizing monoclonal antibodies against Crimean-Congo hemorrhagic fever virus. *Antiviral research*, *146*, 112-120.
162. Hinkula, J., Devignot, S., Åkerström, S., Karlberg, H., Wattrang, E., Bereczky, S., et al. (2017). Immunization with DNA Plasmids Coding for Crimean-Congo Hemorrhagic Fever Virus Capsid and Envelope Proteins and/or Virus-Like Particles Induces Protection and Survival in Challenged Mice. *Journal of virology*, *91*(10), e02076-02016.

163. Scholte, F. E. M., Zivcec, M., Dzimianski, J. V., Deaton, M. K., Spengler, J. R., Welch, S. R., et al. (2017). Crimean-Congo Hemorrhagic Fever Virus Suppresses Innate Immune Responses via a Ubiquitin and ISG15 Specific Protease. *Cell Reports*, *20*(10), 2396-2407.
164. Bergeron, É., Zivcec, M., Chakrabarti, A. K., Nichol, S. T., Albariño, C. G. and Spiropoulou, C. F. (2015). Recovery of Recombinant Crimean Congo Hemorrhagic Fever Virus Reveals a Function for Non-structural Glycoproteins Cleavage by Furin. *PLoS pathogens*, *11*(5), e1004879.
165. Zhao, J., Xia, H., Zhang, Y., Yin, S., Zhang, Z., Tang, S., et al. (2013). Mini-genome rescue of Crimean-Congo hemorrhagic fever virus and research into the evolutionary patterns of its untranslated regions. *Virus research*, *177*(1), 22-34.
166. Carter, S. D., Surtees, R., Walter, C. T., Ariza, A., Bergeron, É., Nichol, S. T., et al. (2012). Structure, Function, and Evolution of the Crimean-Congo Hemorrhagic Fever Virus Nucleocapsid Protein. *Journal of virology*, *86*(20), 10914-10923.
167. Bergeron, E., Albariño, C. G., Khristova, M. L. and Nichol, S. T. (2010). Crimean-Congo hemorrhagic fever virus-encoded ovarian tumor protease activity is dispensable for virus RNA polymerase function. *Journal of virology*, *84*(1), 216-226.
168. Almeida, J. D. and Tyrrell, D. A. (1967). The morphology of three previously uncharacterized human respiratory viruses that grow in organ culture. *J Gen Virol*, *1*(2), 175-178.
169. Tyrrell, D. A. and Almeida, J. D. (1967). Direct electron-microscopy of organ culture for the detection and characterization of viruses. *Arch Gesamte Virusforsch*, *22*(3), 417-425.
170. Chan, J. F., Kok, K. H., Zhu, Z., Chu, H., To, K. K., Yuan, S., et al. (2020). Genomic characterization of the 2019 novel human-pathogenic coronavirus isolated from a patient with atypical pneumonia after visiting Wuhan. *Emerg Microbes Infect*, *9*(1), 221-236.
171. de Wit, E., van Doremalen, N., Falzarano, D. and Munster, V. J. (2016). SARS and MERS: recent insights into emerging coronaviruses. *Nat Rev Microbiol*, *14*(8), 523-534.
172. Huang, C., Wang, Y., Li, X., Ren, L., Zhao, J., Hu, Y., et al. (2020). Clinical features of patients infected with 2019 novel coronavirus in Wuhan, China. *The Lancet*, *395*(10223), 497-506.
173. Zhou, P., Yang, X.-L., Wang, X.-G., Hu, B., Zhang, L., Zhang, W., et al. (2020). A pneumonia outbreak associated with a new coronavirus of probable bat origin. *Nature*, *579*(7798), 270-273.
174. McIntosh, K. COVID-19: Epidemiology, virology, and prevention. (2022). Retrieved 05.12.2022, from *https://www.uptodate.com/contents/covid-19-epidemiology-virology-and-prevention#H1963533542*
175. Temmam, S., Vongphayloth, K., Baquero, E., Munier, S., Bonomi, M., Regnault, B., et al. (2022). Bat coronaviruses related to SARS-CoV-2 and infectious for human cells. *Nature*, *604*(7905), 330-336.
176. Zhou, H., Ji, J., Chen, X., Bi, Y., Li, J., Wang, Q., et al. (2021). Identification of novel bat coronaviruses sheds light on the evolutionary origins of SARS-CoV-2 and related viruses. *Cell*, *184*(17), 4380-4391.e4314.
177. Wacharapluesadee, S., Tan, C. W., Maneeorn, P., Duengkae, P., Zhu, F., Joyjinda, Y., et al. (2021). Evidence for SARS-CoV-2 related coronaviruses

circulating in bats and pangolins in Southeast Asia. *Nature communications*, *12*(1), 972.
178. Murakami, S., Kitamura, T., Suzuki, J., Sato, R., Aoi, T., Fujii, M., et al. (2020). Detection and Characterization of Bat Sarbecovirus Phylogenetically Related to SARS-CoV-2, Japan. *Emerg Infect Dis*, *26*(12), 3025-3029.
179. Zhou, P., Yang, X. L., Wang, X. G., Hu, B., Zhang, L., Zhang, W., et al. (2020). A pneumonia outbreak associated with a new coronavirus of probable bat origin. *Nature*, *579*(7798), 270-273.
180. Rahalkar, M. C. and Bahulikar, R. A. (2020). Lethal Pneumonia Cases in Mojiang Miners (2012) and the Mineshaft Could Provide Important Clues to the Origin of SARS-CoV-2. *Frontiers in Public Health*, *8*.
181. Delaune, D., Hul, V., Karlsson, E. A., Hassanin, A., Ou, T. P., Baidaliuk, A., et al. (2021). A novel SARS-CoV-2 related coronavirus in bats from Cambodia. *Nature communications*, *12*(1), 6563.
182. Liu, P., Jiang, J. Z., Wan, X. F., Hua, Y., Li, L., Zhou, J., et al. (2020). Are pangolins the intermediate host of the 2019 novel coronavirus (SARS-CoV-2)? *PLoS pathogens*, *16*(5), e1008421.
183. Xiao, K., Zhai, J., Feng, Y., Zhou, N., Zhang, X., Zou, J. J., et al. (2020). Isolation of SARS-CoV-2-related coronavirus from Malayan pangolins. *Nature*, *583*(7815), 286-289.
184. Wahba, L., Jain, N., Fire, A. Z., Shoura, M. J., Artiles, K. L., McCoy, M. J., et al. (2020). An Extensive Meta-Metagenomic Search Identifies SARS-CoV-2-Homologous Sequences in Pangolin Lung Viromes. *mSphere*, *5*(3).
185. Zhao, J., Cui, W. and Tian, B.-p. (2020). The Potential Intermediate Hosts for SARS-CoV-2. *Frontiers in microbiology*, *11*.
186. Jackson, B., Boni, M. F., Bull, M. J., Colleran, A., Colquhoun, R. M., Darby, A. C., et al. (2021). Generation and transmission of interlineage recombinants in the SARS-CoV-2 pandemic. *Cell*, *184*(20), 5179-5188.e5178.
187. Rochman, N. D., Wolf, Y. I., Faure, G., Mutz, P., Zhang, F. and Koonin, E. V. (2021). Ongoing global and regional adaptive evolution of SARS-CoV-2. *Proceedings of the National Academy of Sciences of the United States of America*, *118*(29).
188. Ontario, P. H. Additional Routes of COVID-19 Transmission–What We Know So Far. (2021). Retrieved 05.12.2022, from *https://www.publichealthontario.ca/-/media/documents/ncov/covid-wwksf/2020/12/routes-transmission-covid-19.pdf?la=en*
189. Subgenus: Sarbecovirus [Internet]. Current ICTV Taxonomy Release. [cited 05.12.2022]. Available from: https://ictv.global/taxonomy/taxondetails?taxnode_id=202106129.
190. de Haan, C. A. and Rottier, P. J. (2005). Molecular interactions in the assembly of coronaviruses. *Adv Virus Res*, *64*, 165-230.
191. Wu, F., Zhao, S., Yu, B., Chen, Y.-M., Wang, W., Song, Z.-G., et al. (2020). A new coronavirus associated with human respiratory disease in China. *Nature*, *579*(7798), 265-269.
192. PDB, R. SARS-CoV-2 Genome and Proteins. Retrieved 05.12.2022, from *https://pdb101.rcsb.org/learn/flyers-posters-and-other-resources/flyer/sars-cov-2-genome-and-proteins*
193. Rabaan, A. A., Al-Ahmed, S. H., Haque, S., Sah, R., Tiwari, R., Malik, Y. S., et al. (2020). SARS-CoV-2, SARS-CoV, and MERS-COV: A comparative overview. *Infez Med*, *28*(2), 174-184.

194. Fehr, A. R. and Perlman, S. (2015). Coronaviruses: an overview of their replication and pathogenesis. *Methods Mol Biol*, *1282*, 1-23.
195. Whittaker, G. R. (2021). SARS-CoV-2 spike and its adaptable furin cleavage site. *Lancet Microbe*, *2*(10), e488-e489.
196. Laporte, M., Raeymaekers, V., Van Berwaer, R., Vandeput, J., Marchand-Casas, I., Thibaut, H. J., et al. (2021). The SARS-CoV-2 and other human coronavirus spike proteins are fine-tuned towards temperature and proteases of the human airways. *PLoS pathogens*, *17*(4), e1009500.
197. Kung, Y.-A., Lee, K.-M., Chiang, H.-J., Huang, S.-Y., Wu, C.-J. and Shih, S.-R. (2022). Molecular Virology of SARS-CoV-2 and Related Coronaviruses. *Microbiology and Molecular Biology Reviews*, *86*(2), e00026-00021.
198. Zhao, M. M., Yang, W. L., Yang, F. Y., Zhang, L., Huang, W. J., Hou, W., et al. (2021). Cathepsin L plays a key role in SARS-CoV-2 infection in humans and humanized mice and is a promising target for new drug development. *Signal Transduct Target Ther*, *6*(1), 134.
199. Weiss, S. R. (2020). Forty years with coronaviruses. *The Journal of experimental medicine*, *217*(5).
200. Denison, M. R., Graham, R. L., Donaldson, E. F., Eckerle, L. D. and Baric, R. S. (2011). Coronaviruses: an RNA proofreading machine regulates replication fidelity and diversity. *RNA Biol*, *8*(2), 270-279.
201. Wang, J., Jiang, M., Chen, X. and Montaner, L. J. (2020). Cytokine storm and leukocyte changes in mild versus severe SARS-CoV-2 infection: Review of 3939 COVID-19 patients in China and emerging pathogenesis and therapy concepts. *Journal of leukocyte biology*, *108*(1), 17-41.
202. Azkur, A. K., Akdis, M., Azkur, D., Sokolowska, M., van de Veen, W., Brüggen, M. C., et al. (2020). Immune response to SARS-CoV-2 and mechanisms of immunopathological changes in COVID-19. *Allergy*, *75*(7), 1564-1581.
203. Cascella, M., Rajnik, M., Aleem, A., Dulebohn, S. C. and Di Napoli, R. (2022). Features, Evaluation, and Treatment of Coronavirus (COVID-19). *StatPearls*. Treasure Island (FL): StatPearls Publishing

204. Zhang, J., Zeng, H., Gu, J., Li, H., Zheng, L. and Zou, Q. (2020). Progress and Prospects on Vaccine Development against SARS-CoV-2. *Vaccines (Basel)*, *8*(2).
205. Parums, D. V. (2022). Editorial: First Approval of the Protein-Based Adjuvanted Nuvaxovid (NVX-CoV2373) Novavax Vaccine for SARS-CoV-2 Could Increase Vaccine Uptake and Provide Immune Protection from Viral Variants. *Med Sci Monit*, *28*, e936523.
206. Sapoval, N., Liu, Y., Lou, E. G., Hopkins, L., Ensor, K. B., Schneider, R., et al. (2022). QuaID: Enabling Earlier Detection of Recently Emerged SARS-CoV-2 Variants of Concern in Wastewater. *medRxiv*.
207. Kumari, M., Lu, R.-M., Li, M.-C., Huang, J.-L., Hsu, F.-F., Ko, S.-H., et al. (2022). A critical overview of current progress for COVID-19: development of vaccines, antiviral drugs, and therapeutic antibodies. *Journal of Biomedical Science*, *29*(1), 68.
208. Lauring, A. S., Tenforde, M. W., Chappell, J. D., Gaglani, M., Ginde, A. A., McNeal, T., et al. (2022). Clinical severity of, and effectiveness of mRNA vaccines against, covid-19 from omicron, delta, and alpha SARS-CoV-2

variants in the United States: prospective observational study. *BMJ*, *376*, e069761.
209. 2021. China's COVID vaccines have been crucial — now immunity is waning. Nature398-399.
210. WHO. COVID-19 Vaccines with WHO Emergency Use Listing. Retrieved 01.01.2023, from *https://extranet.who.int/pqweb/vaccines/vaccinescovid-19-vaccine-eul-issued*
211. Tanriover, M. D., Doğanay, H. L., Akova, M., Güner, H. R., Azap, A., Akhan, S., et al. (2021). Efficacy and safety of an inactivated whole-virion SARS-CoV-2 vaccine (CoronaVac): interim results of a double-blind, randomised, placebo-controlled, phase 3 trial in Turkey. *The Lancet*, *398*(10296), 213-222.
212. Pavel, S. T., Yetiskin, H., Uygut, M. A., Aslan, A. F., Aydın, G., İnan, Ö., et al. 2021 Development of an Inactivated Vaccine against SARS CoV-2. Vaccines [Internet]. 9(11).
213. Tanriover, M. D., Aydin, O. A., Guner, R., Yildiz, O., Celik, I., Doganay, H. L., et al. (2022). Efficacy, Immunogenicity, and Safety of the Two-Dose Schedules of TURKOVAC versus CoronaVac in Healthy Subjects: A Randomized, Observer-Blinded, Non-Inferiority Phase III Trial. *Vaccines*, *10*(11), 1865.
214. Kalkan Yazıcı, M., Koç, M. M., Çetin, N. S., Karaaslan, E., Okay, G., Durdu, B., et al. (2020). Discordance between Serum Neutralizing Antibody Titers and the Recovery from COVID-19. *The Journal of Immunology*, *205*(10), 2719-2725.
215. Martínez-Sobrido, L. and García-Sastre, A. (2010). Generation of recombinant influenza virus from plasmid DNA. *J Vis Exp*, (42).
216. Zhou, Z.-r., Wang, M.-l., Deng, F., Li, T.-x., Hu, Z.-h. and Wang, H.-l. (2011). Production of CCHF virus-like particle by a baculovirus-insect cell expression system. *Virologica Sinica*, *26*(5), 338.
217. Cao, J., Novoa, E. M., Zhang, Z., Chen, W. C. W., Liu, D., Choi, G. C. G., et al. (2021). High-throughput 5′ UTR engineering for enhanced protein production in non-viral gene therapies. *Nature Communications*, *12*(1), 4138.
218. Li, Z., Zhong, L., He, J., Huang, Y. and Zhao, Y. (2021). Development and application of reverse genetic technology for the influenza virus. *Virus Genes*, *57*(2), 151-163.
219. Dai, S., Wu, Q., Wu, X., Peng, C., Liu, J., Tang, S., et al. (2021). Differential Cell Line Susceptibility to Crimean-Congo Hemorrhagic Fever Virus. *Frontiers in cellular and infection microbiology*, *11*.
220. Lombe, B. P., Miyamoto, H., Saito, T., Yoshida, R., Manzoor, R., Kajihara, M., et al. (2021). Purification of Crimean-Congo hemorrhagic fever virus nucleoprotein and its utility for serological diagnosis. *Sci Rep*, *11*(1), 2324.
221. Lombe, B. P., Saito, T., Miyamoto, H., Mori-Kajihara, A., Kajihara, M., Saijo, M., et al. (2022). Mapping of Antibody Epitopes on the Crimean-Congo Hemorrhagic Fever Virus Nucleoprotein. *Viruses*, *14*(3), 544.
222. Zivcec, M., Metcalfe, M. G., Albariño, C. G., Guerrero, L. W., Pegan, S. D., Spiropoulou, C. F., et al. (2015). Assessment of Inhibitors of Pathogenic Crimean-Congo Hemorrhagic Fever Virus Strains Using Virus-Like Particles. *PLoS Negl Trop Dis*, *9*(12), e0004259.
223. Andersson, I., Bladh, L., Mousavi-Jazi, M., Magnusson, K. E., Lundkvist, A., Haller, O., et al. (2004). Human MxA Protein Inhibits the Replication of

Crimean-Congo Hemorrhagic Fever Virus. *Journal of virology*, *78*(8), 4323-4329.
224. Andersson, C., Henriksson, S., Magnusson, K.-E., Nilsson, M. and Mirazimi, A. (2012). In situ rolling circle amplification detection of Crimean Congo hemorrhagic fever virus (CCHFV) complementary and viral RNA. *Virology*, *426*(2), 87-92.
225. Luytjes, W., Krystal, M., Enami, M., Parvin, J. D. and Palese, P. (1989). Amplification, expression, and packaging of foreign gene by influenza virus. *Cell*, *59*(6), 1107-1113.
226. Pattnaik, A. K. and Wertz, G. W. (1990). Replication and amplification of defective interfering particle RNAs of vesicular stomatitis virus in cells expressing viral proteins from vectors containing cloned cDNAs. *Journal of virology*, *64*(6), 2948-2957.
227. Pattnaik, A. K. and Wertz, G. W. (1991). Cells that express all five proteins of vesicular stomatitis virus from cloned cDNAs support replication, assembly, and budding of defective interfering particles. *Proceedings of the National Academy of Sciences of the United States of America*, *88*(4), 1379-1383.
228. Dunn, E. F., Pritlove, D. C., Jin, H. and Elliott, R. M. (1995). Transcription of a recombinant bunyavirus RNA template by transiently expressed bunyavirus proteins. *Virology*, *211*(1), 133-143.
229. Ferron, F., Weber, F., de la Torre, J. C. and Reguera, J. (2017). Transcription and replication mechanisms of Bunyaviridae and Arenaviridae L proteins. *Virus research*, *234*, 118-134.
230. Hass, M., Gölnitz, U., Müller, S., Becker-Ziaja, B. and Günther, S. (2004). Replicon System for Lassa Virus. *Journal of virology*, *78*(24), 13793-13803.
231. Shi, X., Kohl, A., Léonard, V. H., Li, P., McLees, A. and Elliott, R. M. (2006). Requirement of the N-terminal region of orthobunyavirus nonstructural protein NSm for virus assembly and morphogenesis. *Journal of virology*, *80*(16), 8089-8099.
232. Overby, A. K., Popov, V., Neve, E. P. and Pettersson, R. F. (2006). Generation and analysis of infectious virus-like particles of uukuniemi virus (bunyaviridae): a useful system for studying bunyaviral packaging and budding. *Journal of virology*, *80*(21), 10428-10435.
233. Habjan, M., Penski, N., Wagner, V., Spiegel, M., Overby, A. K., Kochs, G., et al. (2009). Efficient production of Rift Valley fever virus-like particles: The antiviral protein MxA can inhibit primary transcription of bunyaviruses. *Virology*, *385*(2), 400-408.
234. Zhu, Z., Lian, X., Su, X., Wu, W., Marraro, G. A. and Zeng, Y. (2020). From SARS and MERS to COVID-19: a brief summary and comparison of severe acute respiratory infections caused by three highly pathogenic human coronaviruses. *Respir Res*, *21*(1), 224.
235. Siu, Y. L., Teoh, K. T., Lo, J., Chan, C. M., Kien, F., Escriou, N., et al. (2008). The M, E, and N structural proteins of the severe acute respiratory syndrome coronavirus are required for efficient assembly, trafficking, and release of virus-like particles. *Journal of virology*, *82*(22), 11318-11330.
236. Huang, Y., Yang, Z. Y., Kong, W. P. and Nabel, G. J. (2004). Generation of synthetic severe acute respiratory syndrome coronavirus pseudoparticles: implications for assembly and vaccine production. *Journal of virology*, *78*(22), 12557-12565.

237. Mortola, E. and Roy, P. (2004). Efficient assembly and release of SARS coronavirus-like particles by a heterologous expression system. *FEBS Lett*, *576*(1-2), 174-178.
238. Xu, R., Shi, M., Li, J., Song, P. and Li, N. (2020). Construction of SARS-CoV-2 Virus-Like Particles by Mammalian Expression System. *Front Bioeng Biotechnol*, *8*, 862.
239. See, R. H., Petric, M., Lawrence, D. J., Mok, C. P. Y., Rowe, T., Zitzow, L. A., et al. (2008). Severe acute respiratory syndrome vaccine efficacy in ferrets: whole killed virus and adenovirus-vectored vaccines. *J Gen Virol*, *89*(Pt 9), 2136-2146.
240. Liu, Y. V., Massare, M. J., Barnard, D. L., Kort, T., Nathan, M., Wang, L., et al. (2011). Chimeric severe acute respiratory syndrome coronavirus (SARS-CoV) S glycoprotein and influenza matrix 1 efficiently form virus-like particles (VLPs) that protect mice against challenge with SARS-CoV. *Vaccine*, *29*(38), 6606-6613.
241. Lu, X., Chen, Y., Bai, B., Hu, H., Tao, L., Yang, J., et al. (2007). Immune responses against severe acute respiratory syndrome coronavirus induced by virus-like particles in mice. *Immunology*, *122*(4), 496-502.
242. Korber, B., Fischer, W. M., Gnanakaran, S., Yoon, H., Theiler, J., Abfalterer, W., et al. (2020). Tracking Changes in SARS-CoV-2 Spike: Evidence that D614G Increases Infectivity of the COVID-19 Virus. *Cell*, *182*(4), 812-827.e819.
243. Wrapp, D., Wang, N., Corbett, K. S., Goldsmith, J. A., Hsieh, C. L., Abiona, O., et al. (2020). Cryo-EM structure of the 2019-nCoV spike in the prefusion conformation. *Science*, *367*(6483), 1260-1263.
244. Kash, N., Lee, M. A., Kollipara, R., Downing, C., Guidry, J. and Tyring, S. K. (2015). Safety and Efficacy Data on Vaccines and Immunization to Human Papillomavirus. *J Clin Med*, *4*(4), 614-633.
245. Haffar, S., Bazerbachi, F. and Lake, J. R. (2015). Making the case for the development of a vaccination against hepatitis E virus. *Liver Int*, *35*(2), 311-316.
246. Stadler, J., Naderer, L., Beffort, L., Ritzmann, M., Emrich, D., Hermanns, W., et al. (2018). Safety and immune responses after intradermal application of Porcilis PRRS in either the neck or the perianal region. *PloS one*, *13*(9), e0203560.
247. Zhao, C., Ao, Z. and Yao, X. (2016). Current Advances in Virus-Like Particles as a Vaccination Approach against HIV Infection. *Vaccines (Basel)*, *4*(1).
248. Keshavarz, M., Mirzaei, H., Salemi, M., Momeni, F., Mousavi, M. J., Sadeghalvad, M., et al. (2019). Influenza vaccine: Where are we and where do we go? *Rev Med Virol*, *29*(1), e2014.
249. Ong, H. K., Tan, W. S. and Ho, K. L. (2017). Virus like particles as a platform for cancer vaccine development. *PeerJ*, *5*, e4053.
250. Sharifzadeh, M., Mottaghi-Dastjerdi, N. and Soltany Rezae Raad, M. (2022). A Review of Virus-Like Particle-Based SARS-CoV-2 Vaccines in Clinical Trial Phases. *Iran J Pharm Res*, *21*(1), e127042.
251. Ward, B. J., Gobeil, P., Séguin, A., Atkins, J., Boulay, I., Charbonneau, P.-Y., et al. (2020). Phase 1 trial of a Candidate Recombinant Virus-Like Particle Vaccine for Covid-19 Disease Produced in Plants. *medRxiv*, 2020.2011.2004.20226282.

252. Goulet, M.-C., Gaudreau, L., Gagné, M., Maltais, A.-M., Laliberté, A.-C., Éthier, G., et al. (2019). Production of Biopharmaceuticals in Nicotiana benthamiana—Axillary Stem Growth as a Key Determinant of Total Protein Yield. *Frontiers in Plant Science, 10*.
253. Mandal, H. (2021). Achievements of the COVID-19 Turkey Platform in vaccine and drug development with an approach of "co-creation and succeeding together". *Turk J Med Sci, 51*(Si-1), 3139-3149.

CURRICULUM VITAE

Name SURNAME : Nesibe Selma ÇETİN

Place and Date of Birth :

E-mail :

EDUCATION:

- **B.Sc. :** 2013, University of Vienna, Faculty of Life Sciences, Microbiology and Genetics
- **M.Sc. :** 2016, BezmialemVakıfUniversity, Health Sciences Institute, Biotechnology

PROFESSIONAL EXPERIENCE AND REWARDS:

- 2015 Research Assistant at Bezmialem. Vakıf University, Faculty Of Medicine, Department Of Basic Medical Science

PUBLICATIONS, PRESENTATIONS AND PATENTS PRODUCED FROM THE THESIS:

OTHER PUBLICATIONS, PRESENTATIONS AND PATENTS:

- KARAASLAN ELİF, **ÇETİN NESİBE SELMA**, YAZICI MERVE, Hasanoğlu Sevde, KARAKEÇİLİ FARUK, ÖZDARENDELİ AYKUT, KALKAN AHMET, KILIÇ ALİ OSMAN, DOYMAZ MEHMET ZİYA (2021). Immune responses in multiple hosts to Nucleocapsid Protein (NP) of Crimean-Congo Hemorrhagic Fever Virus (CCHFV). PLoS neglected tropical diseases, 15(12), Doi: 10.1371/journal.pntd.0009973
- Kalkan-Yazıcı Merve, KARAASLAN ELİF, **ÇETİN NESİBE SELMA**, Hasanoğlu Sevde, ZEYBEK ŞAKİR ÜMİT, DOYMAZ MEHMET ZİYA (2021). Cross-Reactive Anti-Nucleocapsid Protein Immunity against Crimean-Congo Hemorrhagic Fever Virus and Hazara Virus in Multiple Species. Journal of Virology, 95, Doi: 10.1128/JVI.02156-20
- YAZICI MERVE,MERİÇ KOÇ MELİHA,**ÇETİN NESİBE SELMA**,KARAASLAN ELİF,Okay Gülay,DURDU BÜLENT,SÜMBÜL BİLGE,DOYMAZ MEHMET ZİYA (2020). Discordance between Serum

Neutralizing Antibody Titers and the Recovery from COVID-19. JOURNAL OF IMMUNOLOGY, 205(10), 2719-2725., Doi: 10.4049/jimmunol.2000840

- DOYMAZ MEHMET ZİYA, YAZICI MERVE, **ÇETİN NESİBE SELMA**, KARAASLAN ELİF (2020). Geographical and temporal distribution of SARS-CoV-2 clades in the WHO European Region, January to June 2020. Eurosurveillance, 25(32)
- Investigation Of The Cellular And Humoral Immune Responses Against Nucleoprotein Of Crimean Congo Hemorrhagic Fever Virus (CCHFV) **ÇETİNN.S**. ,KARAASLANE.,DOYMAZM.Z. ,KILIÇA.O. 33.ASM Clinical Virology Symposium, Savanna, USA,7 -10May2017
- Detailed Immonological Analysıis of Recombinant Crimean Congo Hemorrhagic Fever Virus Nucleoprotein. KARAASLANE.,**ÇETİNN.S**. ,Hasanoğlu S.,KILIÇA.O. ,KALKANA.,ÖZDARENDELİA.,DOYMAZM.Z. European Congress of Virology, 28April -01May2019
- Evaluation of CCHFV nucleoprotein as diagnostic tool in ELISA. **ÇETİNN.S.** ,KARAASLANE.,YAZICIM.,Hasanoğlu S.,KALKANA.,KILIÇA.O. ,ÖZDARENDELİA.,DOYMAZM.Z. 2nd International Conference on Crimean-Congo Hemorrhagic Fever,10 -12 September 2017
- Investigation Of Humoral Response Raised Against Bacterially Expressed Nucleoprotein Of Crimean Congo Hemorrhagic Fever Virus Karaaslan.,**Çetinn.**S. ,Kılıça.O. ,Doymazm.Z. 3RD INTERNATIONAL MOLECULAR IMMUNOLOGY IMMUNOGENETICS CONGRESS, 27 -30april2016
- COVİD-19 PANDEMİSİNDE Hastalık/Hastane Yönetimi, Bölüm adı:(COVID-19 ENFEKSİYONUN MİKROBİYOLOJİSİ) (2021)., DOYMAZ MEHMET ZİYA, SÜMBÜL BİLGE, AKBAŞ EMEL, KARAASLAN ELİF, ÇETİN NESİBE SELMA, YAZICI MERVE, Bezmialem Vakıf Üniversitesi Yayınları, Editör:Özdemir, Ramazan; Aydın, Teoman; Su Küçük, Özlem, Basım sayısı:1, Sayfa Sayısı 451, ISBN:978-605-85726-9-0, Türkçe(Bilimsel Kitap), (Yayın No: 7938914)